RESEARCH ARTICLE

REVISED Leaf chamber experiments on sunflowers indicate a temperature-dependent compensation point of carbonyl sulfide

[version 3; peer review: 1 approved, 2 approved with reservations]

Ara Cho[1], Linda M.J. Kooijmans[1], Steven M. Driever[2], Maarten Wassenaar[3], Gerbrand Koren[4], Sophie L. Baartman[1], Leon Mossink[2], Maarten C. Krol[1,5]

[1]Meteorology and Air Quality, Wageningen University & Research, Wageningen, Gelderland, The Netherlands
[2]Centre for Crop Systems Analysis, Wageningen University & Research, Wageningen, Gelderland, The Netherlands
[3]Horticulture and Product Physiology, Wageningen University & Research, Wageningen, Gelderland, The Netherlands
[4]Copernicus Institute of Sustainable Development, Utrecht University, Utrecht, Utrecht, The Netherlands
[5]Institute for Marine and Atmospheric Research, Utrecht University, Utrecht, The Netherlands

v3 **First published:** 05 Aug 2025, **5**:223
https://doi.org/10.12688/openreseurope.20235.1
Second version: 08 Dec 2025, **5**:223
https://doi.org/10.12688/openreseurope.20235.2
Latest published: 10 Apr 2026, **5**:223
https://doi.org/10.12688/openreseurope.20235.3

Abstract

Background

Carbonyl Sulfide (COS) is a potential tracer for estimating gross primary productivity (GPP), due to its co-uptake with CO_2 in leaves and the assumed absence of re-emission. However, the effectiveness of COS as a GPP tracer depends on understanding the differential responses of COS and CO_2 uptake to environmental factors such as temperature and humidity. Methods We conducted three sets of leaf gas exchange experiments on sunflower leaves. In each experiment, we varied only one environmental factor: COS mole fraction (at two temperatures), humidity, or temperature. During the experiments, COS and CO_2 fluxes were measured, and the data were used to optimize a leaf conductance model.

Results

We identified the existence of a COS compensation point, which increases with higher temperatures, suggesting potential emissions at higher temperatures when atmospheric COS concentrations are low. Our gas exchange measurements detected a COS compensation point

Open Peer Review

Approval Status ? ? ✓

	1	2	3
version 3 (revision) 10 Apr 2026			✓ view
version 2 (revision) 08 Dec 2025			? view
version 1 05 Aug 2025	? view	? view	

1. **Jerome Ogee**, Bordeaux Sciences Agro, Villenave d'Ornon, France
Institut National de Recherche pour l'Agriculture l'Alimentation et l'Environnement Centre Nouvelle-Aquitaine Bordeaux (Ringgold ID: 113907), Villenave-d'Ornon, France

2. **Max Berkelhammer**, University of Illinois Chicago, Chicago, USA

of 58.9 ± 52.4 pmol mol^{-1} at 20°C and 139.9 ± 26.0 pmol mol^{-1} at 25°C. As vapor pressure deficit increased and stomatal conductance decreased, we observed that COS leaf uptake decreased more rapidly than CO_2 assimilation. Consequently, the leaf relative uptake ratio (LRU) of COS to CO_2 also decreased when stomatal conductance decreased. The optimized conductance model indicated that the optimum temperature for COS and CO_2 enzymatic uptake was around 35°. However, the maximum net deposition velocity for COS lies between 20 and 25°, due to its temperature-dependent compensation point.

Plain language summary

Carbonyl sulfide (COS) is a trace gas found in the atmosphere that plants take up in a way similar to carbon dioxide (CO_2) during photosynthesis. Because of this shared pathway, COS has been widely used to estimate how much CO_2 plants absorb from the atmosphere—a process known as gross primary production (GPP). In our study, we conducted experiments using sunflower leaves in controlled chambers and found that COS and CO_2 respond differently to changes in temperature and humidity. Surprisingly, we also observed that sunflower leaves may release COS back into the atmosphere when COS levels are low and temperatures are high. This finding challenges the long-standing assumption that plants only absorb COS and do not emit it. Our research highlights that understanding how COS behaves in plants under different environmental conditions is crucial for using it as a reliable tool to estimate how much CO_2 is absorbed by vegetation.

Keywords

Leaf chamber experiment, Leaf conductance model, Carbonyl sulfide, Photosynthesis, Leaf relative uptake, Stomatal conductance, Compensation point

This article is included in the European Research Council (ERC) gateway.

This article is included in the Horizon 2020 gateway.

3. **Anam M. Khan**, Northern Arizona University (Ringgold ID: 3356), Flagstaff, USA

Any reports and responses or comments on the article can be found at the end of the article.

Corresponding author: Ara Cho (ara.cho@wur.nl)

Author roles: Cho A: Conceptualization, Data Curation, Formal Analysis, Investigation, Methodology, Software, Validation, Visualization, Writing – Original Draft Preparation, Writing – Review & Editing; **Kooijmans LMJ**: Conceptualization, Data Curation, Formal Analysis, Investigation, Methodology, Resources, Supervision, Validation, Writing – Original Draft Preparation, Writing – Review & Editing; **Driever SM**: Data Curation, Formal Analysis, Methodology, Resources, Writing – Original Draft Preparation, Writing – Review & Editing; **Wassenaar M**: Data Curation, Formal Analysis, Methodology, Resources, Writing – Review & Editing; **Koren G**: Formal Analysis, Methodology, Software, Writing – Review & Editing; **Baartman SL**: Resources, Writing – Review & Editing; **Mossink L**: Resources, Writing – Review & Editing; **Krol MC**: Conceptualization, Formal Analysis, Funding Acquisition, Investigation, Methodology, Project Administration, Software, Supervision, Writing – Review & Editing

Competing interests: No competing interests were disclosed.

Grant information: This project has received funding from the European Research Council (ERC) under the European Union's Horizon 2020 research and Innovation programme (Grant agreement No. 742798).

How to cite this article: Cho A, Kooijmans LMJ, Driever SM *et al.* **Leaf chamber experiments on sunflowers indicate a temperature-dependent compensation point of carbonyl sulfide [version 3; peer review: 1 approved, 2 approved with reservations]** Open Research Europe 2026, **5**:223 https://doi.org/10.12688/openreseurope.20235.3

First published: 05 Aug 2025, **5**:223 https://doi.org/10.12688/openreseurope.20235.1

REVISED **Amendments from Version 2**

The manuscript was revised in response to the reviewers' comments as summarized below.

First, we clarified why the flux in Equation 2 is normalized using the outflowing mole fraction instead of the inflowing mole fraction. We added an explanation in the Methods section stating that, under the assumption of well-mixed chamber air, the outflowing mole fraction best represents the chamber air mole fraction experienced by the leaf.

Second, we expanded the description of plant growth conditions and experimental timing to improve reproducibility. The Methods section now specifies the greenhouse temperature regime during cultivation as well as the daytime window (10:00–17:00 local time) during which gas exchange measurements were conducted.

Third, the structure of several paragraphs was revised to improve readability and logical flow. In particular, Section 4.1 was reorganized to clearly distinguish experimental limitations from model-related uncertainties.

Finally, minor editorial revisions were made throughout the manuscript, including clarification of model interpretation, small wording improvements, and adjustments to table captions to ensure consistency with the manuscript text.

Any further responses from the reviewers can be found at the end of the article

1. Introduction

Gross primary productivity (GPP) quantifies the largest terrestrial CO_2 uptake flux in the global carbon cycle. However, when measuring the net ecosystem exchange (NEE) of CO_2, separating the GPP signal from respiration is challenging (Reichstein *et al.*, 2005; Wohlfahrt & Gu, 2015). To address this limitation, Carbonyl Sulfide (COS) is an atmospheric trace gas that has been identified as a promising tracer for GPP and several studies have explored its utility extensively (Asaf *et al.*, 2013; Campbell *et al.*, 2008; Kohonen *et al.*, 2022; Montzka *et al.*, 2007). COS primarily originates from anthropogenic sources and oceans, while vegetation predominantly acts as its sink (Berry *et al.*, 2013; Kettle *et al.*, 2002).

The application of COS to estimate GPP has been suggested because COS uptake by leaves proceeds through a stomatal pathway similar to uptake of CO_2. Importantly, COS is assumed not to be released by plants due to its irreversible hydrolysis catalyzed by carbonic anhydrase (CA) (Notni *et al.*, 2007; Protoschill-Krebs *et al.*, 1996; Stimler *et al.*, 2010). With this advantage of COS, the leaf relative uptake ratio (LRU) of deposition velocities of COS and CO_2 has been introduced to scaling COS leaf uptake to photosynthesis (Campbell *et al.*, 2008; Sandoval-Soto *et al.*, 2005) (a detailed LRU description is provided in Section 2.1.2). However, previous studies have emphasized that LRU responds differently to environmental factors such as leaf temperature (T_{leaf}) and vapor pressure deficit (VPD), implying that it is not constant under varying conditions (Cochavi *et al.*, 2021; Kooijmans *et al.*, 2019; Stimler *et al.*, 2010; Sun *et al.*, 2018; Wohlfahrt *et al.*, 2018).

Unlike photosynthesis, COS uptake by CA remains unaffected by light, rendering it a robust proxy for stomatal conductance to water vapor (g_{sw}). Accordingly, recent studies have used ecosystem-level COS exchange as a proxy for g_{sw}, highlighting differences between stomatal and biochemical contributions to CO_2 uptake (Cochavi *et al.*, 2021; Wohlfahrt *et al.*, 2018).

Differences in COS and CO_2 responses to changes in T_{leaf} and VPD were observed under constant light conditions, but their causes remain unclear (Kooijmans *et al.*, 2019; Stimler *et al.*, 2010; Sun *et al.*, 2018). Kooijmans *et al.* (2019) measured that LRU decreases with increasing temperatures (from 13 to 23°C) or increasing VPD (from 0.5 to 2.5 kPa) at the boreal forest site Hyytiälä in Finland, while CO_2 uptake remained relatively stable. Understanding these variations is imperative for utilizing COS measurements to infer information about GPP.

To address these open questions, we investigate three potential explanations for the different responses of COS and CO_2 uptake to increasing T_{leaf} and VPD under high-light conditions. First, the pronounced reduction in COS leaf uptake compared to CO_2 uptake at higher T_{leaf} might be due to a potential COS compensation point (Γ_{COS}) at higher T_{leaf} (Hypothesis 1), which occurs when uptake and production are equal. If the atmospheric mole fraction is higher than Γ_{COS}, it generally indicates a predominance of uptake over production. Conversely, below this point, production exceeds uptake, resulting in a net release of COS to the atmosphere.

Γ_{COS} have been reported in a few vascular plants, algae, crops, and lichen fields (Belviso *et al.*, 2022; Geng & Mu, 2004; Goldan *et al.*, 1988; Kesselmeier & Merk, 1993; Kuhn & Kesselmeier, 2000; Maseyk *et al.*, 2014). These measured Γ_{COS} values are lower than typical atmospheric COS mole fractions (≈500 pmol mol^{-1}), which is why net COS uptake is observed. Stimler *et al.* (2010) also observed a Γ_{COS} of 60.7 pmol mol^{-1}, though statistically indistinguishable from zero,

and interpreted it as a possible diffusional feedback under high COS mole fractions. More recently, Gimeno *et al.* (2017) demonstrated temperature-dependent COS emissions in nonvascular bryophytes, suggesting that biochemical processes such as protein degradation could contribute to COS release at elevated T_{leaf}. However, Γ_{COS} of vascular plants and its temperature dependence remain poorly constrained. We therefore hypothesize that the observed COS uptake results from the coexistence of uptake and production processes, with Γ_{COS} exhibiting temperature dependence.

Second, COS leaf uptake might respond more strongly to stomatal closure than CO_2 uptake (Hypothesis 2). Plants react to variations in VPD to optimize their water use efficiency (Farquhar & Sharkey, 1982). VPD-induced stomatal closure reduces CO_2 inflow, but CO_2 is still consumed within the mesophyll cells. Consequently, the leaf's internal concentration of CO_2 is reduced, increasing the CO_2 gradient between internal and ambient air. This larger gradient could sustain CO_2 uptake despite stomatal closure.

In contrast, the internal COS concentration is assumed to be much lower than ambient levels due to the higher catalytic efficiency of the CA enzyme (Protoschill-Krebs *et al.*, 1996; Seibt *et al.*, 2010; Tcherkez *et al.*, 2006). Assuming that the internal COS concentration is (near-)zero, this concentration cannot reduce much further when stomata close, unlike the CO_2 internal concentration. Consequently, in response to stomatal closure, the COS gradient between internal and ambient air will likely not reduce as much as the CO_2 gradient, and so the COS gradient will not counteract the stomatal closure as is the case for CO_2. Thus, decreasing g_{sw} is expected to reduce COS uptake more than CO_2 uptake.

Third, the enzyme CA could behave optimally at a lower temperature than the RuBisCO enzyme responsible for CO_2 fixation (Cho *et al.*, 2023; Stimler *et al.*, 2010). Consequently, when T_{leaf} rises above the optimum temperature of CA but is still below that of RuBisCO, COS uptake could decrease while CO_2 uptake still increases (Hypothesis 3). Enzyme activity typically increases with temperature until reaching an optimum temperature, and the rate and the optimum temperature might differ between enzymes. Optimum temperatures for the CA enzyme in previous models simulating leaf and soil COS uptake ranged from 15°C to 40°C (Cho *et al.*, 2023; Ogée *et al.*, 2016; Sun *et al.*, 2015), significantly lower than the optimal temperature of 50°C reported for RuBisCO (Salvucci *et al.*, 2001). Together, these hypotheses consider both stomatal and biochemical mechanisms that could explain the differential COS and CO_2 responses.

Disentangling these hypotheses using field measurements is challenging due to interrelated and simultaneous variations of environmental conditions (e.g. T_{leaf}, VPD, and g_{sw}). Laboratory experiments offer the advantage of observing COS and CO_2 uptake changes at a leaf level under controlled conditions while independently varying environmental factors. To complement the experimental analysis and mechanistically interpret the observed gas-exchange responses, we developed a coupled CO_2–COS– H_2O conductance model based on a leaf conductance model previously established for GPP tracers such as the $\Delta_{17}O$ and Δ_{47} isotopic composition of CO_2 (Adnew *et al.*, 2020; Adnew *et al.*, 2021; Adnew *et al.*, 2023). This model serves as a diagnostic tool that enables joint optimization of gas-exchange parameters through the shared stomatal pathway for the three gases and allows inference of internal variables, such as intercellular and chloroplast COS mole fractions, that are not directly measurable.

Finally, to validate the three hypotheses, we aim to investigate the existence of COS compensation points and responses of COS and CO_2 leaf uptake to varying g_{sw} and T_{leaf}. We will present measurement results from leaf gas exchange experiments with sunflowers under controlled environmental conditions. We will interpret the experimental results using the coupled leaf conductance model optimized using the experiments' dataset.

2. Materials and methods

2.1 Leaf gas-exchange measurements

2.1.1 Leaf cuvette system. We measured deposition velocities of COS and CO_2 (V_{COS} and V_{CO2}), i.e. fluxes normalized by mole fractions in air, using a leaf cuvette system. These experiments were conducted using sunflower plants (*Helianthus Annuus* L. cv. 'Sunsation'), which are C_3 photosynthesis type plants cultivated in a local plant nursery (Evanthia, Maasdijk, Netherlands). Plants were cultivated in a greenhouse under a day/night temperature regime of 18–21°C during the day and 15–18°C at night, with ventilation applied above 20°C. Germination occurred at 21–24°C. The species *Helianthus annuus* was originally described by Linnaeus (*Species Plantarum*, Vol. 2, p.904, 1753). Each sunflower plant was used for a maximum of 5 daytime hours to minimize physiological stress caused by prolonged exposure to experimental conditions. Gas exchange measurements were scheduled to align with the plants' photosynthetic rhythm and were conducted during the local daytime window between 10:00 and 17:00 (local time, the Netherlands).

T_{leaf} was monitored within the leaf cuvette using a thermocouple touching the abaxial side of the leaf. A synthetic air mixture, composed of 79% nitrogen and 21% oxygen, was mixed and controlled using mass flow controllers (Bronkhorst,

Veenendaal, the Netherlands) and humidified using a dew point generator (LI-610, Li-Cor). CO_2 and COS were supplied from controlled gas cylinders and then added to the air-stream entering the LI-6800 system. CO_2 mole fractions in the leaf cuvette were kept around 445.1 ± 3.5 μmol mol^{-1}. COS was introduced from a gas mixture with synthetic air with a COS mole fraction of around 700 nmol mol^{-1}, regulated by a mass flow controller (Analyt-MTC, Müllheim, Germany). Except for the first experiment to check Γ_{COS}, COS mole fraction levels were intentionally elevated (in the range of 900 to 1100 pmol mol^{-1}), relative to typically atmospheric mole fractions (approximately 500 pmol mol^{-1}) to improve the detectability of COS uptake. Air in the leaf cuvette was mixed by a fan, operated at approximately 10,000 rpm, and the boundary conductance near the leaf surface was maintained at about 2.44 mol m^{-2} s^{-1}.

To control g_{sw}, adjustments were made to the VPD. Initial g_{sw} (mol m^{-2} s^{-1}) values were estimated by measuring the total conductance of H_2O (g_{tw} (mol m^{-2} s^{-1})) and applying a corresponding boundary conductance of H_2O (g_{bw} (mol m^{-2} s^{-1})) according to the LI-6800 manual. We assumed equal distribution of stomata between the upper to lower side of the leaf and therefore applied a stomatal ratio of K = 0.5.

COS and CO_2 mole fractions of the inflowing and outflowing air were measured using a quantum cascade laser spectrometer (QCLS) (Aerodyne Research Inc., Billerica, MA, USA). The air subjected to QCLS analysis was initially passed through a magnesium perchlorate ($Mg(ClO_4)_2$) drying trap to eliminate water vapor. For this purpose, magnesium perchlorate hexahydrate (99% purity; Sigma-Aldrich, Product Code: 309303-100G, Linear Formula: $Mg(ClO_4)_2 \cdot 6H_2O$) was used. The water vapor scrubber tubes employed were 50 cc stainless steel tubes with 0.25-inch tube fittings. Measurements of air from cylinders with known COS and CO_2 mole fractions were performed for hourly calibration.

Once a leaf reached steady-state under the given conditions, data were recorded. The LI-6800 measured every second and was set to log data automatically every 3 minutes. Each log consisted of an average taken over 15 measurements within the preceding 15 seconds. The QCLS was set to automatically record data every second, totaling 150 measurements over each 150-second period. Then, the median over this 150-second interval was taken as the "data point". Each QCLS interval had a corresponding LI-6800 log.

The air was passed through the analyzer at an approximate flow rate (AF (mol s^{-1})) of 0.35 mmol s^{-1}. Subsequently, leaf assimilation rates (F_{gas}) of COS (F_{COS} (pmol m^{-2} s^{-1})) and CO_2 (F_{CO2} (μmol m^{-2} s^{-1})) were calculated by:

$$F_{gas} = \frac{AF}{S}([gas]_{in} - [gas]_{out}). \quad (1)$$

Here, the $[gas]_{in}$ and $[gas]_{out}$ represent the mole fractions of COS (pmol mol^{-1}) and CO_2 (μmol mol^{-1}) in the air entering and exiting the chamber, which are measured by the QCLS on a dry-air basis. The leaf area S (m^2) was 9 cm^2. Although transpiration slightly increases the outlet air flow due to the addition of water vapor (von Caemmerer & Farquhar, 1981, Appendix 2), the resulting increase in total molar flow (<3% under $[H_2O]_{out}$ = 15–30 mmol mol^{-1}) was neglected in Equation 1 for simplicity. This small effect was not considered in the flux calculations and was consistently omitted throughout the model analysis. The CO_2 leaf assimilation rates obtained from the QCLS measurements closely matched those from the LI-6800 (R = 0.96, mean difference = 0.18 μmol m^{-2} s^{-1}), confirming the accuracy of the CO_2 flux measurements.

Hourly calibration corrected potential QCLS drift, and the data points were excluded when the dew point temperature approached or exceeded the air temperature in any experiment.

To account for COS emissions at higher temperatures from chamber material (Maseyk *et al.*, 2014), we conducted empty chamber experiments using inflowing COS mole fractions of 750 – 900 pmol mol^{-1}, which were adequate for evaluating chamber emissions, across a similar range of temperatures with experimental conditions. Additional experiments with low mole fraction (40 – 75 pmol mol^{-1}) were conducted to evaluate potential emission increases originating from large concentration gradients between sampling air and chamber materials. Figure 1 shows a slight increase in COS emissions with rising temperature, with no significant effect from inflowing COS mole fractions. Measurements were conducted under 40% relative humidity (RH), to avoid potential condensation or other artifacts during the empty chamber experiment. Leaf COS flux measurements were corrected using a linear fit of emissions against temperature in the empty chamber (R^2 = 0.45) with chamber emissions averaging 6.7% of observed leaf COS flux.

2.1.2 Experiments. Table 1 lists the environmental factors that were used in the three experiments. We manipulated inflowing COS mole fractions, humidity, and air temperatures while keeping other environmental conditions constant, as specified in each experimental design. All environmental changes were introduced gradually to allow the leaf sufficient

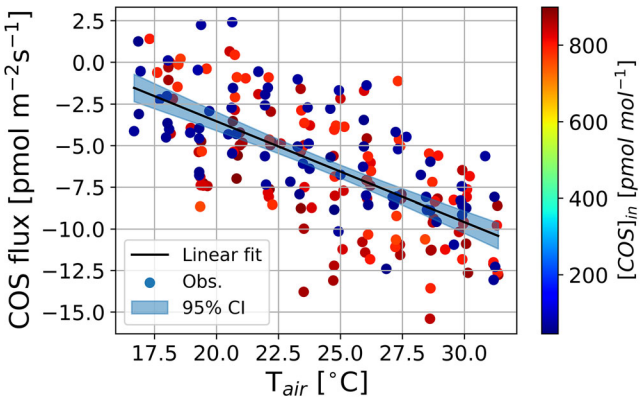

Figure 1. Measurements of COS flux at different air temperatures in the empty chamber. Dots represent measurement data points and their colors indicate injected COS mole fractions in a chamber, black lines are linear fit equations, and filled areas indicate 95% confidential interval.

time to adapt to chamber conditions. For instance, we applied humidity (to achieve a desired g_{sw}) and temperature changes of approximately 0.8 mol m^{-2} s^{-1} and 10°C, respectively, over a period of two hours. This gradual adjustment ensured that measurements reflect steady-state conditions and minimize transient effects from rapid environmental changes. To exclude the effects of light on V_{COS} and V_{CO_2}, high light intensity similar to growth conditions (600 µmol m^{-2} s^{-1}) was maintained throughout all experiments.

The first experiment (Experiment 1) aimed to detect COS compensation points and their temperature dependence. To determine the existence of Γ_{COS} and its temperature response, we measured F_{COS} at four distinct inflow COS mole fractions ranging from 94 to 589 pmol mol^{-1} at two different leaf temperatures (19.8°C and 25.0°C). As in Gimeno *et al.* (2017), the values of the Γ_{COS} were subsequently calculated for each temperature by extrapolating the COS mole fraction at which F_{COS} reaches zero using a linear regression.

The second experiment (Experiment 2) aimed to compare responses of COS and CO_2 uptake to stomatal closure. We examined the responses of V_{COS} and V_{CO_2} to g_{sw} while keeping other environmental factors constant, including air temperature (approximately 25°C). Thus, changes in V_{COS} and V_{CO2} predominantly reflect responses to changes in g_{sw}. The modulation of g_{sw} was accomplished by adjusting humidity within the leaf cuvette – hence modifying VPD – using the humidifier.

The last experiment (Experiment 3) aimed to compare responses of COS and CO_2 uptake to changing temperatures. We observed V_{COS} and V_{CO_2} while controlling the air temperature (T_{air}) within the leaf cuvette and maintaining other variables constant, including g_{sw}. The desired g_{sw} value was sustained by manipulating chamber humidity and thus VPD when necessary. The resulting leaf temperatures varied between 19.0 and 30.9°C.

Regarding a repetition of experiments, Experiment 1 was executed once with a single sunflower plant (Sunflower 1), while Experiments 2 and 3 were replicated with three different sunflower plants over three days (Sunflower 2, 3, and 4). During the measurement of COS, CO_2, and H_2O mole fractions in Experiment 3, the complete temperature range could not be covered consistently across all three repetitions due to fluctuating g_{sw} conditions. Due to this limitation, data from Sunflower 3 were omitted from the analysis of Experiment 3. Overall, we collected 15 data points from Experiment 1 and 48 data points from Experiments 2 and 3.

The measured V_{COS} and V_{CO_2} were used to calculate the LRU (-), which was used to characterize differing responses of COS and CO_2 from Experiments 2 and 3 (Sandoval-Soto et al., 2005; Campbell et al., 2008):

$$LRU = \frac{V_{COS}}{V_{CO2}} = \frac{A_{COS}}{[COS]_{out}} \frac{[CO_2]_{out}}{A_{CO2}}, \quad (2)$$

where A_{COS} (pmol m^{-2} s^{-1}) and A_{CO2} (µmol m^{-2} s^{-1}) are assimilation rates of COS and CO_2, respectively. These rates were normalized by outflowing concentrations $[COS]_{out}$ and $[CO_2]_{out}$, which are assumed to be the concentrations the plants are exposed to due to the well-mixed conditions (see Section 2.2.1).

Table 1. Environmental conditions during the three experiments. The range of controlled and constant variables for each experiment is expressed as minimum ~ maximum and mean ± standard deviation, respectively. Experiment 1 (Sunflower 1) aims to detect COS compensation points at two temperatures. Experiments 2 (Sunflower 2, 3, and 4) and 3 (Sunflower 2 and 4) are designed to investigate responses of V_{COS} and V_{CO2} to stomatal conductance (g_s) and leaf temperature (T_{leaf}), respectively, with T_{leaf} acting as a primary driver of mesophyll conductance (g_m). We controlled a designated variable in each experiment while other variables including light intensity, air flow rate, and mixing fan speed were kept constant.

Experiment (Control)	**Experiment 1 ($[COS]_{in}$)**		**Experiment 2 (g_{sw})**			**Experiment 3 (T_{leaf})**	
Sunflower number (-)	**1**	**1**	**2**	**3**	**4**	**2**	**3**
g_{sw} (mol $m^{-2}s^{-1}$)	0.8 ± 0.0	0.9 ±0.1	0.4 ~ 1.1	0.3 ~ 1.0	0.3 ~ 0.6	0.6 ± 0.1	0.6 ± 0.0
VPD (kPa)	0.5 ± 0.0	0.5 ± 0.0	0.6 ± 0.1	0.7 ± 0.2	0.9 ± 0.3	0.7 ± 0.2	0.9 ± 0.3
T_{leaf} (°C)	19.8 ± 0.0	25.0 ±0.3	25.1 ± 0.0	26.4 ± 0.1	24.8 ± 0.3	19.1 ~ 30.9	19.0 ~ 29.8
$[COS]_{in}$ (pmol $m^{-2}s^{-1}$)	94.11 ~ 589.05	104.50 ~ 706.96	1096.4 ± 12.6	1181.9 ± 11.1	914.4 ± 29.6	1087.7 ± 41.1	926.8 ± 14.0
$[CO_2]_{in}$ (µmol $m^{-2}s^{-1}$)	446.5 ± 0.1	449.1 ± 0.3	441.0 ± 0.4	446.2 ± 1.5	447.5 ± 1.7	439.9 ± 3.1	447.3 ± 1.4

Open Research Europe 2026, 5:223 Last updated: 12 MAY 2026

2.2 Conductance model

2.2.1 General concept. Since the observations were somewhat limited in exploring internal leaf processes, we developed a conductance model and applied an optimization method using 48 data points from Experiments 2 and 3. Experiment 1 (15 data points) was used to provide initial information of Γ_{COS} and its temperature dependence to the model (Section 3.2.2). This modeling framework was designed to mechanistically link experimental observations to internal gas-exchange processes.

Our leaf conductance model simulates the concurrent exchange of COS, CO_2, and H_2O in a plant leaf with the conditions of the laboratory experiments. Since these gases share the same stomatal pathway, their simultaneous modeling stomatal pathway, their simultaneous modeling helps us understand the mechanisms of leaf conductance. The model calculates mole fractions on a wet-air basis, while the measurements are reported on a dry-air basis. Accordingly, conversions between dry- and wet-air mole fractions were applied when comparing modeled and observed concentrations (see Section 2.1.1). Additionally, the model assumes that gas exchange reaches an equilibrium that we tried to attain in the conducted experiments. All model variables that remain constant in the model are listed in Table 2. Variables that are excluded from Table 2 are targets for optimization as explained in Section 2.3.

Figure 2a schematically illustrates the methodology for the gas exchange experiments. As described in Section 2.1.2, environmental conditions, including $[COS]_{in}$, T_{air}, and VPD, were manipulated to test the hypotheses while keeping other variables, such as light levels, constant. The cuvette received controlled mole fractions of the three gases via the airflow. Figure 2b depicts the exchange pathways of COS, CO_2, and H_2O within the sunflower leaf, which form the basis for the conductance model. We assumed that COS, CO_2, and H_2O production or consumption within the plant were governed by three conductances: boundary layer conductance (g_b (mol m^{-2} s^{-1})), stomatal conductance (g_s (mol m^{-2} s^{-1})), and mesophyll conductance (g_m (mol m^{-2} s^{-1})) limited by physical or biochemical processes

With a designated set of conductance values, the model simulates the mole fractions of the three gases in each layer: ambient air ($[gas]_a$), boundary layer ($[gas]_b$), and inter-cellular airspace ($[gas]_i$)), and mesophyll level ($[gas]_c$). The mole fractions of COS, CO_2, and H_2O are represented in units of pmol mol^{-1}, µmol mol^{-1}, and mmol mol^{-1}, respectively.

The following rate equations describe the gas exchanges tendencies, assuming they achieve a steady state:

$$\frac{d[gas]_a}{dt}\left(\frac{V_{cv}}{V_m S}\right) = -g_b([gas]_a - [gas]_b) + \frac{AF}{S}([gas]_{in} - [gas]_a) = 0, \quad (3)$$

Table 2. Model constants used in the model. Variables in all gases were used for all models, while those specific to COS, CO_2, and H_2O were applied to their respective model. The molar volume (V_m) is at standard temperature (298 K) and pressure (100 kPa).

Gas	Symbol	Description	Unit	Value	Q_{10}
All	S	Leaf area	cm^2	9.0	
	R	Universal molar gas constant	J K^{-1} mol^{-1}	8.314	
	V_m	Molar volume	m^3 mol^{-1}	0.0248	
	V_{cv}	Cuvette volume	cm^3	109[a]	
COS	$\Delta H_{a,CA}$	Activation energy of CA	kJ mol^{-1}	40[b]	
	$\Delta H_{eq,CA}$	Enthalpy change of CA	kJ mol^{-1}	100[b]	
CO_2	$\tau_{298\ K}$	Specificity factor between CO_2 and O_2 at 298 K	-	2600[c]	0.57
	$K_{c,\ 298\ K}$	Michaelis-Menten constant for carboxylation at 298 K	Pa	30[c]	2.1
	$K_{o,\ 298\ K}$	Michaelis-Menten constant for oxygenation at 298 K	Pa	30000[c]	1.2
	R_d	Dark respiration at 298 K	µmol m^{-2} s^{-1}	3.0[c]	2.0
	$p[O_2]_i$	Partial pressure of internal O_2	Pa	20900[c]	
H_2O	g_{mw}	Mesophyll conductance for H_2O	mol m^{-2} s^{-1}	10	

[a]LI-COR-6800 documents.
[b]Cho *et al.* (2023).
[c]Collatz *et al.* (1991).

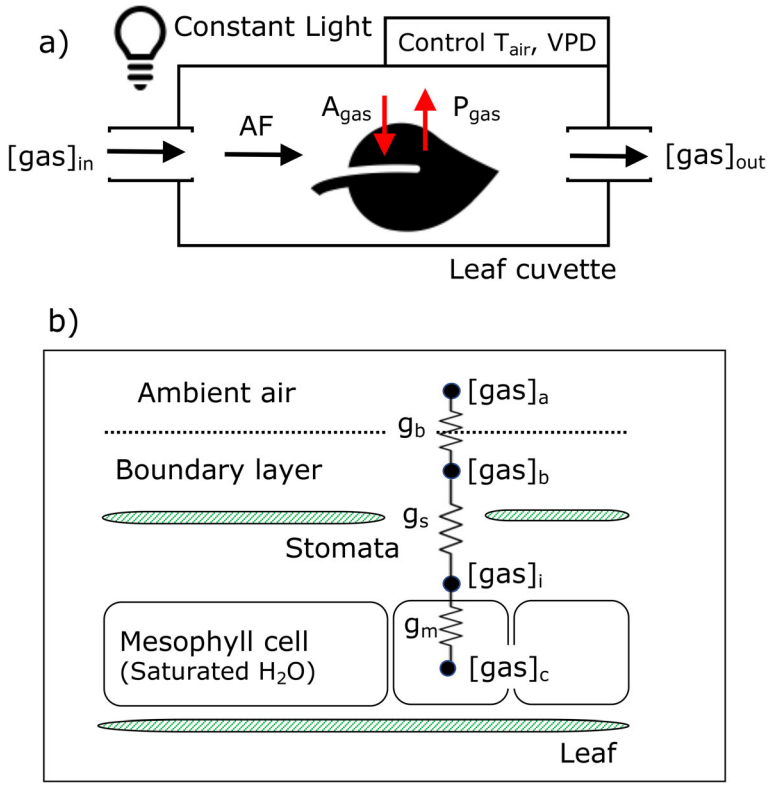

Figure 2. Schemes of leaf cuvette experiments (a) and diffusion pathways of COS, CO_2, and H_2O into and out of a leaf in the conductance model (b). A_{gas} and P_{gas} indicate the assimilation rate and production rate of each gas. g_b, g_s, and g_m represent boundary, stomatal, and mesophyll conductance, respectively.

$$\frac{d[gas]_b}{dt}\left(\frac{V_{cv}}{V_m S}\right) = g_b([gas]_a - [gas]_b) - g_S([gas]_b - [gas]_i) = 0, \quad (4)$$

$$\frac{d[gas]_i}{dt}\left(\frac{V_{cv}}{V_m S}\right) = g_S([gas]_b - [gas]_i) - g_m([gas]_i - [gas]_c) = 0. \quad (5)$$

Here, V_m (m^3 mol^{-1}) is the molar volume, and V_{cv} (m^3) is the effective air volume representing the gas-exchange region near the leaf surface. Under steady-state conditions, the first term on the left-hand side of Equation 3, Equation 4, and Equation 5, which represents the rate of gas accumulation, becomes negligible. To account for the different properties of COS and CO_2 to H_2O, the stomatal conductances ($g_{s,COS}$ and g_{s,CO_2}) and the boundary layer conductances ($g_{b,COS}$ and g_{b,CO_2}) are scaled proportionally to the conductance of water vapor (g_{sw} and g_{bw}) ($g_{s,CO_2} = g_{sw}/1.6$, $g_{b,CO_2} = g_{bw}/1.4$, $g_{s,COS} = g_{sw}/1.94$, $g_{b,COS} = g_{bw}/1.56$) (Bonan, 2008; Seibt *et al.*, 2010; Stimler *et al.*, 2010).

For the COS and CO_2 exchange at the stomatal level, a ternary system with H_2O and air should be considered, because the transpiration (F_{H_2O} (mol m^{-2} s^{-1})) is significantly larger than COS and CO_2 assimilation (Jarman, 1974; von Caemmerer & Farquhar, 1981). Thus, we added the ternary term in Equation 4 and Equation 5 for the COS and CO_2 models:

$$\frac{d[gas]_b}{dt}\left(\frac{V_{cv}}{V_m S}\right) = g_b([gas]_a - [gas]_b) - g_S([gas]_b - [gas]_i) + \frac{F_{H_2O}([gas]_b + [gas]_i)}{2} = 0, \quad (6)$$

$$\frac{d[gas]_i}{dt}\left(\frac{V_{cv}}{V_m S}\right) = g_s([gas]_b - [gas]_i) - \frac{F_{H_2O}([gas]_b + [gas]_i)}{2} - g_m([gas]_i - [gas]_c) = 0. \quad (7)$$

Although accounting for the H_2O ternary system is important, its influence on the calculated mole fractions was found to be negligible. The smaller ternary effects within the leaf boundary layer were therefore not included, as they scale with E/g_{bw} (von Caemmerer & Farquhar, 1981, Equation B10) and are expected to be negligible under our experimental conditions (large g_{bw} and small E). Note that the mole fractions calculated by the model are expressed on a wet-air basis, whereas the observed mole fractions are reported on a dry-air basis. The moisture correction applied to model outputs is described at the end of this section.

To test Hypothesis 2, we analyzed how the intercellular mole fraction $[gas]_i$ influences the net flux. The flux was computedusing Equation 3, Equation 6, and Equation 7 to determine $[gas]_i$, and then applied to the flux-gradient relationship:

$$F_{gas} = g_{b\sim s}([gas]_a - [gas]_i). \tag{8}$$

Here, $g_{b\sim s}$ denotes the conductance from the leaf boundary layer to the stomata. The deposition velocity (V_{gas} (mol m^{-2} s^{-1})) can be calculated as follows:

$$V_{gas} = g_{b\sim s}\left(1 - \frac{[gas]_i}{[gas]_a}\right). \tag{9}$$

The term (1-$[gas]_i$ $[gas]_a^{-1}$) represents the effect of changes between internal and ambient mole fractions on the gas conductance and deposition velocity, termed Ambient Fraction Remaining (AFR). This concept is utilized in Section 3.2.3 for interpreting Hypothesis 2. Strictly speaking, the mass flow difference between the inlet and outlet and the ternary effect should be considered in Equation 8 and Equation 9. However, these effects are expected to be minor under our experimental conditions (see above), and Equation 8 and Equation 9 were used only to examine the conceptual relationship between $[gas]_i$ and flux. Therefore, for simplicity, these correction terms were omitted. Note that this omission does not affect the interpretation of AFR in Section 3.2.3.

This set of coupled rate equations can be solved analytically, resulting in mole fractions of the three gases in each layer. Conductance at the mesophyll level (g_m) and $[gas]_c$ were calculated using a different model for each gas. Descriptions of the individual biophysical processes at the mesophyll level for each gas are provided in subsequent sections.

From experiments, we measured $[gas]_{out}$, while the leaf conductance model calculates $[gas]_a$. Because the chamber air was well mixed, the modeled $[gas]_{out,est}$ is considered equivalent to $[gas]_a$ for model-observation comparison. Thus, $[gas]_{out,est}$ is used for $[gas]_a$ to interpret experimental data.

In the model, the estimated mole fractions for COS and CO_2 are based on wet air, whereas the QCLS measures dry-air mole fractions. Therefore, to compare model results with observations, the modeled wet-air mole fractions were converted to their dry-air equivalents using the observed outgoing H_2O mole fractions ($[H_2O]_{out,obs}$ (mmol mol^{-1})):

$$[gas]_{out,est} = [gas]_a\left(1 - \frac{[H_2O]_{out,obs}}{1000}\right)^{-1}. \tag{10}$$

For $[COS]_{in,obs}$, which was measured after moisture removal, the same correction (Equation 10) was applied using $[H_2O]_{in,obs}$ instead of $[H_2O]_{out,obs}$ to convert from the dry-air to the wet-air basis before use in the conductance model.

Finally, net fluxes of the three gases were calculated using the same methodology as employed for the observations (Equation 1).

2.2.2 Water vapor model. In our experiments, we observed water evaporation from leaves. We aimed to model this evaporation at the mesophyll level and its subsequent transport out of the leaves, governed by g_{sw}. The unit of H_2O mole fractions in all layers is mmol mol^{-1}, and the unit of the flux is mmol m^{-2} s^{-1}.

To represent the internal water vapor conditions, $[H_2O]_c$ was calculated assuming that water vapor within the mesophyll intercellular airspace is saturated. However, we allowed for relative humidity within the intercellular airspace (RH_i (%)) to be less than 100%, based on previous studies (Cernusak *et al.*, 2018; Wong *et al.*, 2022). To achieve this, we introduced a mesophyll conductance for water vapor (g_{mw}) and set it to an arbitrary value of 10 mol m^{-2} s^{-1}, approximately ten times the largest observed value of g_{sw}. This parameter was included to test the sensitivity of the model to possible non-saturation within the intercellular airspace.

The expression for $[H_2O]_c$ relies on T_{leaf} (°C) and air pressure (P_{air} (Pa)):

$$[H_2O]_c = 1000\frac{P_{H_2O}}{P_{air}}, \text{ with} \tag{11}$$

$$P_{H_2O} = 613.5\exp\left(\frac{17.502\,T_{leaf}}{T_{leaf} + 240.97}\right). \tag{12}$$

Using these assumptions, we calculated the water vapor mole fractions in the atmosphere ($[H_2O]_a$), boundary layer ($[H_2O]_b$), and interior ($[H_2O]_i$) by solving Equation 3, Equation 4, and Equation 5. Finally, we estimated the RH_i (%) from the calculated $[H_2O]_c$ and $[H_2O]_i$:

$$RH_i = 100\,\frac{[H_2O]_i}{[H_2O]_c}. \tag{13}$$

2.2.3 CO_2 model. We aimed to simulate the gross CO_2 flux (F_{CO_2}, μmol m^{-2} s^{-1}) and mole fractions of CO_2 in each layer (μmol mol^{-1}) using the model proposed by Farquhar *et al.* (1980). In this model, the gross CO_2 uptake rate is calculated as the minimum value among assimilation limited by enzymes (A_m), light (A_E), and sucrose synthesis (A_S), minus the dark respiration (R_d) :

$$F_{CO2} \approx \min(A_m, A_E, A_S) - R_d. \tag{14}$$

Our experiments were conducted under a constant light intensity (PAR = 600 μmol m^{-2} s^{-1}). We assumed that the A_E and A_S pathways were saturated, as light saturation points previously were obtained above 500 μmol m^{-2} s^{-1} (Lobo *et al.*, 2013). Consequently, we calculated g_{m,CO_2} ($[CO_2]_i - [CO_2]_c$) in Equation 7 with $A_m - R_d$. R_d was estimated by Collatz *et al.* (1991).

A_m is calculated by multiplying the maximum rate of RuBisCO carboxylation ($V_{max,Rub}$) with the partial pressure changes from RuBP partitioning between the CO_2 carboxylation and O_2 oxygenation reactions:

$$A_m = \frac{V_{max,Rub} f_{rub}(T_{leaf})(p[CO_2]_i - \Gamma^*_{CO_2})}{p[CO_2]_i + K_C\left(1 + \frac{p[O_2]_i}{K_o}\right)}, \tag{15}$$

where p $[CO_2]_i$ (Pa) and p $[O_2]_i$ (Pa) are the partial pressures of CO_2 and O_2 in the inter-cellular air space. K_c (Pa) and K_o (Pa) are Michaelis-Menten constants for CO_2 and O_2, respectively. $\Gamma^*_{CO_2}$ (Pa) stands for the CO_2 compensation point independent of dark respiration.

Strictly speaking, RuBisCO carboxylation occurs within the chloroplast stroma and should depend on the chloroplast CO_2 partial pressure (p $[CO_2]_c$), rather than p $[CO_2]_i$. However, our model does not explicitly include mesophyll conductance (g_{m,CO_2}), and thus p $[CO_2]_c$ cannot be directly resolved. Accordingly, $p[CO_2]_i$ was used as a proxy for $p[CO_2]_c$, following the classical formulation of Farquhar *et al.* (1980).

The estimation of Γ^*_{CO2} is based on the partial pressure of oxygen linked to the side reaction of RuBisCO:

$$R_2 = R_1 Q_{10}^{\frac{(T_2 - T_1)}{10}}. \tag{16}$$

Here, T_2 corresponds to T_{leaf}, and T_1 is 25°C for the CO_2 parameters K_c, K_o, and $\Gamma^*_{CO_2}$. The temperature function of $V_{max,Rub}$ (μmol m^{-2} s^{-1}) at T_{leaf} (°C) is calculated by (Badger & Collatz, 1977):

$$f_{Rub}(T_{leaf}) = \exp\left(\frac{((T_{leaf} + 273.15) - T_{ref,Rub})\Delta H_{a,Rub}}{T_{ref,Rub} R (T_{leaf} + 273.15)}\right), \tag{17}$$

where $\Delta H_{a,Rub}$ (J mol^{-1}) is the activation energy of RuBisCO, valued at 60.0 kJ mol^{-1} (von Caemmerer & Evans, 2015), and $T_{ref,Rub}$ (K) is the reference temperature (298 K). R is the universal molar gas constant (8.314 J K^{-1} mol^{-1}).

2.2.4 COS model. We constructed the COS model to estimate the gross COS flux rate (F_{COS}, pmol m^{-2} s^{-1}) and mole fractions of COS in each layer (pmol mol^{-1}). Accurate modeling of COS leaf uptake requires representing mesophyll conductance, which integrates both the diffusional transport of COS and biochemical conversion by CA.

Earlier approaches treated mesophyll diffusion and CA activity as linearly proportional to Rubisco's V_{max} (Berry *et al.*, 2013). However, this simplification was shown to bias COS flux estimates, leading to the introduction of a revised CA-based temperature formulation (Cho *et al.*, 2023). More recently, Lai *et al.* (2024) emphasized the importance of explicitly accounting for mesophyll diffusion in COS uptake models but also noted the lack of reliable parameterization for COS-specific mesophyll diffusion.

Building on these previous findings, we modeled biochemical conductance of COS in the mesophyll ($g_{m,COS}$ (mol m^{-2} s^{-1})) using the CA activity–based function proposed by Cho *et al.* (2023), which implicitly represents mesophyll diffusion while minimizing estimation bias through its revised temperature dependence. This function describes the temperature dependence of CA activity using a specified Arrhenius equation and Michaelis-Menten Kinetics (Cho *et al.*, 2023; Daniel *et al.*, 2010; Ogée *et al.*, 2016; Sun *et al.*, 2015):

$$g_{m,COS} = V_{max,CA} f_{CA}(T_{leaf}) = V_{max,CA} A_T \frac{(T_{leaf} + 273.15) \exp\left[-\frac{\Delta H_{a,CA}}{R(T_{leaf}+273.15)}\right]}{1 + \exp\left[-\frac{\Delta H_{eq,CA}}{R}\left(\frac{1}{T_{leaf}} - \frac{1}{T_{eq,CA}+273.15}\right)\right]}. \quad (18)$$

Here, $V_{max,CA}$ (mol m^{-2} s^{-1}) is the maximum catalyzation velocity of CA, $\Delta H_{a,CA}$ (J mol^{-1}) represents the activation free energy of CA and $\Delta H_{eq,CA}$ (J mol^{-1}) is the enthalpy change when the enzyme transits from activation to inactivation. $T_{eq,CA}$ (°C) stands for the optimum temperature at which the concentrations of activated and inactivated enzymes are equal (Daniel *et al.*, 2010; Ogée *et al.*, 2016; Sun *et al.*, 2015). We adopted the normalization factor A_T as the value of f_{CA} $(T_{eq,CA})^{-1}$.

To incorporate temperature-dependent compensation point behavior, applied the Γ_{COS} into $[COS]_c$. We proposed four temperature functions of Γ_{COS} based on Experiment 1 data. For model S1, Γ_{COS} was set to zero across all temperatures, assuming no compensation point effects. For model S2, Γ_{COS} was represented as a linear function:

$$\Gamma_{COS}(T_{leaf}) = f_{\Gamma COS}(T_{leaf}) = m_{COS}(T_{leaf} - T_{ref}). \quad (19)$$

where T_{ref} (°C) is the intercept temperature (16.4°C), determined from the linear regression of two Γ_{COS} values detected in Experiment 1 (Section 3.1.1). The slope m_{COS} (pmol mol^{-1} K^{-1}) was set to 16.2 pmol mol^{-1} K^{-1}, also derived from Experiment 1. At low temperatures, where Γ_{COS} becomes negative, we assumed Γ_{COS} = 0.

For model S3, Γ_{COS} was calculated using the Arrhenius function with a observation-based value of 55.0 pmol mol^{-1} at 293 K from Experiment 1:

$$\Gamma_{COS}(T_{leaf}) = 55.0 \exp\left(\frac{((T_{leaf} + 273.15) - 293)\Delta H_{a,\Gamma}}{293 R (T_{leaf} + 273.15)}\right), \quad (20)$$

and for model S4, Γ_{COS} was similarly computed using a reference value of 138.7 pmol mol^{-1} at 298 K:

$$\Gamma_{COS}(T_{leaf}) = 138.7 \exp\left(\frac{((T_{leaf} + 273.15) - 298)\Delta H_{a,\Gamma}}{298 R (T_{leaf} + 273.15)}\right), \quad (21)$$

where $\Delta H_{a,\Gamma}$ (kJ mol^{-1}) represents the activation energy for Γ_{COS}. By solving for $\Delta H_{a,\Gamma}$ using the two derived Γ_{COS} values, we determined an initial activation energy of 134.3 kJ mol^{-1}.

Figure 3 shows these four Γ_{COS} functions (S1–S4) representing the prior temperature-dependent parameterizations tested in the modeling framework with their imposed uncertainties. The figure also shows the experimental Γ_{COS} estimates from Experiment 1, included solely for reference to illustrate the initial parameter alignment.

2.3 Indirectly derived COS compensation point

Because the temperature-dependent behavior of Γ_{COS} in Experiment 1 was derived from a limited set of measurements under a few temperature levels, additional validation was required to test whether the modeled Γ_{COS} functions are consistent across broader environmental conditions. To support this validation, we incorporated the indirectly derived Γ_{COS} from 48 data points in Experiments 2 and 3. By calculating $[COS]_c$ using our optimized model parameters in Equation 3, Equation 6, and Equation 7, we were able to indirectly estimate Γ_{COS} and compare it with the modeled Γ_{COS}.

First, we calculated $[COS]_b$ from the measured COS mole fractions with the rearranged Equation 3:

$$[COS]_b = [COS]_a + \frac{AF}{S g_{b,COS}}([COS]_a - [COS]_{in}), \quad (22)$$

where $[COS]_{in}$ and $[COS]_a$, along with AF, S, and $g_{b,COS}$, were applied from Experiments 2 and 3. Due to thorough mixing within the cuvette, we assumed $[COS]_{out}$ to be equivalent to $[COS]_a$ and used it accordingly (refer to Section 2.2). Although transpiration slightly increases the outlet air flow, this effect (<3%) was neglected to retain easy analytical

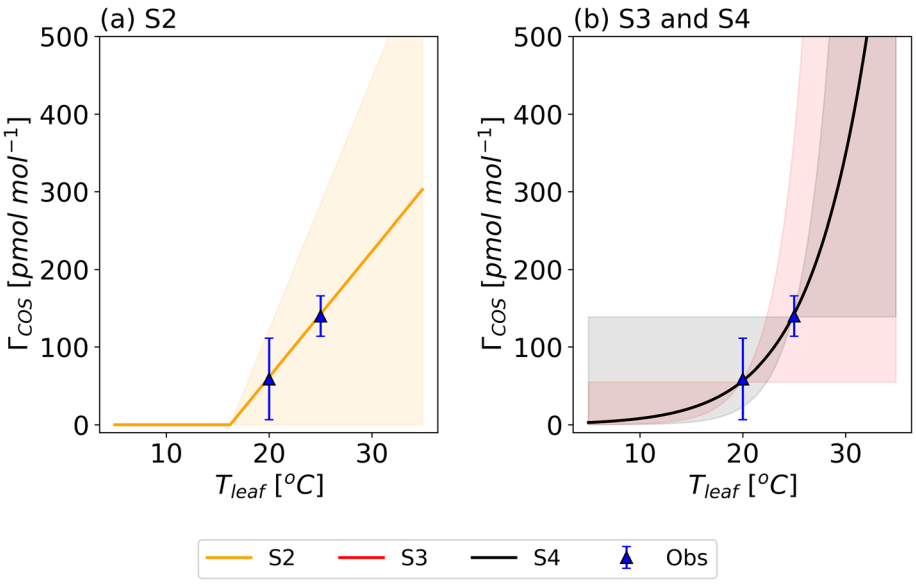

Figure 3. Prior temperature functions of the COS compensation point (Γ_{COS}) (lines) with their error ranges (shaded area). Blue triangles show the regression-derived Γ_{COS} from Experiment 1, included for reference to illustrate the initial parameter setup. The S1 model assumed Γ_{COS} = 0 pmol mol^{-1}. Model S2 describes Γ_{COS} as a linear relationship with T_{leaf} (a), while models S3 and S4 use an Arrhenius equation (b).

expressions, consistent with the assumptions described in Equation 1. This formulation follows the same assumptions as in Equation 3 regarding ternary effects at the boundary layer, which were found to be negligible under our experimental conditions. Here, $[COS]_{in}$ and $[COS]_{out}$ were converted from a dry air basis to a wet air basis. We then used the derived $[COS]_b$ to calculate $[COS]_i$ using the rearranged Equation 6:

$$[COS]_i = (-g_{b,COS}[COS]_a + g_{b,COS}[COS]_b + g_{s,COS}[COS]_b - 0.5F_{H2O}[COS]_b)(g_{s,COS} + 0.5F_{H_2O})^{-1}. \quad (23)$$

F_{H_2O} was calculated using Equation 1 with the observed $[H_2O]_{in}$ and the modeled $[H_2O]_a$ obtained by the H_2O model. We used optimized g_{sw} value in the the H_2O model and $g_{s,COS}$. The reason for using the model-calculated $[H_2O]_a$ instead of the observed $[H_2O]_{out}$ is to consider the optimized g_{sw} in F_{H_2O}.

Finally, $[COS]_i$ is used in Equation 7 to derive $[COS]_c$:

$$[COS]_c = -\frac{g_{s,COS}}{g_{m,COS}}([COS]_b - [COS]_i) + \frac{F_{H2O}}{g_{m,COS}}([COS]_b + [COS]_i) + [COS]_i, \quad (24)$$

where $g_{m,COS}$ was determined using Equation 18 with optimized parameters $V_{max,CA}$ and $T_{eq,CA}$. These indirectly calculated Γ_{COS} values vary depending on the chosen temperature-dependent functions of Γ_{COS}, which influence other parameters. Consequently, the indirectly derived Γ_{COS} values differ from Γ_{COS} functions due to their impact on the optimized parameters used in the calculations.

2.4 Parameter optimization

2.4.1 Optimization setting. Beginning with the model state parameter (x), we calculated $[gas]_{out,est}$ and compared these to the observed values $[gas]_{out,obs}$ on a dry-air basis. We aimed to minimize the differences between our model and the observations during each optimization step. To accomplish this, we defined a cost function (J_{tot}) consisting of a background term (J_{bg}) and three observational terms that account for the differences between model estimations and observations of COS (J_{COS}), CO_2 (J_{CO_2}), and H_2O (J_{H_2O}):

$$J_{tot} = J_{bg} + J_{COS} + J_{CO_2} + J_{H_2O} = \frac{(x - x_a)^2}{W_{bg}\sigma^2} + \frac{([COS]_{out,est} - [COS]_{out,obs})^2}{W_{COS}(\sigma_{COS})^2} + \frac{([CO_2]_{out,est} - [CO_2]_{out,obs})^2}{W_{CO_2}(\sigma_{CO_2})^2} + \frac{([H_2O]_{out,est} - [H_2O]_{out,obs})^2}{W_{H_2O}(\sigma_{H_2O})^2}. \quad (25)$$

The first term of the cost function penalizes deviations of the state x from the prior state vector x_a. This penalty depends on σ, which represents the prior error in the state vector. This background term is introduced to keep state variables within reasonable boundaries (Brasseur & Jacob, 2017). The last three terms of the cost function calculate the costs associated with deviations between modeled ($[gas]_{out,est}$) and observed mole fractions ($[gas]_{out,obs}$) for for COS, CO_2, and H_2O, respectively. Each term is normalized by its observational uncertainty to ensure consistent treatment of measurement errors, and each is scaled by optimization weights (W_{bg}, W_{COS}, W_{CO_2}, and W_{H_2O}) to balance the relative influence of each gas. These weights do not modify the observational errors but instead prevent any single gas—particularly CO_2—from dominating the total cost. The determination of these weights is described in the following section.

The costs related to observations (J_{COS}, J_{CO_2}, and J_{H_2O}) are influenced by observational errors (σ_{COS}, σ_{CO_2}, and σ_{H_2O}), derived from the measured COS, CO_2, and H_2O mole fractions. These observational errors were determined as the standard deviation of the measured mole fractions at outflow within the data point interval (150-second). Formally, σ_{COS}, σ_{CO_2}, and σ_{H_2O} should also reflect model errors caused by model parameters not included in the state or by processes that were not modeled (Brasseur & Jacob, 2017). Note that we excluded data from Experiment 1 to validate the optimized temperature function of Γ_{COS} in Section 3.2.2.

Due to the larger relative error in $[H_2O]_{out,obs}$ and $[COS]_{out,obs}$ than in $[CO_2]_{out,obs}$, the optimization procedure tended to focus on minimizing preliminary J_{CO_2}. To better utilize the non-CO_2 observations, we introduced optimization weights for each cost component. The observed $[CO_2]_{out,obs}$ values ranged from 379.4 to 390.0 μmol mol^{-1}, with an average observational error of only 0.2 μmol mol^{-1} (0.05%). $[COS]_{out,obs}$ values ranged from 748.2 to 1032.4 pmol mol^{-1}, with an average error of 16.7 pmol mol^{-1} (1.91%). $[H_2O]_{out,obs}$ values ranged from 15.2 to 32.5 mmol mol^{-1} with a mean error of 0.3 mmol mol^{-1} (1.14%).

The targeted state parameters, along with their initial values and errors, are listed in Table 3. We assumed that the parameters related to the temperature response of mesophyll cells are consistent across all experiments, as all sunflowers were cultivated in a similar climate. We constructed state vectors with variables that significantly impact the total cost and better quantify the combined leaf exchanges: $V_{max,CA}$, $T_{eq,CA}$, and m_{COS} for COS, $V_{max,Rub}$ and $\Delta H_{a,Rub}$ for CO_2, and g_{sw} for all gases.

Although we selected sunflower leaves at similar development stages, variations in biochemical functioning existed among individual leaves. Therefore, we optimized $V_{max,CA}$ and $V_{max,Rub}$ for each individual plant, as these largely

Table 3. State parameters (x) and their prior and posterior values with their errors based on model S2. Posterior errors are calculated from 200 optimizations in a Monte Carlo method (Section 2.5). The last column denotes the error reduction. Prior and Posterior values for g_{sw} are averaged values across the dataset from Experiments 2 and 3. Values in "Bounds" column with brackets indicate lower and higher bounds provided to the optimization.

Parameter	Description	Unit	Bounds	Prior ± Error	Posterior ± Error	(b-a)/a[1] (%)
$V_{max,CA}$	Maximum velocity for CA	mol m^{-2} s^{-1}	[0.01, 0.50]	0.125 ± 0.060	0.217 ± 0.037[2]	38
					0.189 ± 0.029[3]	52
					0.230 ± 0.042[4]	30
$T_{eq,CA}$	Optimum temperature for CA	°C	[1, 60]	30.0 ± 15.0	39.7 ± 5.0	66
m_{COS}	Slope of Γ_{COS}	pmol mol^{-1} K^{-1}	[1, 300]	16.2 ± 16.2	22.4 ± 5.3	67
$V_{max,Rub}$	Maximum velocity for RuBisCO	μmol m^{-2} s^{-1}	[1, 200]	90.0 ± 20.0	94.4 ± 0.3[2]	98
					87.4 ± 0.5[3]	98
					82.9 ± 0.3[4]	98
$\Delta H_{a,Rub}$	Activation energy for RuBisCO	kJ mol^{-1}	[1, 100]	60.0 ± 12.0	54.5 ± 0.9	92
g_{sw}	Stomatal conductance of H_2O	mol m^{-2} s^{-1}	[0, 3]	0.62 ± 0.09	0.64 ± 0.05	43

[1] 'a' is a prior error and 'b' is a posterior error. They are used to calculate the error reduction.
[2–4]The values are obtained for Sunflower 2, 3, and 4, respectively.

determine mesophyll conductance (Cho *et al.*, 2023; Le Roux *et al.*, 2001; Williams & Flanagan, 1996). The initial $V_{max,CA}$ was based on the averaged $V_{max,CA}$ across different phenological stages from two observation sites, Hyytiälä (Finland) and Harvard Forest (United States), as introduced by Cho *et al.* (2023). The standard deviation of $V_{max,CA}$ was used as the state error. For $V_{max,Rub}$, we set the initial value as $V_{max,CA}$ divided into the scaling factor 1400, derived from laboratory measurements of gas exchange in C_3 plants (Berry *et al.*, 2013; Stimler *et al.*, 2010; Stimler *et al.*, 2011).

$T_{eq,CA}$ is more crucial in determining CA's temperature function compared to other kinetic variables (Cho *et al.*, 2023). We adopted the initial value and state error of $T_{eq,CA}$ directly from Cho *et al.* (2023), ensuring consistency with previous characterizations of CA kinetics.

To further evaluate the temperature dependence of Γ_{COS} , four temperature functions (S1 to S4) were tested within the conductance model. Each function was optimized and compared against observation-based Γ_{COS}. The S1 model excludes Γ_{COS}, while S2 applies a linear function with m_{COS} of 16.2 pmol mol^{-1}. Both S3 and S4 use a temperature dependence described by an Arrhenius relationship. All models were initialized with the same prior error for Γ_{COS}, including the zero-compensation point, as shown in Figure 3.

For the CO_2 parameters, we optimized $\Delta H_{a,Rub}$, as it is an unknown parameter for Sunflowers. We determine the initial value and error of $\Delta H_{a,Rub}$ using the mean and standard deviation across nine species reported by von Caemmerer and Evans (2015). Other temperature-dependent parameters were adopted from Collatz *et al.* (1991).

The LI-6800 derives g_{sw} from water vapor exchange with its own uncertainties. Because g_{sw} similarly affects the exchange of H_2O, CO_2, and COS through the same shared stomatal pathway, we optimize g_{sw} in a coupled framework using flux information from all three gases to ensure internal consistency across species. The novelty of this framework lies in explicitly coupling these fluxes to derive a more physically consistent constraint on g_{sw}, while also addressing potential uncertainties in g_{sw} derived from LI-6800 measurements (e.g., stomatal ratio parameter K; Section 2.1.1).

Initial values for g_{sw} were taken from the LI-6800 measurements during Experiments 2 and 3. We applied a random error of 0.08 mol m^{-2} s^{-1}, representing the standard deviation of g_{sw} from Experiment 3, despite efforts to maintain a constant g_{sw} ($\pm$ 0.06 mol m^{-2} s^{-1}). In addition, we considered an extra measurement uncertainty of 0.02 mol m^{-2} s^{-1}, based on known sources of instrumental bias—such as the leaf temperature underestimation (Garen *et al.*, 2022) and background total leaf conductance to water observed in empty chambers (Hussain *et al.*, 2024). We also added individual $[H_2O]_{out,obs}$ errors by normalizing $[H_2O]_{\ out,obs}$. The averaged initial g_{sw} value and its standard deviation (prior error) are 0.61 mol m^{-2} s^{-1} and 0.09 mol m^{-2} s^{-1}, respectively.

Assuming a Gaussian probability density function for the state parameters could lead to nonphysical values in the optimization process. Thus, we minimized J_{tot} using the Sequential Least SQuares Programming optimizer (SLSQP) from the SciPy Python library. This optimizer enables the specification of lower and upper bounds on the state space and is well-suited for solving nonlinear problems. The parameter bounds are listed in Table 3.

2.4.2 Weight determination. We selected weights to achieve more balanced prior costs across four components in Equation 25. The prior chi-squared value (χ^2_{prior}) was used to check the cost balance in prior condition. We set seven possible weights, and the corresponding χ^2_{prior} value ranged from 3 to 200, as listed in Table 4. Then, we optimized parameters and calculated cost reduction rates for each part of the cost function. For H_2O, we found a χ^2_{prior} value of about 3, indicating that the H_2O model already performs well with the prior parameter settings.

Table 4. Candidates for weights in the observational terms (W_{COS}, W_{CO_2}, W_{H_2O}) based on the chosen χ^2_{prior} values.

χ^2_{prior}	W_{COS}	W_{CO_2}	W_{H_2O}
3	0.337	238.8	3.24
10	0.101	71.6	0.97
30	0.034	23.9	0.32
50	0.020	14.3	0.19
100	0.010	7.2	0.10
150	0.007	4.8	0.06
200	0.005	3.6	0.05

We finally selected the weight combination that minimized the averaged reduction rates of J_{COS} and $J_{CO\ 2}$ and ensured that each χ^2_{poste} exceeded the value of 0.6 to avoid over-fitting, including J_{bg}. The selected weights ($W_{COS} = 0.034$, $W_{CO_2} = 7.2$, $W_{H_2O} = 3.24$, $W_{bg} = 1.0$), correspond to χ^2_{prior} values of 30, 100, and 3 for COS, CO_2, and H_2O, respectively. These weights lead to a more balanced ratio of χ^2_{prior} across the observational parts (COS: CO_2: H_2O = 10: 33: 1), compared to the ratio without weights (1: 329: 4). Note that the prior value of J_{bg} is zero by design.

2.5 Error statistics

We evaluated the model performance using χ^2 values, mean bias errors (MBEs), and root mean square errors (RMSEs). The χ^2 metric was calculated by dividing the partial cost function by the number of observations or state variables (Tarantola, 2005). A posterior chi-squared value (χ^2_{poste}) of 1 indicates a good fit, as the model predictions fall within the error distribution fall within the error distribution of the observations. A χ^2_{poste} significantly greater than 1 indicates a poor fit, while a value smaller than 1 suggests potential overfitting. MBE indicates bias, with a positive value for over-estimation and a negative value for underestimation. RMSE is the quadratic mean of the differences between estimation and observation, with a value of 0 indicating a perfect fit.

Note that the optimization process targets for χ^2_{poste} to reach 1.0, but we also give the improvement in MBEs and RMSEs for completeness. To assess the posterior error associated with the optimized state, we employed a Monte Carlo method. In this process, we optimized the parameters using 200 distinct ensemble members, introducing random noise within the bounds of the respective state and observational errors (Bosman & Krol, 2023; Chevallier *et al.*, 2007; Cho *et al.*, 2023).

Furthermore, we conducted 500 perturbed forward simulations to assess the spread in both prior and posterior models. Parameters were randomly sampled from Gaussian distributions of both the prior and posterior. Prior uncertainties were assumed uncorrelated, while for the posterior parameters, we used the correlations that were determined using the Monte Carlo optimization. We quantified the posterior covariance matrix and considered the cross-parameter correlations when sampling the parameters to evaluate the posterior model. Parameters more than three standard deviations from the mean were discarded. These simulations were conducted with designated environmental input variables: pressure = 103,100 Pa, air flow rate (AF) = 0.00035 mol s^{-1}, $[CO_2]_{in}$ = 400 μmol mol^{-1}, $[COS]_{in}$ = 1000 pmol mol^{-1}, $[H_2O]_{in}$ = 15 mmol mol^{-1}, g_{bw} = 2.44 mol m^{-2} s^{-1}, g_{sw} = 0.6 mol m^{-2} s^{-1}, and T_{leaf} = 25°C. We only varied one variable at the time, to evaluate its impact on the simulation.

3. Results

3.1 Experiments

3.1.1 COS Compensation Point (Experiment 1). Figure 4 presents the results from Experiment 1 with Sunflower 1, aimed at determining Γ_{COS} by measuring F_{COS} while controlling $[COS]_{out}$ and maintaining constant g_{sw} and T_{leaf}. Minor fluctuations in g_{sw} occurred during temperature adjustments, increasing from 0.76 to 0.90 mol m^{-2} s^{-1} higher temperatures. F_{COS} shows a linear increase with increasing $[COS]_{out}$, in agreement with findings from earlier studies (Gimeno *et al.*, 2017; Kesselmeier & Merk, 1993; Stimler *et al.*, 2010).

We quantified the regression-based Γ_{COS} using a linear function at two temperatures: Γ_{COS} was 55.0 ± 53.2 pmol mol^{-1} at 19.8°C and 138.7 ± 26.1 pmol mol^{-1} at 25.0°C (error estimates denote 95% confidence interval). These results indicate that Γ_{COS} increases with rising T_{leaf}, suggesting a potential temperature dependence.

Although the empty-chamber regression effectively removed the baseline COS emission, some residual variability likely remained (RMSE = 6.9 pmol mol^{-1} for $[COS]_a$ and 2.73 pmol m^{-2} s^{-1} for F_{COS}). To evaluate the potential influence of this unresolved background variability, we propagated these errors to the regression-derived Γ_{COS}. When the uncertainty is included, the 95% confidence interval of Γ_{COS} widened from ± 53.2 to ± 93.4 pmol mol^{-1} at 19.8°C and from ± 26.1 to ± 48.9 pmol mol^{-1} at 25.0°C.

The large uncertainty at 19.8°C indicates that the corresponding Γ_{COS} value is statistically indistinguishable from zero. By contrast, the Γ_{COS} measured at 25°C remains significant even when this is propagated and instrumental uncertainty is considered. Even accounting for the reported QCLS uncertainty of approximately 7.5 pmol mol^{-1} for COS (Kooijmans *et al.*, 2016), the Γ_{COS} value at 25°C remains statistically robust.

3.1.2 Responses to Stomatal Conductance (Experiment 2). Figure 5 illustrates the observed relationships of V_{COS}, V_{CO_2}, and LRU with optimized g_{sw} for three sunflower plants. The observed values show that both V_{COS} and V_{CO_2} decrease with declining g_{sw}, albeit at a slower rate at higher g_{sw} values. Specifically, as g_{sw} decreases from 1.0 mol m^{-2} s^{-1} to 0.4 mol m^{-2} s^{-1}, V_{COS} declines by approximately 40%, compared to a decline of about 10% in V_{CO_2}. This difference persists even after accounting for the g_{sw} ratio between COS and CO_2 (1.21).

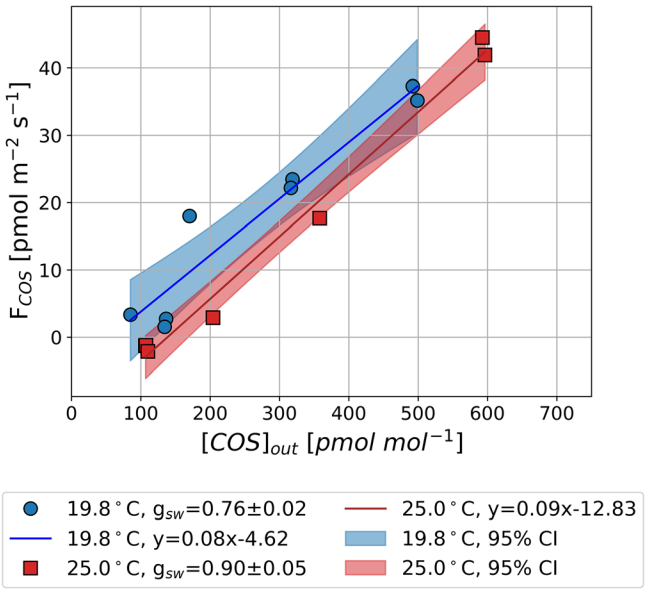

Figure 4. Observed mean COS net flux (F_{COS}) along an outflowing COS mole fraction ($[COS]_{out}$) in the light at 25.0°C (rectangle and red areas) and 19.8°C (circle and blue areas) in Experiment 1. Lines and shaded areas represent linear fits with 95% confidence intervals. Positive values in F_{COS} (y axis) indicate COS uptake, and negative values indicate COS emissions.

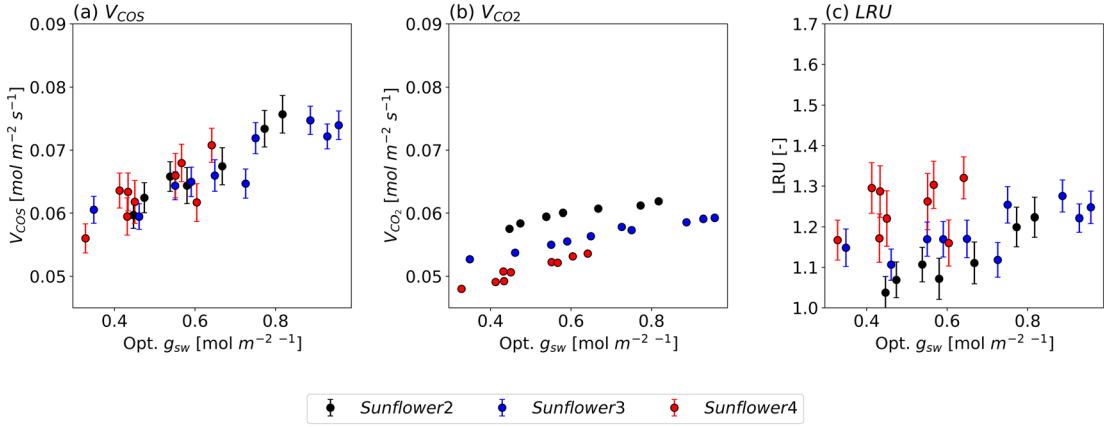

Figure 5. COS (a) and CO_2 (b) deposition velocities and LRU changes (c) along the optimized g_{sw} under leaf temperatures of approximately 25°C for three different sunflower plants, each represented in a different color. The circles and error bars represent the median values and standard deviations of the data points for their respective 150-second intervals.

The greater sensitivity of V_{COS} to changes in g_{sw} is also reflected in the LRU, which consistently increases with g_{sw} across all sunflowers. These findings support the hypothesis that COS uptake is more sensitive to variations in g_{sw} compared to CO_2 uptake. Meanwhile, slight differences in V_{COS} and V_{CO_2} values among individual sunflowers result in variations in LRU as well.

3.1.3 Responses to Leaf Temperature (Experiment 3). Figure 6 shows the observed V_{COS} and V_{CO_2}, and LRU against T_{leaf} for two sunflowers, with g_{sw} held approximately constant. For all sunflowers, V_{COS} decreases when temperatures exceed 25°C, whereas V_{CO2} increases with T_{leaf} up to approximately 30°C. The absolute rate of decrease in V_{COS} is larger than the rate of increase in V_{CO_2}. Consequently, LRU decreases as T_{leaf} increases. This trend can be attributed to the temperature responses of Γ_{COS} or/and the lower optimum temperature for CA than RuBisCO.

The temperature-dependent variations in V_{COS} and V_{CO2} also differ slightly between individual sunflower plants. While V_{COS} exhibited relatively large observational errors, V_{CO2} showed minimal errors. This suggests that while experimental

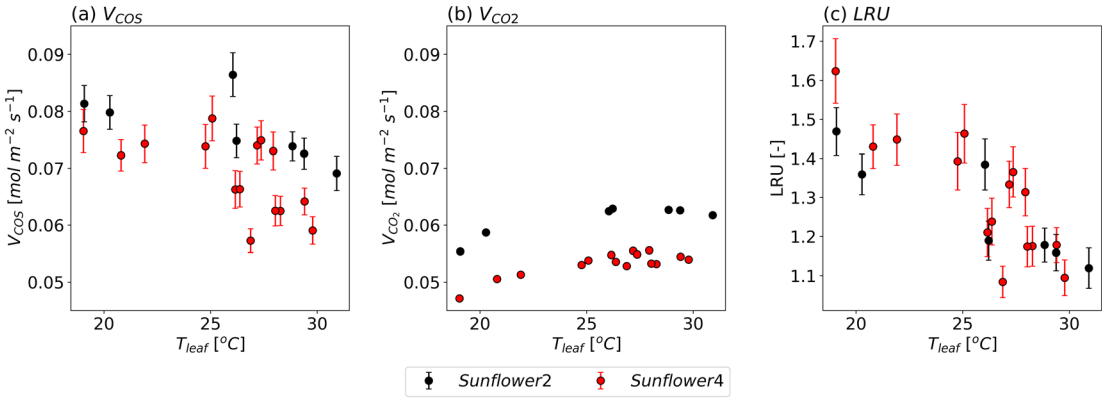

Figure 6. Same as Figure 5, but as a function of T_{leaf} with maintained stomatal conductance at 0.6 ± 0.1 mol m^{-2} s^{-1} (mean ± standard deviation).

uncertainties may influence V_{COS}, the variations in both V_{COS} and V_{CO_2} are likely driven by micro-environmental differences, plant-to-plant variability, or other natural conditions, even within the same species grown in similar environments.

3.2 Model-assisted analysis

3.2.1 Optimization Performance. We present the optimized results of model S2, which provides the best fit to the observations (Section 3.2.2).

Table 5 quantifies how well the optimized model estimates $[COS]_{out}$, $[CO_2]_{out}$, and $[H_2O]_{out}$ compared to observations. The optimized model simulated the mole fractions of all three gases more accurately, reflected by mostly reduced values of χ^2, MSE, and MBE. Notably, the model biases were mitigated, as shown by the low posterior MBE values for $[COS]_{out}$ (0.15 pmol mol^{-1}), $[CO_2]_{out}$ (– 0.01 µmol mol^{-1}), and $[H_2O]_{out}$ (0.07 mmol mol^{-1}). The χ^2_{poste} values for $[COS]_{out}$, $[CO_2]_{out}$, $[H_2O]_{out}$, and the state variables are 6.65, 1.68, 2.24, and 1.00, respectively. The large χ^2_{poste} and RMSE for $[COS]_{out}$ likely result from its relatively larger observational error.

To visualize these improvements, Figure 7 presents scatter plots comparing the simulated atmospheric mole fractions from the prior and posterior models to the observed values. The optimized atmospheric mole fractions exhibit improved agreement with the observed values across all sunflowers, improving the performance of the prior simulations. The optimized model explains the variability in the observations with high R^2 values from 0.93 to 0.99. The simulation errors, represented by the standard deviation of 500 forward simulations, were substantially reduced after optimization. Specifically for $[COS]_{out}$, errors decreased from 47.4 pmol mol^{-1} to 12.5 pmol mol^{-1}, for $[CO_2]_{out}$ from 10.8 µmol mol^{-1} to 0.8 µmol mol^{-1}, and for $[H_2O]_{out}$ from 0.6 mmol mol^{-1} to 0.3 mmol mol^{-1}. However, discrepancies remain, such as in Sunflower 2. Several posterior $[COS]_{out}$ and $[CO_2]_{out}$ values of Sunflower 2 fall outside the weighted observational error range, likely due to measurement uncertainties.

In addition to reproducing the observations well, the optimization also reduced the parameter uncertainties. The optimized state values and their posterior errors, along with error reductions, are presented in Table 2. As expected, errors associated with all target parameters were significantly reduced, with an average error reduction of 48%. An error

Table 5. The statistical indices of the prior and posterior estimated $[COS]_{out}$, $[CO_2]_{out}$, and $[H_2O]_{out}$ from model S2 compared to the observations with χ^2 changes of state term (*x*). The units of RMSE and MBE of $[COS]_{out}$ are pmol mol^{-1}, $[CO_2]_{out}$ is in µmol mol^{-1}, and $[H_2O]_{out}$ is mmol mol^{-1}.

Index	$[COS]_{out}$		$[CO_2]_{out}$		$[H_2O]_{out}$		Background (State *x*)	
	Prior	Posterior	Prior	Posterior	Prior	Posterior	Prior	Posterior
χ^2	30.00	6.65	100.00	1.68	3.00	2.24	0.00	1.00
RMSE	16.71	7.93	3.63	0.71	0.30	0.45	-	-
MBE	11.77	0.15	-1.52	-0.01	-0.14	0.07	-	-

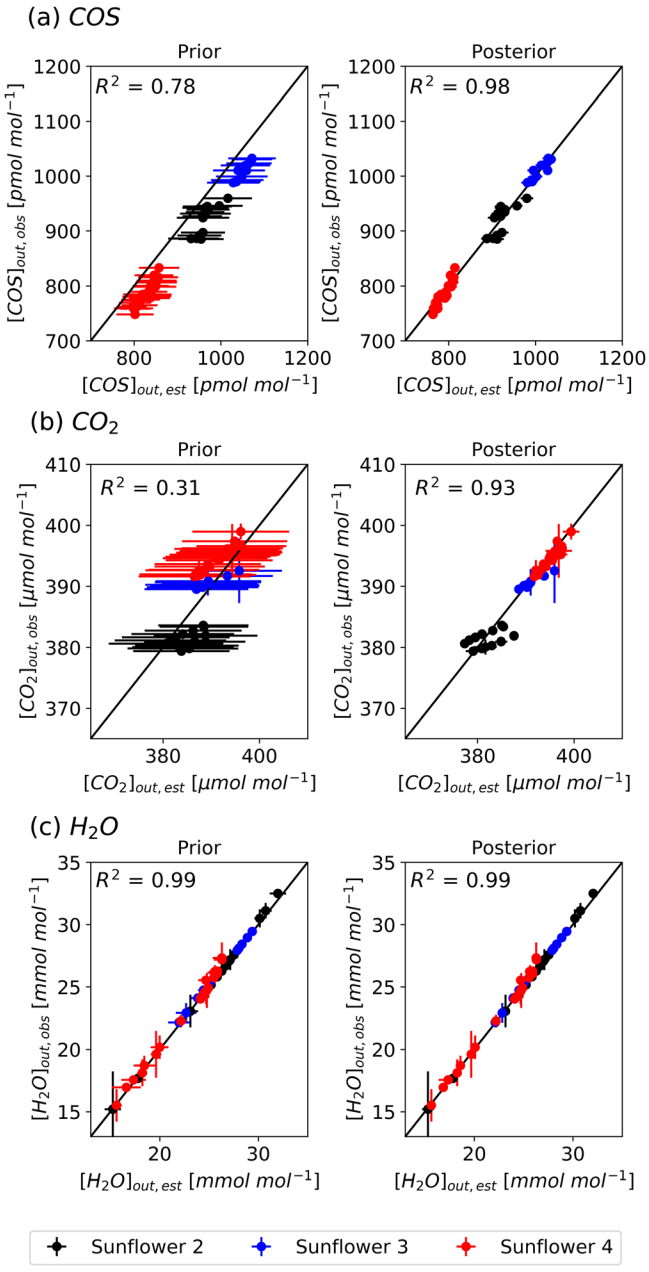

Figure 7. Scatter plots comparing the simulated (model S2) and observed atmospheric mole fractions of COS (a), CO_2 (b), and H_2O (c) with the prior parameters (left) and optimized parameters (right) with a 1:1 line indicating perfect agreement. The vertical error bars represent weighted observational errors, taken as the standard deviations of measurements, and the horizontal error bars represent prior errors (left) and posterior errors (right). Colors indicate different sunflower plants (black: Sunflower 2, blue: Sunflower 3, red: Sunflower 4).

reduction of more than 92% was achieved for CO_2 parameters $\Delta H_{a,Rub}$ and $V_{max,Rub}$. Prior uncertainties of $T_{eq,CA}$, m_{COS}, and $V_{max,CA}$ were reduced by more than 30%, and the error reduction for g_{sw} was about 43%.

Parameter values also shifted meaningfully after optimization. The optimized slope of Γ_{COS} (m_{COS}, 22.4 pmol mol^{-1} K^{-1}) is slightly increased to the initial setting (16.2 pmol mol^{-1} K^{-1}). With the optimized value of m_{COS}, the variable $T_{eq,CA}$ was adjusted to 39.7°C, and the values of $V_{max,CA}$ for each plant were optimized ranging from 0.189 to 0.230 mol m^{-2} s^{-1}. These values increased significantly from their priors, 30.0°C and 0.125 mol m^{-2} s^{-1}, indicating higher optimum temperatures and higher catalyzation velocities compared to the prior settings. The optimized $V_{max,Rub}$ ranged

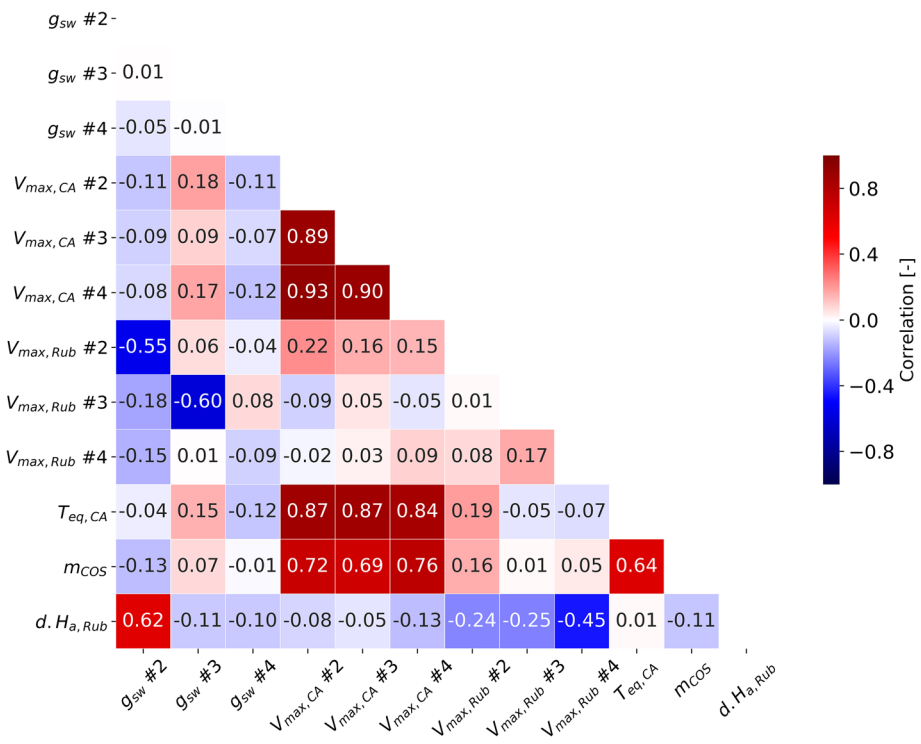

Figure 8. The covariance matrix for state variables. Regarding g_{sw}, only the first data point of each sunflower is marked.

from 82.9 to 94.4 µmol m^{-2} s^{-1}, while $\Delta H_{a,Rub}$ did not change substantially. The ratio of $V_{max,CA}$ to $V_{max,Rub}$ which is crucial for calculating CA activity from $V_{max,Rub}$ based on the assumption of a linear relationship, ranges from 2160 to 2770.

The optimized g_{sw} also showed consistent behavior. Comparisons of the optimized mean g_{sw} values of 0.64 mol m^{-2} s^{-1} with the prior values of 0.62 mol m^{-2} s^{-1} reveal slight differences. Errors in g_{sw} were reduced from 0.09 to 0.05 mol m^{-2} s^{-1}. The optimized model yielded an average relative humidity within the leaf (RH_i) of 98.82 ± 0.04%. These results confirm that allowing for slight non-saturation in the intercellular airspace (through g_m,H_2O) had a negligible impact on the modeled fluxes, validating the assumption that the air within the intercellular airspace was effectively saturated under our experimental conditions. Simulations further confirmed that varying g_{mw} (<10 mol m^{-2} s^{-1}) did not alter the modeled fluxes or mole fractions, indicating that its effect was negligible under our experimental conditions.

Figure 8 illustrates the posterior covariance matrix derived from Monte Carlo calculations. Although several state variables were highly correlated after optimization (values above 0.7), they were retained as state parameters because their simulation errors were substantially reduced. For instance, three variables of COS parameters ($T_{eq,CA}$, m_{COS}, and $V_{max,CA}$) were highly correlated, with values ranging from 0.69 to 0.87, as these parameters are all related to the mesophyll uptake of COS.

3.2.2 COS Compensation Point (Hypothesis H1). Table 6 summarizes the changes in total cost (J_{tot}) between prior and posterior estimations for each Γ_{COS} temperature function. Among the tested models, the lowest total cost was achieved with the linear model (S2), followed by the Arrhenius models S4 and S3, and the model without a compensation point (S1). These results confirm that incorporating Γ_{COS} with a linear temperature function into the leaf exchange model provides the best agreement with observations, as it minimizes the overall cost function and improves model performance. However, the total cost difference between the S2 model and the S4 model was only 1 unit.

To further evaluate the performance of these models, Figure 9 compares estimated Γ_{COS} with two types of observation-based values across temperatures. The first type is regression-based measurements from 15 data points at two temperatures in Experiment 1 (blue triangles; see Figure 4). The second type is indirectly derived Γ_{COS} in Experiments 2 and 3.

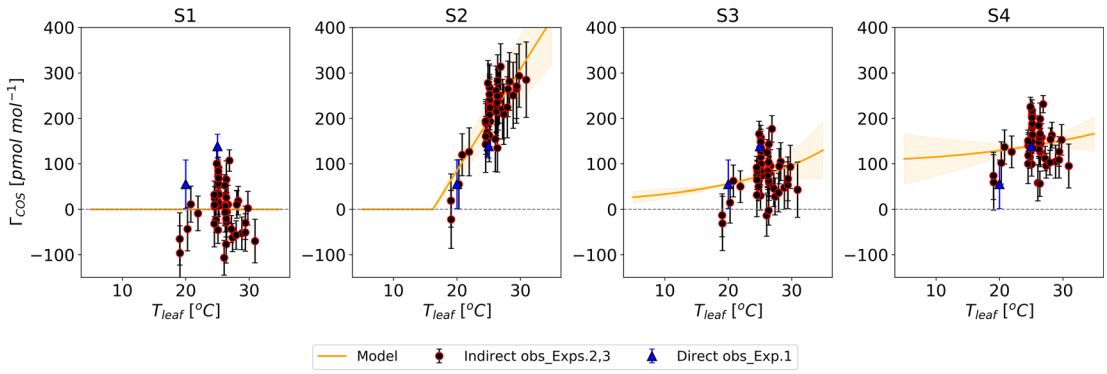

Figure 9. Posterior temperature functions for Γ_{COS} from S1 to S4 models, shown with orange lines and error ranges from 200 Monte Carlo simulations. These are compared with Γ_{COS} values from Experiment 1 (blue triangles, regression-derived from two temperature points) and Experiments 2 and 3 (black circles with red edges, derived indirectly). Regression-derived Γ_{COS} measurements are 55.0 ± 53.2 pmol mol^{-1} at 19.8°C and 138.7 ± 26.1 pmol mol^{-1} at 25.0°C, detailed in Section 3.1.1). Indirectly derived values are averages with standard deviation error bars, calculated from parameters optimized through 200 Monte Carlo simulations (See Section 2.5.).

The optimized S2 model best captures the Γ_{COS} measurements derived from both regression and indirect methods, compared to other models. Specifically, the S2 model achieved the lowest RMSE with the indirect derived Γ_{COS} (39 pmol mol^{-1}). The RMSE values for the other models were: S1 = 50 pmol mol^{-1}, S3 = 49 pmol mol^{-1}, and S4 = 41 pmol mol^{-1}, respectively.

3.2.3 Response to stomatal conductance (Hypothesis H2). In Experiment 2, we confirmed that V_{COS} responds more strongly than V_{CO2} at low g_{sw} values. To further interpret this behavior mechanistically, we explore how changes in deposition velocity due to g_{sw} are influenced by interactions with mesophyll conductance. We calculated AFR values ($1 - [gas]_i/[gas]_a$) for both gases using the optimized S2 model, as these values cannot be directly measured (Figure 10). Simulations were performed at a constant T_{leaf} of 25°C.

The model results indicate that for both gases, AFR decreases as g_{sw} increases, which provides support for Hypothesis 2. However, contrary to Hypothesis 2, which assumes that $[COS]_i$ is nearly zero thus resulting in AFR for COS close to

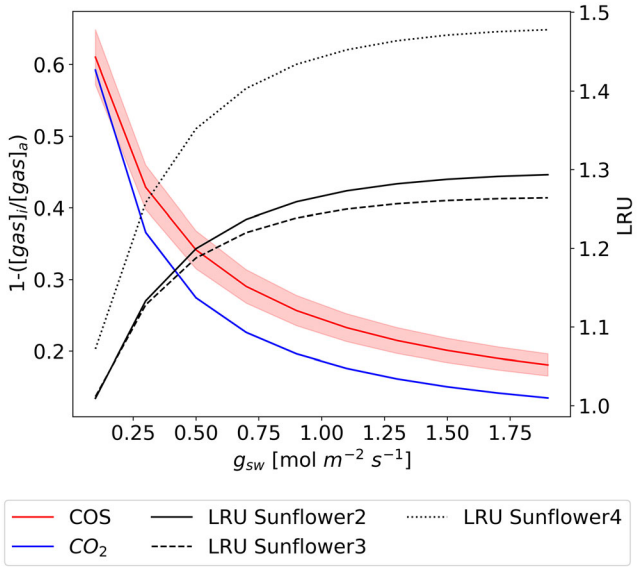

Figure 10. Simulated changes in (1 – $[gas]_i/[gas]_a$) for COS (red) and CO_2 (blue) averaged among sunflowers 2, 3, and 4, with LRU (black, secondary y-axis) as a function of g_{sw} each sunflower (Results from the S2 model). The lines represent averages, and the filled areas indicate the standard deviation of 500 simulations using posterior error propagation.

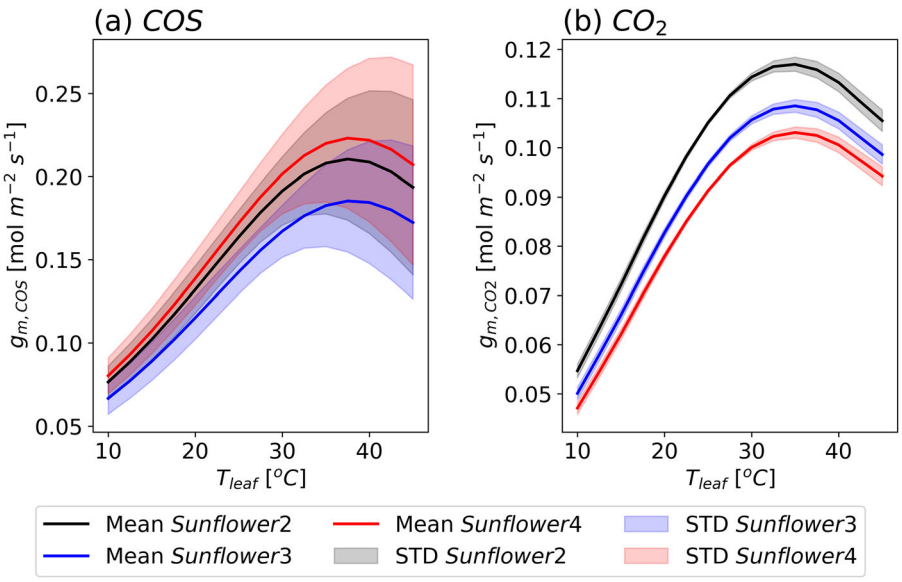

Figure 11. Modeled response of mesophyll conductances (g_m) to leaf temperatures (T_{leaf}) for COS (a) and CO_2 (b) with three sunflowers (black: sunflower 2, blue: sunflower 3, red: sunflower 4, results from the S2 model). The lines represent averaged values, and the filled areas indicate the standard deviation from 500 simulations using posterior error propagation.

1, the actual modeled values range from 0.2 to 0.6 depending on g_{sw}. This deviation indicates that $[COS]_i$ is not negligible and suggests a dynamic COS consumption within the leaf that does not bring $[COS]_i$ close to zero.

The model also reveals a distinct LRU pattern, showing sharp increases at low g_{sw} values followed by stabilization at higher g_{sw}. This response is consistent with observations from Experiment 2, where LRU exhibited similar trends in response to g_{sw}. These results underscore the differing sensitivities of COS and CO_2 uptake to g_{sw}, as reflected in both experimental and modeled data.

3.2.4 Response to leaf temperature (Hypothesis H3). To investigate the temperature function of enzyme activity separated from Γ_{COS} in V_{COS}, we calculated $g_{m,COS}$ and g_{m,CO_2} using the optimized model S2. Figure 11 shows the temperature dependency of $g_{m,COS}$ and g_{m,CO_2} for three sunflowers. The magnitudes of these dependencies vary among plants due to differences in optimized V_{max} values. The optimum temperature for $g_{m,COS}$ is around 35 to 40°C, while for g_{m,CO_2} it is approximately 35°C, which contradicts Hypothesis 3, proposing a lower optimum temperature for $g_{m,COS}$ than for g_{m,CO_2}.

The observed decline in V_{COS} above 25°C in Experiment 3 (Figure 6a) is explained by the model-predicted impact of Γ_{COS} on COS uptake. While the optimum temperature for $g_{m,COS}$ is approximately 35 to 40°C, the influence of temperature-dependent Γ_{COS} results in a much lower optimum temperature for V_{COS}, around 20°C. This is significantly lower than the optimum temperature for V_{CO_2}, which is approximately 30°C.

Overall, the model results suggest that the temperature dependence of Γ_{COS} plays a critical role in shaping the distinct responses of V_{COS} and V_{COS_2}.

4. Discussion

This study aimed to investigate how leaf COS and CO_2 fluxes respond differently to environmental changes and to identify which internal processes within leaves govern these differences. Laboratory experiments were conducted under controlled conditions to isolate the effects of stomatal conductance and temperature. However, to provide more insights in the internal processes that control COS exchange, we developed and optimized a coupled CO_2–COS–H_2O conductance model to mechanistically interpret the measurement data. Although the model involves some simplified representations of internal processes, these simplifications are minor and do not affect the overall interpretation. In this section, we discuss the uncertainties in both observations and model representations, the physiological implications of the observed COS compensation points, and their broader significance for biochemical parameters and the global COS budget.

4.1 Uncertainties in measurements and models

Before discussing measurement uncertainties, we emphasize that potential leakage effects were minimized in our experimental setup. Through improvements in our experimental setup, especially with the LI-6800 system incorporating new gasket materials (Advanced Polymer, Polyethylene, and Neoprene) and optimized flow paths, we minimized the gas leakage issues prevalent in previous systems like the LI-6400. No significant pressure differentials were observed during experiments, supporting the effectiveness of these enhancements. Additionally, maintaining the cuvette under slight positive pressure reduces the risk of inward leakage.

Nevertheless, several experimental limitations remain. First, the temperature range explored in this study was relatively restricted. Our optimization was based on data from Experiments 2 and 3, conducted at temperatures ranging from 19.0°C to 29.8°C. Therefore, additional experiments across a broader temperature range are necessary to confirm the existence and assess the temperature dependence of Γ_{COS}.

The choice of elevated COS concentration in the cuvette also introduces interpretative considerations. In our experiment, we increased the COS mole fraction in the cuvette to approximately 1000 pmol mol^{-1}, significantly above natural ambient levels, to enhance signal detection and reduce noise. The primary purpose of our empty chamber experiments was to eliminate the effects of emissions from chamber materials. Conducting these tests at similarly high mole fractions also helped mitigate any emissions that could arise from this higher mole fraction setting.

This high COS mole fraction possibly contributed to slightly higher AFR (Figure 10) because the high ambient mole fraction may influence the internal concentration. $[COS]_i/[COS]_a$ values of about 0.63 $\pm$ 0.13 were observed under elevated ambient $[COS]_a$ conditions (Stimler *et al.*, 2010), aligning with our results. Stimler *et al.* (2010) also reported a linear relationship between $[COS]_i/[COS]_a$ and $[COS]_a$, likely due to retro-diffusion from the leaves. Therefore, when applying our results to natural conditions ($[COS]_a$ about 500 pmol mol^{-1}, the AFR may decrease. However, the high AFR is also possibly due to the influence of Γ_{COS}. The simulated $[CO_2]_i/[CO_2]_a$ ranges from 0.4 to 0.9, consistent with values previously reported for C_3 plants (0.5 – 0.8) (Black & Jones, 1985; Seibt *et al.*, 2010; Tanner & Sinclair, 2015). Nevertheless, in Experiments 2 and 3, despite the high COS mole fractions, their consistent level throughout the experiments likely negated any impact on analyzing how g_{sw} and temperatures relate to V_{COS} and V_{CO_2}.

In addition to the experimental limitations discussed above, a practical limitation arises from the mole fraction range used for model optimization. Model parameters were optimized using data obtained under relatively high COS mole fraction conditions (~1000 pmol mol^{-1}) to ensure stable and precise flux measurements, whereas Γ_{COS} was determined from experiments conducted at lower inflowing concentrations (100–600 pmol mol^{-1}). This discrepancy in concentration ranges may introduce some uncertainty when extrapolating parameters between optimization and compensation-point estimation. Nevertheless, the model formulation remains internally consistent, and the derived parameters are valid for interpreting the relative temperature-dependent behavior of COS exchange. Future experiments targeting near-ambient COS mole fraction levels will be valuable to further validate the applicability of these optimized parameters and to evaluate potential retro-diffusion effects under more natural conditions.

From a modeling perspective, only the enzyme CA is considered in determining the mesophyll conductance of COS. However, other enzymes, such as RuBisCO and phosphoenolpyruvate carboxylase (PEP-C), are known to also catalyze COS uptake (Lorimer & Pierce, 1989; Protoschill-Krebs & Kesselmeier, 1992). The contribution of RuBisCO to COS uptake is relatively minor compared to CA (Protoschill-Krebs *et al.*, 1996), and its activity has not yet been quantified.

An additional source of uncertainty arises from the simplified representation of COS mesophyll conductance in our model. While mesophyll diffusion was not explicitly parameterized, it was implicitly represented through the temperature-dependent CA activity function (Cho *et al.*, 2023) that integrates both diffusional and biochemical processes. Nevertheless, this implicit treatment may not fully capture variations in diffusional resistance under different environmental or structural conditions, and thus its influence on the temperature dependence of COS uptake cannot be completely excluded. Future modeling studies incorporating explicit mesophyll diffusion parameterization—beyond the current CA-based formulation—would help to disentangle the relative contributions of diffusional and biochemical controls, as well as potential COS emissions from leaves, in regulating COS exchange.

Beyond these structural uncertainties in the model, it is important to note that the conductance model was designed as an exploratory diagnostic tool. Its purpose was to integrate the coupled behavior of CO_2, COS, and H_2O exchange and to mechanistically interpret the observed fluxes. Despite its simplifications in not considering minor features, such as outlet mass flow change and boundary ternary effect, this framework represents the first attempt to jointly optimize gas exchange for the three gases, thereby providing a process-based means to independently estimate the COS compensation

Table 6. Prior (Pri) and posterior (Poste) contributions to the cost function of the state term, H_2O, CO_2, and COS parts, depending on the prescription of Γ_{COS} and its temperature dependence. J_{tot} is the sum of costs for the states (J_{bg}), H_2O (J_{H_2O}), CO_2 (J_{CO_2}), and COS (J_{COS}).

No.	Description of Γ_{COS}		Cost							
			J_{bg}	J_{H_2O}		J_{CO_2}		J_{COS}		J_{tot}
	Function	Based T [°C]	Post	Pri	Post	Pri	Post	Pri	Post	Post
S1	Γ_{COS} = 0	-	54	144	97	4800	80	2437	349	580
S2	Linear	16.4	57		107		81	1440	320	564
S3	Arrhenius	19.8	59		100		80	2634	335	574
S4		25.0	61		106		80	2634	319	565

point. Overall, this approach highlights the potential of combined gas-exchange measurement and modeling to advance our understanding of COS biogeochemistry.

Taken together, the remaining uncertainties in both COS measurements and model structure require careful interpretation. Concerning Hypothesis 1, Model S2 was selected as the best model due to its minimal posterior costs and lowest RMSE with observation-based Γ_{COS}, despite higher H_2O and background costs compared to S1, as shown in Table 6. Furthermore, the minor differences in posterior costs and RMSE with indirectly derived Γ_{COS} between S2 and S4 suggest that S4 is a viable alternative. The strong correlation between the temperature dependence of Γ_{COS} (m_{COS}) and $V_{max,CA}$ complicates the precise and independent determination of these two parameters. Although S2 and S4 employ different temperature-dependent formulations of Γ_{COS}, both model structures consistently support the presence of a COS compensation point.

Accordingly, the exact value and temperature dependence of Γ_{COS} remain uncertain, but including a compensation point in the models, as in models S2 and S4, significantly improves their alignment with observations. Even if S4 were to better represent the true underlying mechanism, both model structures indicate an increase in Γ_{COS} with temperature, although the optimum temperature derived under Hypothesis 3 may shift slightly depending on the assumed functional form of the temperature response of CA activity.

4.2 Possible causes of a COS compensation point

COS emission can occur due to leaf stress induced by external factors during experiments. To minimize the risk of mechanical damage or stress, the chamber was gently attached, and leaves were inspected post-experiment for physical damage such as bruising, desiccation, or discoloration. No visible damage was observed, and the limited measurement duration further reduced the likelihood of stress-induced COS emissions.

Previous studies on COS leaf exchange experiments have reported positive Γ_{COS} values, but often concluded these are statistically indistinguishable from zero due to high variability. For example, Stimler *et al.* (2010) observed a Γ_{COS} of 60.7 pmol mol^{-1} at 25°C, and attributed it to potential retro-diffusion under high COS mole fractions. Similarly, our Γ_{COS} at 20.0°C (55.0 ± 53.2 pmol mol^{-1}) was statistically insignificant, whereas a significant Γ_{COS} (138.7 ± 26.1 pmol mol^{-1}) was detected at 25°C. Considering that our experiments, like those of Stimler *et al.* (2010), were conducted under relatively high COS mole fractions, this pattern suggests that higher temperature may enhance diffusion-driven feedbacks. It should also be noted that our COS model does not explicitly account for mesophyll diffusion conductance, and thus part of the apparent emission function could be interpreted as an effect of internal diffusion-related mechanisms (e.g., retro-diffusion) within the leaf.

In addition to retro-diffusion, temperature-induced stress could also contribute to the observed COS compensation point. Previous studies, typically conducted below 25°C, did not assess temperature dependence. Our modeling revealed a linear relationship between Γ_{COS} and temperature, consistent with Gimeno *et al.* (2017), who reported higher Γ_{COS} in mosses at elevated temperatures. Although no visible stress was observed in our plants, temperature stress may have influenced Γ_{COS}. Gimeno *et al.* (2017) suggested that COS emissions could result from protein degradation under stress, releasing COS through the breakdown of sulfur-containing amino acids. This highlights the role of temperature-driven biochemical pathways in shaping Γ_{COS} values and supports the inclusion of Γ_{COS} in leaf gas exchange models.

Beyond temperature-driven stress, differences in species physiology also contribute to Γ_{COS}. Mosses studied by Gimeno *et al.* (2017) exhibited higher Γ_{COS} values than in vascular plants, likely due to enzymatic activity of associated fungi and bacteria. While microbial activity is not directly applicable to vascular plants, it underscores the importance of

species-specific factors in determining COS emissions. In vascular plants, rapeseed is known to produce COS due to its high sulfur content, with Γ_{COS} exceeding 100 pmol mol^{-1} during ripening and senescence (Belviso *et al.*, 2022). However, no experiments have previously been conducted to detect Γ_{COS} in sunflowers.

Previous studies (e.g., Maseyk *et al.*, 2014; Belviso *et al.*, 2022) reported that COS emissions occur during the ripening and senescence phases, indicating that senescence-related processes could explain COS emissions rather than active uptake from living tissues. In Maseyk *et al.* (2014) part of these emissions may have originated from the soil, whereas Belviso *et al.* (2022) provided strong evidence for plant-derived senescence emissions. Additionally, Kesselmeier and Merk (1993) reported Γ_{COS} values ranging from 57 to 328 pmol mol^{-1} in rapeseed and corn during flowering. In our study, measurements were conducted during the flowering phase, which could explain the observed COS emissions, although the exact source remains unclear. Sulfur emissions during senescence have been linked to the translocation of sulfur-containing amino acids and sulfur regulation in plant cells (Rennenberg, 1991).

Apart from biological factors, methodological advances may explain the discrepancies between our results and previous studies. We employed the Li-6800 system, which offers improved measurement accuracy, and evaluated an optimized conductance model incorporating temperature-dependent Γ_{COS}. Our findings confirm that all observations support an increase in Γ_{COS} with temperature.

Taken together, the existence of Γ_{COS} and its increase at higher temperatures may result from a combination of the factors discussed above. However, our current formulation of Γ_{COS} is expressed solely as a temperature-dependent function and does not explicitly include retro-diffusion effects. As a result, while the observed increase in Γ_{COS} with temperature is consistent with thermally driven processes, the potential contribution of internal diffusion feedbacks—particularly under elevated COS mole fractions—cannot be fully excluded.

At present, reliable measurements can only be obtained under relatively high COS mole fractions, which limits our ability to fully constrain Γ_{COS} dynamics near ambient conditions. Improving detection precision at low COS concentrations and incorporating explicit representations of internal diffusion in future models would enable a more direct evaluation of whether Γ_{COS} variability originates from retro-diffusion or from physiological and biochemical processes. Moreover, extending such measurements to different phenological stages and species, and exploring interactions with microbial associations and environmental stressors, will be essential for developing a more mechanistic understanding of COS exchange in plants.

4.3 Impact of COS compensation point on $V_{max,CA}$

When Γ_{COS} was explicitly considered in the optimization, the optimized ratio between $V_{max,CA}$ and $V_{max,Rub}$ ranges from 2160 to 2770, which is higher than previously obtained values of approximately 1200 from laboratory measurements with C_3 plants (Berry *et al.*, 2013). Kooijmans *et al.* (2021) reported an average ratio of 1616 ± 562 based on field observations in summer months. In contrast, when Γ_{COS} was excluded (model S1), the optimized $V_{max,CA}$ became smaller, resulting in ratios of 1197–1327, closely matching the values reported in previous studies. Thus, models that incorporate Γ_{COS} result in higher optimized values of $V_{max,CA}$ and consequently to higher ratios between $V_{max,CA}$ and $V_{max,Rub}$, indicating a higher maximum catalyzation velocity of CA.

4.4 Consequences for the COS global budget

Our evidence of decreasing V_{COS} between 20 and 25°C (Figure 6a) supports lower biosphere uptake in high temperature regions. The current COS budget has a missing source of roughly 400 GgS year^{-1}, mainly due to the large biosphere sink calculated by the Simple Biosphere model (SiB4) in the tropics (Berry *et al.*, 2013). In warm tropical forests, biosphere uptake would be significantly reduced.

The presence of Γ_{COS} could have implications for the global COS budget and the utilization of COS in estimating GPP, especially under conditions such as drought, where high temperatures and low humidity persist. Despite the uncertainty concerning Γ_{COS} in our experiments, including Γ_{COS} in our model better reproduced CO_2 and COS observations. This suggests that incorporating Γ_{COS} into global biosphere models could enhance the accuracy of COS flux estimates. Differences in temperatures and humidity responses between CO_2 and COS should also be considered. To further improve the large-scale modeling, it is recommended to measure Γ_{COS} and enzyme activity across diverse plant types, specifically tropical plants.

While our study focused on controlled conditions with a single species, larger variations would indeed be expected under natural conditions and across different species. Consequently, future research should therefore explore these factors in more diverse environmental settings to validate and generalize these findings.

Ethics and consent

Ethical approval and consent were not required.

Data availability

All datasets generated from the experiments are available on GitHub and have been archived on Zenodo under a CC-BY 4.0 license.

- DOI: [https://doi.org/10.5281/zenodo.15489794] (Cho *et al.*, 2025)

- GitHub: [https://github.com/dkfkcho/COS_sunflower]

Software availability

- Source code available from: [https://github.com/dkfkcho/COS_sunflower]

- Archived software available from: [https://doi.org/10.5281/zenodo.15489794] (Cho *et al.*, 2025)

- License: MIT License

Acknowledgements

We gratefully acknowledge Steven van Heuven (Energy and Sustainability Research Institute Groningen) for his valuable technical contributions, including providing access to the gas chromatography system and advising on experimental setup and calibration. Additionally, we would like to express our sincere gratitude to Nerea Ubierna Lopez (Florida Department of Environmental Protection, FL, USA) and reviewers for their invaluable and insightful comments, which greatly improved the quality of this work. The manuscript was prepared with the assistance of ChatGPT (GPT-4, OpenAI), used for improving English readability.

References

Adnew GA, Hofmann ME, Pons TL, *et al.*: **Leaf scale quantification of the effect of photosynthetic gas exchange on Δ_{47} of CO_2.** *Sci Rep.* 2021; **11**(1): 14023.
PubMed Abstract | **Publisher Full Text** | **Free Full Text**

Adnew GA, Pons TL, Koren G, *et al.*: **Leaf-scale quantification of the effect of photosynthetic gas exchange on $\delta^{17}O$ of atmospheric CO_2.** *Biogeosciences.* 2020; **17**(14): 3903–3922.
Publisher Full Text

Adnew GA, Pons TL, Koren G, *et al.*: **Exploring the potential of $\Delta^{17}O$ in CO_2 for determining mesophyll conductance.** *Plant Physiol.* 2023; **192**(2): 1234–1253.
PubMed Abstract | **Publisher Full Text** | **Free Full Text**

Asaf D, Rotenberg E, Tatarinov F, *et al.*: **Ecosystem photosynthesis inferred from measurements of carbonyl sulphide flux.** *Nat Geosci.* 2013; **6**(3): 186–190.
Publisher Full Text

Badger M, Collatz G: *Studies on the kinetic mechanism of ribulose-1,5-bisphosphate carboxylase and oxygenase reactions with particular reference to the effect of temperature on kinetic parameters.* Carnegie Institution of Washington Yearbook; 1977, **76**(1961).

Belviso S, Abadie C, Montagne D, *et al.*: **Carbonyl Sulfide (COS) emissions in two agroecosystems in central France.** *PLoS One.* 2022; **17**(12): e0278584.
PubMed Abstract | **Publisher Full Text** | **Free Full Text**

Berry J, Wolf A, Campbell JE, *et al.*: **A coupled model of the global cycles of carbonyl sulfide and CO_2: a possible new window on the carbon cycle.** ***JGR. Biogeosciences.*** 2013; **118**(2): 842–852.
Publisher Full Text

Black VJ, Jones HG: **Plants and microclimate.** *J Appl Ecol.* 1985; **22**(2): 605–606.
Publisher Full Text

Bonan GB: **Forests and climate change: forcings, feedbacks, and the climate benefits of forests.** *Science.* 2008; **320**(5882): 1444–1449.
PubMed Abstract | **Publisher Full Text**

Bosman PJ, Krol MC: **ICLASS 1.1, a variational Inverse modelling framework for the Chemistry land-surface atmosphere soil slab model: description, validation, and application.** *Geosci Model Dev.* 2023; **16**(1): 47–74.
Publisher Full Text

Brasseur GP, Jacob DJ: **Modeling of atmospheric chemistry.** 2017.
Publisher Full Text

Campbell JE, Carmichael GR, Chai T, *et al.*: **Photosynthetic control of atmospheric carbonyl sulfide during the growing season.** *Science.* 2008; **322**(5904): 1085–1088.
PubMed Abstract | **Publisher Full Text**

Cernusak LA, Ubierna N, Jenkins MW, *et al.*: **Unsaturation of vapour pressure inside leaves of two conifer species.** *Sci Rep.* 2018; **8**(1): 7667.
PubMed Abstract | **Publisher Full Text** | **Free Full Text**

Chevallier F, Bréon FM, Rayner PJ: **Contribution of the Orbiting Carbon Observatory to the estimation of CO_2 sources and sinks: theoretical study in a variational data assimilation framework.** *J Geophys Res Atmos.* 2007; **112**(9).
Publisher Full Text

Cho A, Kooijmans LMJ, Driever SM, *et al.*: **COS_sunflower: dataset and software for: leaf chamber experiments on sunflowers indicate a temperature (v1.0).** *Zenodo.* 2025.
Publisher Full Text

Cho A, Kooijmans LM, Kohonen KM, *et al.*: **Optimizing the carbonic anhydrase temperature response and stomatal conductance of carbonyl sulfide leaf uptake in the Simple Biosphere model (SiB4).** *Biogeosciences.* 2023; **20**(13): 2573–2594.
Publisher Full Text

Cochavi A, Amer M, Stern R, *et al.*: **Differential responses to two heatwave intensities in a mediterranean citrus orchard are identified by combining measurements of fluorescence and carbonyl Sulfide (COS) and CO_2 uptake.** *New Phytol.* 2021; **230**(4): 1394–1406.
PubMed Abstract | **Publisher Full Text**

Collatz GJ, Ball JT, Grivet C, *et al.*: **Physiological and environmental regulation of stomatal conductance, photosynthesis and transpiration: a model that includes a laminar boundary layer.** *Agric For Meteorol.* 1991; **54**(2–4): 107–136.
Publisher Full Text

Daniel RM, Peterson ME, Danson MJ, *et al.*: **The molecular basis of the effect of temperature on enzyme activity.** *Biochem J.* 2010; **425**(2): 353–360.
PubMed Abstract | **Publisher Full Text**

Farquhar GD, Sharkey TD: **Stomatal conductance and photosynthesis.** *Annu Rev Plant Physiol.* 1982; **33**(1): 317–345.
Publisher Full Text

Farquhar GD, von Caemmerer S, Berry JA: **A biochemical model of photosynthetic CO_2 assimilation in leaves of C_3 species.** *Planta.* 1980; **149**(1): 78–90.
PubMed Abstract | **Publisher Full Text**

Garen JC, Branch HA, Borrego I, *et al.*: **Gas exchange analysers exhibit large measurement error driven by internal thermal gradients.** *New Phytol.* 2022; **236**(2): 369–384.
PubMed Abstract | **Publisher Full Text**

Geng C, Mu Y: **Carbonyl sulfide and dimethyl sulfide exchange between lawn and the atmosphere.** *J Geophys Res D: Atmos.* 2004; **109**(12).
Publisher Full Text

Gimeno TE, Ogée J, Royles J, *et al.*: **Bryophyte gas-exchange dynamics along varying hydration status reveal a significant Carbonyl Sulphide (COS) sink in the dark and COS source in the light.** *New Phytol.* 2017; **215**(3): 965–976.
PubMed Abstract | **Publisher Full Text** | **Free Full Text**

Goldan PD, Fall R, Kuster WC, *et al.*: **Uptake of COS by growing vegetation: a major tropospheric sink.** *J Geophys Res.* 1988; **93**(D11): 14186–14192.
Publisher Full Text

Hussain SB, Stinziano J, Pierre MO, *et al.*: **Accurate photosynthetic parameter estimation at low stomatal conductance: effects of cuticular conductance and instrumental noise.** *Photosynth Res.* 2024; **160**(2–3): 111–124.
PubMed Abstract | **Publisher Full Text** | **Free Full Text**

Jarman PD: **The diffusion of carbon dioxide and water vapour through stomata.** *J Exp Bot.* 1974; **25**(5): 927–936.
Publisher Full Text

Kesselmeier J, Merk L: **Exchange of Carbonyl Sulfide (COS) between agricultural plants and the atmosphere: Studies on the deposition of COS to peas, corn and rapeseed.** *Biogeochemistry.* 1993; **23**(1): 47–59.
Publisher Full Text

Kettle AJ, Kuhn U, Von Hobe M, *et al.*: **Global budget of atmospheric Carbonyl Sulfide: temporal and spatial variations of the dominant sources and sinks.** *J Geophys Res.* 2002; **107**(22): ACH 25-1–ACH 25-16.
Publisher Full Text

Kohonen KM, Dewar R, Tramontana G, *et al.*: **Intercomparison of methods to estimate gross primary production based on CO_2 and COS flux measurements.** *Biogeosciences.* 2022; **19**(17): 4067–4088.
PubMed Abstract | **Publisher Full Text** | **Free Full Text**

Kooijmans LM, Cho A, Ma J, *et al.*: **Evaluation of Carbonyl Sulfide biosphere exchange in the Simple Biosphere Model (SiB4).** *Biogeosciences.* 2021; **18**(24): 6547–6565.
Publisher Full Text

Kooijmans LMJ, Sun W, Aalto J, *et al.*: **Influences of light and humidity on Carbonyl Sulfide-based estimates of photosynthesis.** *Proc Natl Acad Sci U S A.* 2019; **116**(7): 2470–2475.
PubMed Abstract | **Publisher Full Text** | **Free Full Text**

Kooijmans LMJ, Uitslag NAM, Zahniser MS, *et al.*: **Continuous and high-precision atmospheric concentration measurements of COS, CO_2, CO and H_2O using a Quantum Cascade Laser Spectrometer (QCLS).** *Atmos Meas Tech.* 2016; **9**(11): 5293–5314.
Publisher Full Text

Kuhn U, Kesselmeier J: **Environmental variables controlling the uptake of Carbonyl Sulfide by lichens.** *J Geophys Res.* 2000; **105**(D22): 26783–26792.
Publisher Full Text

Lai J, Kooijmans LMJ, Sun W, *et al.*: **Terrestrial photosynthesis inferred from plant carbonyl sulfide uptake.** *Nature.* 2024; **634**(8035): 855–861.
PubMed Abstract | **Publisher Full Text**

Le Roux X, Bariac T, Sinoquet H, *et al.*: **Spatial distribution of leaf water-use efficiency and carbon isotope discrimination within an isolated tree crown.** *Plant, Cell and Environment.* 2001; **24**(10): 1021–1032.
Publisher Full Text

Lobo FA, de Barros MP, Dalmagro HJ, *et al.*: **Fitting net photosynthetic light-response curves with *Microsoft Excel* - a critical look at the models.** *Photosynthetica.* 2013; **51**(3): 445–456.
Publisher Full Text

Lorimer GH, Pierce J: **Carbonyl sulfide: an alternate substrate for but not an activator of ribulose-1,5-bisphosphate carboxylase.** *J Biol Chem.* 1989; **264**(5): 2764–2772.
PubMed Abstract | **Publisher Full Text**

Maseyk K, Berry JA, Billesbach D, *et al.*: **Sources and sinks of Carbonyl Sulfide in an agricultural field in the Southern Great Plains.** *Proc Natl Acad Sci U S A.* 2014; **111**(25): 9064–9069.
PubMed Abstract | **Publisher Full Text** | **Free Full Text**

Montzka SA, Calvert P, Hall BD, *et al.*: **On the global distribution, seasonality, and budget of atmospheric Carbonyl Sulfide (COS) and some similarities to CO_2.** *J Geophys Res.* 2007; **112**(9).
Publisher Full Text

Notni J, Schenk S, Protoschill-Krebs G, *et al.*: **The missing link in COS metabolism: a model study on the reactivation of carbonic anhydrase from its hydrosulfide analogue.** *ChemBioChem.* 2007; **8**(5): 530–536.
PubMed Abstract | **Publisher Full Text**

Ogée J, Sauze J, Kesselmeier J, *et al.*: **A new mechanistic framework to predict OCS fluxes from soils.** *Biogeosciences.* 2016; **13**(8): 2221–2240.
Publisher Full Text

Protoschill-Krebs G, Kesselmeier J: **Enzymatic pathways for the Consumption of Carbonyl Sulphide (COS) by higher plants.** *Bot Acta.* 1992; **105**(3): 206–212.
Publisher Full Text

Protoschill-Krebs G, Wilhelm C, Kesselmeier J: **Consumption of Carbonyl Sulphide (COS) by higher plant Carbonic Anhydrase (CA).** *Atmos Environ.* 1996; **30**(18): 3151–3156.
Publisher Full Text

Reichstein M, Falge E, Baldocchi D, *et al.*: **On the separation of net ecosystem exchange into assimilation and ecosystem respiration: review and improved algorithm.** *Glob Chang Biol.* 2005; **11**(9): 1424–1439.
Publisher Full Text

Rennenberg H: *The significance of higher plants in the emission of sulfur compounds from Terrestrial Ecosystems.* Trace Gas Emissions by Plants. 1991.
Publisher Full Text

Salvucci ME, Osteryoung KW, Crafts-Brandner SJ, *et al.*: **Exceptional sensitivity of Rubisco activase to thermal denaturation *in vitro* and *in vivo*.** *Plant Physiol.* 2001; **127**(3): 1053–1064.
PubMed Abstract | **Publisher Full Text** | **Free Full Text**

Sandoval-Soto L, Stanimirov M, von Hobe M, *et al.*: **Global uptake of Carbonyl Sulfide (COS) by terrestrial vegetation: estimates corrected by deposition velocities normalized to the uptake of carbon dioxide (CO_2).** *Biogeosciences.* 2005; **2**(2): 125–132.
Publisher Full Text

Seibt U, Kesselmeier J, Sandoval-Soto L, *et al.*: **A kinetic analysis of leaf uptake of COS and its relation to transpiration, photosynthesis and carbon isotope fractionation.** *Biogeosciences.* 2010; **7**(1): 333–341.
Publisher Full Text

Stimler K, Berry JA, Montzka SA, *et al.*: **Association between Carbonyl Sulfide uptake and $^{18}\Delta$ during gas exchange in C_3 and C_4 leaves.** *Plant Physiol.* 2011; **157**(1): 509–517.
PubMed Abstract | **Publisher Full Text** | **Free Full Text**

Stimler K, Montzka SA, Berry JA, *et al.*: **Relationships between Carbonyl Sulfide (COS) and CO_2 during leaf gas exchange.** *New Phytol.* 2010; **186**(4): 869–878.
PubMed Abstract | **Publisher Full Text**

Sun W, Kooijmans LM, Maseyk K, *et al.*: **Soil fluxes of Carbonyl Sulfide (COS), carbon monoxide, and carbon dioxide in a boreal forest in southern Finland.** *Atmos Chem Phys.* 2018; **18**(2): 1363–1378.
Publisher Full Text

Sun W, Maseyk K, Lett C, *et al.*: **A soil diffusion-reaction model for surface COS flux: COSSM v1.** *Geosci Model Dev.* 2015; **8**(10): 3055–3070.
Publisher Full Text

Tanner CB, Sinclair TR: **Efficient water use in crop production: research or re-search?** *In: Limitations to Efficient Water Use in Crop Production.* 2015: 1–27.
Publisher Full Text

Tarantola A: **Inverse problem theory and methods for model parameter estimation.** 2005.
Publisher Full Text

Tcherkez GG, Farquhar GD, Andrews TJ: **Despite slow catalysis and confused substrate specificity, all ribulose bisphosphate carboxylases may be nearly perfectly optimized.** *Proc Natl Acad Sci USA.* 2006; **103**(19): 7246–7251.
PubMed Abstract | **Publisher Full Text** | **Free Full Text**

von Caemmerer S, Evans JR: **Temperature responses of mesophyll conductance differ greatly between species.** *Plant Cell Environ.* 2015; **38**(4): 629–637.
PubMed Abstract | **Publisher Full Text**

von Caemmerer S, Farquhar GD: **Some relationships between the biochemistry of photosynthesis and the gas exchange of leaves.** *Planta.* 1981; **153**(4): 376–387.
PubMed Abstract | **Publisher Full Text**

Williams TG, Flanagan LB: **Effect of changes in water content on photosynthesis, transpiration and discrimination against $^{13}CO_2$ and $C^{18}O^{16}O$ in *Pleurozium* and *Sphagnum*.** *Oecologia.* 1996; **108**(1): 38–46.
PubMed Abstract | **Publisher Full Text**

Wohlfahrt G, Gerdel K, Migliavacca M, *et al.*: **Sun-induced fluorescence and gross primary productivity during a heat wave.** *Sci Rep.* 2018; **8**(1): 14169.
PubMed Abstract | **Publisher Full Text** | **Free Full Text**

Wohlfahrt G, Gu L: **The many meanings of gross photosynthesis and their implication for photosynthesis research from leaf to globe.** *Plant Cell Environ.* 2015; **38**(12): 2500–2507.
PubMed Abstract | **Publisher Full Text** | **Free Full Text**

Wong SC, Canny MJ, Holloway-Phillips M, *et al.*: **Humidity gradients in the air spaces of leaves.** *Nat Plants.* 2022; **8**(8): 971–978.
PubMed Abstract | **Publisher Full Text**

Open Peer Review

Current Peer Review Status: ? ? ✓

Version 3

Reviewer Report 12 May 2026

https://doi.org/10.21956/openreseurope.25391.r72168

✓ **Anam M. Khan**
Northern Arizona University (Ringgold ID: 3356), Flagstaff, Arizona, USA

I have no further comments. I approve of this manuscript.

Competing Interests: No competing interests were disclosed.

Reviewer Expertise: deposition velocity, stomatal conductance, surface-atmosphere exchange

I confirm that I have read this submission and believe that I have an appropriate level of expertise to confirm that it is of an acceptable scientific standard.

Version 2

Reviewer Report 04 February 2026

https://doi.org/10.21956/openreseurope.23939.r66532

? **Anam M. Khan**
Northern Arizona University (Ringgold ID: 3356), Flagstaff, Arizona, USA

The authors present interesting gas exchange data for COS and CO_2 from sunflower. They demonstrate the existence of a significant COS compensation point at a temperature of 25C, and they find that sunflower emits COS at low ambient [COS] at this temperature. The comparison between the response of COS and CO_2 leaf uptake to stomatal conductance is interesting.

However, some clarifications are needed to ensure reproducibility, and the calculation of deposition velocity needs more clarification as well.

Specific comments:

1. In the case of depositing a gas from ambient air to intercellular spaces, the deposition velocity (Vd) is a flux divided by the concentration gradient between the ambient air and the intercellular space, Vd = flux/(ambient [gas] – intercellular [gas]). For some gasses, it is assumed that intercellular [gas] is 0. Then, the Vd is simply flux / ambient [gas]. The assumption of intercellular [gas] = 0 does not hold for CO_2, and the modeling in this study seems to suggest that it does not hold for COS either. The authors should describe the rationale used to calculate Vd in equation 2. Why is the flux being normalized by the $[gas]_{out}$? The $[gas]_{out}$ has no significance without knowing the $[gas]_{in}$. The decrease in the concentration of the gas in the ambient air of the leaf chamber ($[gas]_{in}$ – $[gas]_{out}$) approximates the uptake by the plant material in the chamber. If the goal was to normalize the flux by ambient [gas], then $[gas]_{in}$ approximates the ambient [gas] that the plant material was exposed to. The $[gas]_{out}$ is just the [gas] after the uptake or emission has taken place in the chamber. There might be adequate reason for calculating Vd as it was calculated in equation 2, but it is not clear.
2. The growth conditions of the plants and the timings of measurements need to be explained if the experiment is going to be reproduced. What were the plants' growing conditions? Which time of the day were gas exchange measurements taken?
3. The modeling reveals issues of model equifinality where two different model structures, S2 and S4, have a very similar agreement with observations. The authors briefly mention that S4 is a viable alternative to S2. Can they expand on which structure reflects the true mechanisms if both have very similar agreement with observations?

Minor comments:

1. Consider submitting manuscripts for peer review with line numbers.
2. The paragraph structure of the manuscript needs extensive editing.
3. Caption for Table 1 might need revision. It says, "designed to investigate responses of V_{COS} and V_{CO2} to g_s and g_m, respectively." Was experiment 3 investigating the response to T_{leaf} or g_m? I'm assuming T_{leaf} since that is what the table header and manuscript text says.

Is the work clearly and accurately presented and does it cite the current literature?
Partly

Is the study design appropriate and does the work have academic merit?
Yes

Are sufficient details of methods and analysis provided to allow replication by others?
Partly

If applicable, is the statistical analysis and its interpretation appropriate?
Yes

Are all the source data underlying the results available to ensure full reproducibility?
Yes

Are the conclusions drawn adequately supported by the results?
Yes

Competing Interests: No competing interests were disclosed.

Reviewer Expertise: deposition velocity, stomatal conductance, surface-atmosphere exchange

I confirm that I have read this submission and believe that I have an appropriate level of expertise to confirm that it is of an acceptable scientific standard, however I have significant reservations, as outlined above.

Author Response 17 Mar 2026

Ara Cho

The authors present interesting gas exchange data for COS and CO_2 from sunflower. They demonstrate the existence of a significant COS compensation point at a temperature of 25C, and they find that sunflower emits COS at low ambient [COS] at this temperature. The comparison between the response of COS and CO_2 leaf uptake to stomatal conductance is interesting. However, some clarifications are needed to ensure reproducibility, and the calculation of deposition velocity needs more clarification as well. Specific comments:

1. In the case of depositing a gas from ambient air to intercellular spaces, the deposition velocity (Vd) is a flux divided by the concentration gradient between the ambient air and the intercellular space, Vd = flux/(ambient [gas] – intercellular [gas]). For some gasses, it is assumed that intercellular [gas] is 0. Then, the Vd is simply flux / ambient [gas]. The assumption of intercellular [gas] = 0 does not hold for CO_2, and the modeling in this study seems to suggest that it does not hold for COS either. The authors should describe the rationale used to calculate Vd in equation 2. Why is the flux being normalized by the $[gas]_{out}$? The $[gas]_{out}$ has no significance without knowing the $[gas]_{in}$. The decrease in the concentration of the gas in the ambient air of the leaf chamber ($[gas]_{in}$ – $[gas]_{out}$) approximates the uptake by the plant material in the chamber. If the goal was to normalize the flux by ambient [gas], then $[gas]_{in}$ approximates the ambient [gas] that the plant material was exposed to. The $[gas]_{out}$ is just the [gas] after the uptake or emission has taken place in the chamber. There might be adequate reason for calculating Vd as it was calculated in equation 2, but it is not clear.

We thank the reviewer for this thoughtful question. Indeed, the difference between C_{in} and C_{out} provides a measure of plant uptake within the chamber. As stated in the Methods section, deposition velocities were calculated using the outgoing mole fraction (C_{out}). The rationale for this choice is the assumption of a well-mixed chamber, under which C_{out} is considered representative of the air mole fraction surrounding the experienced by the leaf. We therefore regard C_{out} as the most appropriate bulk mole fraction for normalizing the flux. We have clarified this explicitly in the manuscript immediately following Equation 2. 2.1.2. Experiments The measured V_{COS} and V_{CO2} were used to calculate the LRU (-), which was used to characterize differing response of COS and CO_2 from Experiments 2 and 3 (Sandoval-Soto et al., 2005; Campbell et al., 2008) : ...Equation 2... where A_{COS} (pmol m^{-2} s^{-1}) and A_{CO2} (μmol m^{-2} s^{-1}) are assimilation rates of COS and CO_2, respectively. These rates were normalized by outflowing concentrations $[COS]_{out}$ and $[CO_2]_{out}$, which are

assumed to be the concentrations the plants are exposed to due to the well-mixed conditions (see Sect. 2.2.1)

2. The growth conditions of the plants and the timings of measurements need to be explained if the experiment is going to be reproduced. What were the plants' growing conditions? Which time of the day were gas exchange measurements taken?
We thank the reviewer for this comment. We have clarified both the growth conditions of the plant material and the timing of the gas exchange measurements in the Methods section to improve reproducibility. Sunflower plants were obtained from a local plant nursery (Evanthia, Maasdijk, the Netherlands) and cultivated in a greenhouse under a day/night temperature regime of 18–21 °C during the day and 15–18 °C at night, with ventilation applied above 20 °C. Germination occurred at 21–24 °C. In addition, we now specify that gas exchange measurements were scheduled to align with the plants' photosynthetic rhythm and were conducted within the local daytime window between 10:00 and 17:00 (local time, the Netherlands), with each individual plant measured for a maximum duration of 5 daytime hours.
We measured deposition velocities of COS and CO_2 (V_{COS} and V_{CO2}), i.e., fluxes normalized by mole fractions in air, using a leaf cuvette system. These experiments were conducted using sunflower plants (Helianthus annuus L. cv. 'Sunsation'), which are C_3 photosynthesis type plants cultivated in a local plant nursery (Evanthia, Maasdijk, the Netherlands). Plants were cultivated in a greenhouse under a day/night temperature regime of 18–21 °C during the day and 15–18 °C at night, with ventilation applied above 20 °C. Germination occurred at 21–24 °C. Each sunflower plant was used for a maximum of 5 daytime hours to minimize physiological stress caused by prolonged exposure to experimental conditions. Gas exchange measurements were scheduled to align with the plants' photosynthetic diurnal rhythm and were conducted during the local daytime window between 10:00 and 17:00 (local time, the Netherlands).

1. The modeling reveals issues of model equifinality where two different model structures, S2 and S4, have a very similar agreement with observations. The authors briefly mention that S4 is a viable alternative to S2. Can they expand on which structure reflects the true mechanisms if both have very similar agreement with observations?

We agree that models S2 and S4 show similar performance and therefore cannot be uniquely distinguished based on the available data. Both model structures assume the presence of a COS compensation point, but differ in the steepness of its temperature dependence. While posterior costs were comparable, S2 consistently showed the lowest RMSE and most closely reproduced the observations from Experiment 1 (Fig. 2.9). Based on this overall performance across multiple metrics, S2 was therefore selected as the best-performing model in this study. We have expanded the Discussion to clarify this rationale and to note that, even if S4 were to better represent the true mechanism, the key conclusion of a temperature-dependent COS compensation point remains unchanged, although the exact optimum temperature associated with Hypothesis H3 may vary slightly.
4.1. Uncertainties in measurements and models Taken together, the remaining uncertainties in both COS measurements and model structure require careful interpretation. Concerning Hypothesis 1, Model S2 was selected as the best model due to its

minimal posterior costs and lowest RMSE with observation-based Γ_{COS}, despite higher H_2O and background costs compared to S1, as shown in Table 2.6. Furthermore, the minor differences in posterior costs and RMSE with indirectly derived Γ_{COS} between S2 and S4 suggest that S4 is a viable alternative. The strong correlation between the temperature dependence of Γ_{COS} (m_{COS}) and $V_{max,CA}$ complicates the precise and independent determination of these two parameters. Although S2 and S4 employ different temperature-dependent formulations of Γ_{COS}, both model structures consistently support the presence of a COS compensation point. Accordingly, the exact value and temperature dependence of Γ_{COS} remain uncertain, but including a compensation point in the models, as in models S2 and S4, significantly improves their alignment with observations. Even if S4 were to better represent the true underlying mechanism, both model structures indicate an increase in Γ_{COS} with temperature, although the optimum temperature derived under Hypothesis 3 may shift slightly depending on the assumed functional form of the temperature response of CA activity.

Minor comments:

1. Consider submitting manuscripts for peer review with line numbers.

We thank the reviewer for this suggestion. The manuscript template from Open Research Europe does not support the inclusion of line numbers. We will contact Open Research Europe to clarify whether line numbers can be included within the provided manuscript template.

1. The paragraph structure of the manuscript needs extensive editing.

We thank the reviewer for this comment. We carefully revisited the manuscript to improve paragraph structure and overall readability. In particular, Section 4.1 has been reorganized to more clearly separate experimental limitations from model-related uncertainties, and several long paragraphs were divided and streamlined to ensure that each paragraph addresses a single, well-defined topic. Transitions between experimental constraints and structural model assumptions were clarified to improve logical flow. Minor adjustments were also made in other sections to enhance coherence and reduce redundancy. We believe these revisions substantially improve the readability and structural clarity of the manuscript.

1. Caption for Table 1 might need revision. It says, “designed to investigate responses of V_{COS} and V_{CO2} to g_s and g_m, respectively.” Was experiment 3 investigating the response to T_{leaf} or g_m? I’m assuming T_{leaf} since that is what the table header and manuscript text says.

We thank the reviewer for pointing this out. The reviewer is correct that Experiment 3 investigated responses to leaf temperature (T_{leaf}). While T_{leaf} was the manipulated variable, this experiment was designed to explore temperature-driven changes in mesophyll conductance (g_m), for which T_{leaf} is a major controlling factor. We have revised the caption of Table 1 accordingly to clarify this distinction and ensure consistency with the table header and manuscript text.

Table 1. Environmental conditions during the three experiments. The range of controlled and constant variables for each experiment is expressed as minimum–maximum and mean ± standard deviation, respectively. Experiment 1 (Sunflower 1) aimed to detect COS

compensation points at two temperatures. Experiments 2 (Sunflower 2, 3, and 4) and 3 (Sunflower 2 and 4) were designed to investigate responses of V_{COS} and V_{CO2} to stomatal conductance (g_s) and leaf temperature (T_{leaf}), respectively, with T_{leaf} acting as a primary driver of mesophyll conductance (g_m) . We controlled a designated variable in each experiment while other variables including light intensity, air flow rate, and mixing fan speed were kept constant.

Competing Interests: No competing interests were disclosed.

Version 1

Reviewer Report 24 September 2025

https://doi.org/10.21956/openreseurope.21895.r58703

?

Max Berkelhammer
University of Illinois Chicago, Chicago, USA

This paper presents a set of leaf chamber and modeling experiments to test fundamental and poorly constrained aspects of the leaf-level exchange of OCS. The authors show evidence of a temperature-dependent compensation point and indicate how the differential effects of temperature and VPD on OCS and CO2 change the relative uptake of these two gases. Firstly, I'd like to commend the authors on difficult lab experiments that were well-designed and executed. Secondly, the modeling experiments allowed the authors to clearly test three fundamental hypotheses. While the sources of uncertainty in the experiments are large, the manuscript raises a lot of interesting questions that open the door for interesting work to come. So while I support the publication of the manuscript, I do feel that the structure and style of the manuscript requires some careful considerations.

1. The paper is written in a strange style where many paragraphs seem to be one sentence and essentially like a bullet point. I am not sure if this was intentional or some artifact of the formatting. Nevertheless, paragraphs should be structured in a more standard format where the reader knows the purpose of the paragraph from the opening sentence and the end of the paragraph sets up the next paragraph. The issue is not just about following traditional writing structure but, as is, the flow of the paper is not great. I think the authors should consider improving the flow, removing some superfluous text and following standard formatting. That said, the individual sentences were generally well-written and there were barely any grammatical issues.
2. As I was reading the paper, I found myself thinking a lot about the Stimler experiments and how they compared. The authors bring in the details of the Stimler paper in the Discussion but this should be part of the Introduction. For example, the fact that Stimler also saw a

compensation point at around pmol mol should be discussed in the beginning of the paper. Furthermore, it would be interesting, if reasonable, to actually add some of the Stimler results to your figures so the authors can directly see how the results compare.

3. The authors note some ecosystem studies like those of Maseyk that suggest a compensation point or emission at high temperature but, I believe, these were emissions after the crops had senesced and were possibly from the soil. Please clarify if they actually documented emissions from living wheat.
4. Perhaps this was discussed in previous studies but is there any documentation here on how the uncertainty of the instrument varies with OCS concentration. At these low concentrations – around 100 pmol mol – how uncertain are the measurements?
5. Insufficient attention was paid to the potential importance of the temperature-dependent OCS uptake from the empty cuvette. For example, at 25C, the uptake of OCS varies from 0 to -12.5. This is a big range and obviously highly significant when considering the question of compensation points and very low fluxes at low [OCS] concentrations. When I see in Figure 4 that the uncertainty of the flux is about 5 pmol m-2 s-1 at 100 pmol mol-1, this seems discordant with such a potentially large range in fluxes from the empty chamber. I acknowledge that this may be dealt with in the statistics so I am not, per se, questioning the result but just asking for more careful deliberation about the potential impacts of the empty chamber flux.
6. The authors acknowledge this in the Discussion but I also found myself concerned by the fact that the experiments were optimized using observations conducted under conditions where [OCS] was an order of magnitude higher than the compensation point yet these simulations were used to study compensation point dynamics. I understand the operational reasons for this and I think the authors were transparent about this but it leaves quite a lot of room for future studies.

No page numbers.
Line 1: “quantifies the _____ gross CO2….” Should that “largest gross”?
Top of Page 5: “stomatal closure like the case”
Page 10: The text following Equation 7 needs to be rewritten

Is the work clearly and accurately presented and does it cite the current literature?
Yes

Is the study design appropriate and does the work have academic merit?
Yes

Are sufficient details of methods and analysis provided to allow replication by others?
Yes

If applicable, is the statistical analysis and its interpretation appropriate?
Yes

Are all the source data underlying the results available to ensure full reproducibility?
Yes

Are the conclusions drawn adequately supported by the results?

Partly

Competing Interests: No competing interests were disclosed.

Reviewer Expertise: Atmosphere, Climate and Ecosystems

I confirm that I have read this submission and believe that I have an appropriate level of expertise to confirm that it is of an acceptable scientific standard, however I have significant reservations, as outlined above.

Author Response 03 Dec 2025

Ara Cho

1. The paper is written in a strange style where many paragraphs seem to be one sentence and essentially like a bullet point. I am not sure if this was intentional or some artifact of the formatting. Nevertheless, paragraphs should be structured in a more standard format where the reader knows the purpose of the paragraph from the opening sentence and the end of the paragraph sets up the next paragraph. The issue is not just about following traditional writing structure but, as is, the flow of the paper is not great. I think the authors should consider improving the flow, removing some superfluous text and following standard formatting. That said, the individual sentences were generally well-written and there were barely any grammatical issues.

We sincerely thank the reviewer for this valuable comment and fully agree that the previous version of the manuscript suffered from an overly fragmented paragraph structure, which reduced the overall readability and logical flow. To address this issue, we thoroughly revised the manuscript to ensure that each paragraph now follows a clear logical structure: an opening statement that introduces the main idea, supporting sentences that develop the argument, and a concluding sentence that transitions smoothly to the next paragraph. In particular, we merged overly short bullet-like paragraphs and added linking sentences.As a result, we hope that the manuscript now reads more easily, and that the connection between experimental observations, model results, and their broader implications is clearer.
Because these revisions were made throughout the manuscript to improve the overall readability and flow, we did not mark them individually in the main text.

2. As I was reading the paper, I found myself thinking a lot about the Stimler experiments and how they compared. The authors bring in the details of the Stimler paper in the Discussion but this should be part of the Introduction. For example, the fact that Stimler also saw a compensation point at around pmol mol should be discussed in the beginning of the paper. Furthermore, it would be interesting, if reasonable, to actually add some of the Stimler results to your figures so the authors can directly see how the results compare.

We thank the reviewer for this helpful suggestion. In the revised manuscript, we have incorporated the key details of the Stimler et al. (2010) study into the Introduction, providing a clearer background and establishing the context for our investigation of the COS compensation point. Specifically, we now mention that Stimler et al. observed a

compensation point of 60.7 pmol mol^{-1}, despite it being statistically indistinguishable from zero, and interpreted it as a diffusional feedback under high COS mole fractions. This helps frame our study within prior findings and emphasizes the motivation for exploring temperature-dependent behavior in vascular plants. However, we have chosen not to include the Stimler et al. (2010) results in our figures, because direct graphical comparison is not scientifically consistent across species and experimental conditions. Stimler et al. (2010) investigated *Salvia indigo spires*, while Kesselmeier and Merk (1993) reported Γ_{COS} values of 90 pmol mol^{-1} for *rapeseed* and 144 pmol mol^{-1} for *corn*, and our study focused on *Helianthus annuus* (sunflower). These species differ substantially in leaf anatomy, sulfur metabolism, and stomatal physiology, leading to large inherent variations in COS compensation points. Moreover, experimental setups (e.g., light intensity, humidity, chamber design, etc) and analytical precision differed between studies, making a direct quantitative comparison potentially misleading.

Γ_{COS} have been reported in a few vascular plants, algae, crops, and lichen fields (Belviso et al., 2022; Geng & Mu, 2004; Goldan et al., 1988; Kesselmeier & Merk, 1993; Kuhn & Kesselmeier, 2000; Maseyk et al., 2014). These measured Γ_{COS} values are lower than typical atmospheric COS mole fractions ($\approx$ 500 pmol mol -1), which is why net COS uptake is observed. Stimler et al. (2010) also observed a Γ_{COS} of 60.7 pmol mol -1, though statistically indistinguishable from zero, and interpreted it as a possible diffusional feedback under high COS mole fractions. More recently, Gimeno et al. (2017) demonstrated temperature-dependent COS emissions in nonvascular bryophytes, suggesting that biochemical processes such as protein degradation could contribute to COS release at elevated T_{leaf}. However, Γ_{COS} of vascular plants and its temperature dependence remain poorly constrained. We therefore hypothesize that the observed COS uptake results from the coexistence of uptake and production processes, with Γ_{COS} exhibiting temperature dependence.

4.2. Possible causes of a COS compensation point> Previous studies on COS leaf exchange experiments have reported positive Γ_{COS} values, but often concluded these are statistically indistinguishable from zero due to high variability. For example, Stimler et al. (2010) observed a Γ_{COS} of 60.7 pmol mol^{-1} at 25 °C and attributed it to potential retro-diffusion under high COS mole fractions. Similarly, our Γ_{COS} at 20.0 °C (55.0 ± 53.2 pmol mol^{-1}) was statistically insignificant, whereas a significant Γ_{COS} (138.7 ± 26.1 pmol mol^{-1}) was detected at 25 °C. Considering that our experiments, like those of Stimler et al. (2010), were conducted under relatively high COS mole fractions, this pattern suggests that higher temperature may enhance diffusion-driven feedbacks. It should also be noted that our COS model does not explicitly account for mesophyll diffusion conductance, and thus part of the apparent emission function could be interpreted as an effect of internal diffusion-related mechanisms (e.g., retro-diffusion) within the leaf. The authors note some ecosystem studies like those of Maseyk that suggest a compensation point or emission at high temperature but, I believe, these were emissions after the crops had senesced and were possibly from the soil. Please clarify if they actually documented emissions from living wheat. We thank the reviewer for this insightful comment. Both Maseyk et al. (2014) and Belviso et al. (2022) reported transitions from COS uptake to COS emission during the ripening and senescence phases of wheat (and rapeseed). These emissions are therefore likely associated with senescence-related processes rather than active

uptake or release from photosynthetically functioning tissues. Maseyk et al. (2014) additionally noted that part of the observed emissions could originate from the soil, whereas Belviso et al. (2022) provided stronger evidence for plant-derived emissions during senescence. Based on this, we clarify this point and discuss these studies only in the context of senescence-related ecosystem COS emissions.

4.2. Possible causes of a COS compensation point> Previous studies (e.g., Maseyk et al., 2014; Belviso et al., 2022) reported that COS emissions occur during the ripening and senescence phases, indicating that senescence-related processes could explain COS emissions rather than active uptake from living tissues. In Maseyk et al. (2014) part of these emissions may have originated from the soil, whereas Belviso et al. (2022) provided strong evidence for plant-derived senescence emissions. Additionally, Kesselmeier and Merk (1993) reported Γ_{COS} values ranging from 57 to 328 pmol mol^{-1} in rapeseed and corn during flowering. Perhaps this was discussed in previous studies but is there any documentation here on how the uncertainty of the instrument varies with OCS concentration. At these low concentrations – around 100 pmol mol – how uncertain are the measurements? To our knowledge, specific evaluations of QCLS precision as a function of COS mole fraction at low level have not been explicitly reported in the literature. However, previous studies have demonstrated a typical precision of approximately 7.5 pmol mol^{-1} for COS at low ambient mole fractions (Kooijmans et al., 2016). We have now added this information to the Results section (Section 3.1.1) and included a quantitative uncertainty analysis that propagates both instrumental and regression-derived errors (from empty chamber) into the estimation of Γ_{COS}. This addition clarifies that, even when accounting for this uncertainty, the Γ_{COS} value observed at 25 °C remains statistically robust.

<3.1.1. COS Compensation Point (Experiment 1)>
We quantified the regression-based Γ_{COS} using a linear function at two temperatures: Γ_{COS} was 55.0 ± 53.2 pmol mol^{-1} at 19.8 °C and 138.7 ± 26.1 pmol mol^{-1} at 25.0 °C (error estimates denote 95 % confidence interval). These results indicate that Γ_{COS} increases with rising T_{leaf}, suggesting a potential temperature dependence. Although the empty-chamber regression effectively removed the baseline COS emission, some residual variability likely remained (RMSE = 6.9 pmol mol^{-1} for $[COS]_a$ and 2.73 pmol m^{-2} s^{-1} for F_{COS}). To evaluate the potential influence of this unresolved background variability, we propagated these residual errors to the regression-derived Γ_{COS}. When the uncertainty is included, the 95% confidence interval of Γ_{COS} widened from ± 53.2 to ± 93.4 pmol mol^{-1} at 19.8 °C and from ± 26.1 to ± 48.9 pmol mol^{-1} at 25.0 °C. The large uncertainty at 19.8 °C indicates that the corresponding Γ_{COS} value is statistically indistinguishable from zero. By contrast, the Γ_{COS} measured at 25 °C remains significant even when this propagated and instrumental uncertainty is considered. Even accounting for the reported QCLS uncertainty of approximately 7.5 pmol mol^{-1} for COS (Kooijmans et al., 2016), the Γ_{COS} value at 25 °C remains statistically robust.
Kooijmans LMJ, Uitslag NAM, Zahniser MS, et al.: Continuous and high-precision atmospheric concentration measurements of COS, CO2, CO and H2O using a quantum cascade laser spectrometer (QCLS). Atmos. Meas. Tech. 2016;9. 10.5194/amt-9-5293-2016 Insufficient attention was paid to the potential importance of the temperature-

dependent OCS uptake from the empty cuvette. For example, at 25C, the uptake of OCS varies from 0 to -12.5. This is a big range and obviously highly significant when considering the question of compensation points and very low fluxes at low [OCS] concentrations. When I see in Figure 4 that the uptake of the flux is about 5 pmol m-2 s-1 at 100 pmol mol-1, this seems discordant with such a potentially large range in fluxes from the empty chamber. I acknowledge that this may be dealt with in the statistics so I am not, per se, questioning the result but just asking for more careful deliberation about the potential impacts of the empty chamber flux. We appreciate the reviewer's insightful comment highlighting the potential influence of temperature-dependent COS uptake from the empty cuvette. We agree that variations in background COS flux could affect the estimation of low leaf fluxes and compensation points, particularly under low COS mole fraction conditions. In the revised manuscript, we have clarified how this issue was quantitatively addressed. Specifically, we incorporated the residual variability of the empty chamber into the uncertainty analysis by propagating the RMSEs of 6.9 pmol mol^{-1} for $[COS]_a$ and 2.73 pmol m^{-2} s^{-1} for F_{COS} into the regression-derived Γ_{COS}. This approach effectively accounts for the potential influence of empty-cuvette temperature dependence on the estimated compensation point. Furthermore, as shown in Section 3.1.1, we explicitly report that the Γ_{COS} value at 19.8 °C is statistically indistinguishable from zero when this propagated uncertainty is considered, while the Γ_{COS} at 25 °C remains significantly positive. This result indicates that, although some temperature-dependent background variability may remain, it does not alter the overall conclusion that Γ_{COS} increases with temperature. We have now added a short statement in Section 3.1.1 to explicitly acknowledge this potential influence and clarify that it was incorporated into our total uncertainty estimation.

<3.1.1. COS Compensation Point (Experiment 1)>
We quantified the regression-based Γ_{COS} using a linear function at two temperatures: Γ_{COS} was 55.0 ± 53.2 pmol mol^{-1} at 19.8 °C and 138.7 ± 26.1 pmol mol^{-1} at 25.0 °C (error estimates denote 95 % confidence interval). These results indicate that Γ_{COS} increases with rising T_{leaf}, suggesting a potential temperature dependence. Although the empty-chamber regression effectively removed the baseline COS emission, some residual variability likely remained (RMSE = 6.9 pmol mol^{-1} for $[COS]_a$ and 2.73 pmol m^{-2} s^{-1} for F_{COS}). To evaluate the potential influence of this unresolved background variability, we propagated these errors to the regression-derived Γ_{COS}. When the uncertainty is included, the 95% confidence interval of Γ_{COS} widened from ± 53.2 to ± 93.4 pmol mol^{-1} at 19.8 °C and from ± 26.1 to ± 48.9 pmol mol^{-1} at 25.0 °C. The large uncertainty at 19.8 °C indicates that the corresponding Γ_{COS} value is statistically indistinguishable from zero. By contrast, the Γ_{COS} measured at 25 °C remains significant even when this propagated and instrumental uncertainty is considered. Even accounting for the reported QCLS uncertainty of approximately 7.5 pmol mol^{-1} for COS (Kooijmans et al., 2016), the Γ_{COS} value at 25 °C remains statistically robust. The authors acknowledge this in the Discussion but I also found myself concerned by the fact that the experiments were optimized using observations conducted under conditions where [OCS] was an order of magnitude higher than the compensation point yet these simulations were used to study compensation point dynamics. I understand the operational reasons for this and I think the authors were transparent

about this but it leaves quite a lot of room for future studies. We agree that the optimization was performed under high COS mole fractions, which may limit the interpretation of compensation point dynamics under near-ambient concentrations. Our COS model indeed parameterizes Γ_{COS} as a temperature-dependent function and does not explicitly include a diffusivity or the impact of inflowing COS mole fractions due to the limited stability of COS detection at low ambient levels. We have now clarified this limitation in the Discussion, noting that current measurement systems allow reliable detection only under elevated COS levels. We also emphasize that future work with improved precision at low COS concentrations will help determine whether Γ_{COS} varies with ambient [COS] due to retro-diffusion or other physiological mechanisms.

<4.1. Uncertainties in measurements and models> In addition to the experimental limitations discussed above, a practical limitation arises from the mole fraction range used for model optimization. Model parameters were optimized using data obtained under relatively high COS mole fraction conditions (~1000 pmol mol^{-1}) to ensure stable and precise flux measurements, whereas Γ_{COS} was determined from experiments conducted at lower inflowing concentrations (100–600 pmol mol^{-1}). This discrepancy in concentration ranges may introduce some uncertainty when extrapolating parameters between optimization and compensation-point estimation. Nevertheless, the model formulation remains internally consistent, and the derived parameters are valid for interpreting the relative temperature-dependent behavior of COS exchange. Future experiments targeting near-ambient COS mole fraction levels will be valuable to further validate the applicability of these optimized parameters and to evaluate potential retro-diffusion effects under more natural conditions. <4.2. Possible causes of a COS compensation point> Taken together, the existence of Γ_{COS} and its increase at higher temperatures may result from a combination of the factors discussed above. However, our current formulation of Γ_{COS} is expressed solely as a temperature-dependent function and does not explicitly include retro-diffusion effects. As a result, while the observed increase in Γ_{COS} with temperature is consistent with thermally driven processes, the potential contribution of internal diffusion feedbacks—particularly under elevated COS mole fractions—cannot be fully excluded. At present, reliable measurements can only be obtained under relatively high COS mole fractions, which limits our ability to fully constrain Γ_{COS} dynamics near ambient conditions. Improving detection precision at low COS concentrations and incorporating explicit representations of internal diffusion in future models would enable a more direct evaluation of whether Γ_{COS} variability originates from retro-diffusion or from physiological and biochemical processes. Moreover, extending such measurements to different phenological stages and species, and exploring interactions with microbial associations and environmental stressors, will be essential for developing a more mechanistic understanding of COS exchange in plants. No page numbers.
Line 1: "quantifies the ____ gross CO2…." Should that "largest gross"? We have modified the sentence to "Gross primary productivity (GPP) quantifies the largest terrestrial CO_2 uptake flux in the global carbon cycle." Top of Page 5: "stomatal closure like the case" We have revised the sentence to improve clarity. The phrase "like is the case for CO_2" has been replaced with "as is the case for CO_2" to ensure

grammatical correctness and a smoother flow. Page 10: The text following Equation 7 needs to be rewritten We appreciate the reviewer's suggestion. The sentence has been revised for clarity. It now reads: <2.2.1. General concept> Although accounting for the H_2O ternary system is important, its influence on the calculated mole fractions was found to be negligible. The smaller ternary effects within the leaf boundary layer were therefore not included, as they scale with E / g_{bw} (von Caemmerer & Farquhar, 1981, Equation B10) and are expected to be negligible under our experimental conditions (large g_{bw} and small E). Note that the mole fractions calculated by the model are expressed on a wet-air basis, whereas the observed mole fractions are reported on a dry-air basis. The moisture removal applied to model outputs is described at the end of this section. To test Hypothesis 2, we analyzed how the intercellular mole fraction $[gas]_i$ influences the net flux. The flux was computed using Equation 3, Equation 6, and Equation 7 to determine $[gas]_i$, and then applied to the flux-gradient relationship:

Competing Interests: No competing interests were disclosed.

Reviewer Report 23 September 2025

https://doi.org/10.21956/openreseurope.21895.r58706

?

Jerome Ogee
[1] Bordeaux Sciences Agro, Villenave d'Ornon, France
[2] ISPA, Institut National de Recherche pour l'Agriculture l'Alimentation et l'Environnement Centre Nouvelle-Aquitaine Bordeaux (Ringgold ID: 113907), Villenave-d'Ornon, Aquitaine-Limousin-Poitou-Charentes, France

The manuscript presents original gas exchange data of COS and CO2 fluxes on sunflower leaves that indicate COS emissions from leaves that increase with temperature. This is a rather unique dataset because very few groups have managed to measure leaf COS gas exchange due to the presence of COS-emitting surfaces in such systems that complicate the interpretation of the results (and the identification of COS emissions from the leaf itself). The authors seem to have addressed this issue rather well, and the data seems of good quality, and in support of what is advanced in the title and abstract.

Despite all these very good points, writing the review was quite difficult because I found some issues in the manuscript that needed to be addressed and wanted to propose the most constructive way of doing so. I think I came up with a good plan that I hope the authors will agree with and follow. In particular, I did not find the modelling aspect of the study very convincing, as many assumptions and shortcuts were not well justified (see below). More importantly, I think that the modelling exercise is not needed and weakens the study (because of those many assumptions and shortcuts) and therefore I strongly suggest to refocus the paper strictly on the data, which is

sufficient to support the main findings (or test the three main hypotheses). By doing so, the authors will need to revise their data analysis as well, because the equations to compute the gas exchange fluxes and conductances seem to contain some mistakes (in the text at least, I have not checked the code), leaving the reader with the impression that the theory behind has been misunderstood or at least wrongly applied. This is a concern because the data seems of good quality and there are good chances that the results may not change much after corrections, but we can never be sure until those changes are made. I think by refocusing the paper on the data analysis only would make the manuscript much shorter and stronger, with a clearer message. The modelling part could be the topic of another (separate) study, but this would require a better justification of some modelling assumptions beforehand. Below I have listed my major concerns and provide directions to address them.

Because the manuscript has no line numbers, I refer below to equation or section numbers instead of line numbers.

In Eq 1 the authors do not account for the change of air flow on the outlet of the cuvette due to the extra moisture brought about by transpiration (see Appendix 2 of von Caemmerer and Farquhar 1981 - noted vCF81 from now - or the LICOR's manual). These equations also do not account for the fact that, unlike the LICOR's IRGA, the QCLS instrument measures CO2 (and COS) mixing ratios on a dry air basis. Note also that a different equation should be used to estimate transpiration (see Eq B5 in vCF81).

In Eqs 3-5 and 6-7, the air volume in the storage term should not be the entire chamber volume, and also because the ternary correction terms are not accounted for properly. Also, in Eq 3, the flux calculation should account for the difference in mass flow entering and exiting the leaf cuvette (see comment about Eq 1) and the "flux-gradient" calculation should include ternary corrections. Eq 6 implicitly assumes that the ternary correction is only important within the stomata, and not in the leaf boundary layer, and Eqs 6-7 are inconsistent with Eq 8 that neglects ternary correction. Fortunately, these "step-by-step" equations are not needed to interpret gas exchange data, and global equations like Eq B17 in vCF81 should be used instead (but with a clear distinction of mixing ratios on a dry or wet air basis).

In Eq 8, ternary corrections are missing (see above and Eq B17 in vCF81).

Eq 10 is correct but the distinction between mixing ratios on a dry and wet air should be made earlier. Also, the whole sentence leading to this Eq 10 is extremely confusing and should be rewritten and simplified.

Eq 11 and the notion of "mesophyll conductance" for water vapour is quite debated (i.e. assuming that the air is not saturated in the leaf stomatal cavity) and unjustified here where the leaves were not exposed to very dry air or high temperature or light levels. Also the value of 10 mol/m2/s for that conductance is so high (4 times larger than the boundary-layer conductance) that its effect is probably negligible, and so introducing this new variable (and Eq 13 below) is pointless. I would recommend to neglect it, as it is normally done in the LiCOR manual.

Eqs 14-17 are not needed to interpret gas exchange data, and test the three hypotheses, because only fluxes and LRU values are shown afterwards. Also in Eq 15, it should, not be CO2_i but CO2_c (at the chloroplast level).

In Eq 18, why assuming that mesophyll conductance to COS is only biochemical? There should be a diffusional part considered. But again, this parameterisation of mesophyll conductance for COS is not needed for testing the three hypotheses and interpret gas exchange data.

Eqs. 19-21 present three possible temperature responses for the estimated “compensation point" for COS. It is a bit strange to show results (Figure 3 with observational data points) here. I think this section (and Eq 19-21) should be brought in the Results section directly. It is not part of the Methods.

Eqs 22 neglects changes in mass flow between the inlet and outlet (see Eq B7 in vCF81) and Eqs 23-24 are also incorrect (see comment above on Eq 6-7). I don’t understand why stomatal conductance is not derived directly from the measurements (see LiCOR’s manual or Eq B14-15 in vCF81). Given the high boundary-layer conductance (about 3-4 times stomatal conductance), the sensitivity of stomatal conductance to the exact choice of “K" is very small (see LICOR manual) and it is much more reliable than an “optimized” value based on a simplified model of photosynthesis (and COS uptake), with lots of unknown parameter values. Also, it seems odd to estimate a compensation point for COS using a model that requires a parameterisation of this compensation point. If the idea is to compute the COS concentration in the intercellular air space, an equation similar to Eq B18 In vCF81 could be used (see also Stimler et al 2010). But in the end, the compensation point for COS is only estimated from the intercept of the regression line of FCOS vs [COS]a (Figure 4) so only COS flux calculations are needed, and sections 2.2.3, 2.2.4 and 2.3 could be removed from the manuscript.

Section 2.4 could also be removed if the modelling part is taken out (as I suggest). There is no need of a biochemical model that needs to be “parameterised” to discuss the gas exchange results presented here. As I explained above, what needs to be done instead is to compute gas exchange parameters (fluxes, conductances, etc) following the LICOR manual (but accounting for the fact that the QCLS computes mixing ratios on this dry air basis). This would make the manuscript much shorter and easier to read and follow.

The discussion about measurement errors on stomatal conductance at the end of section 2.4.1 lacks some justification (where does the extra measurement error comes from?). But this part should be removed anyway, because this measurement error was only used for the biochemical model optimization that I propose to get rid of.

In section 2.4.2 and Eq 25, the introduction of “weights" in the cost function is difficult to understand because it seems that those weights are there to wipe out differences in observational error between CO2, COS and H2O. But the cost function is normalised by these error terms for a reason, no? And again if the biochemical model optimization is removed, section 2.4 is also removed, and this comment is not relevant anymore.

In section 3.1.1, you mention a “20% increase" of what? Stomatal conductance? Also it would be good to propagate errors due to the COS emission from the chamber (the scatter on Fig 1 is rather large) and clearly state whether the retrieved composition point are all statistically different from zero.

I have not finalized the review of the end of the manuscript but I see that Figs 7-9 and most Tables

except Table 1 could be removed as they show results from the biochemical model optimization that, to me, should be removed because I do not see what it brings to the study. My suggestions would make the paper much more digest and strong, and the main message should stay almost unchanged. I hope the authors will agree with this suggestion.

Is the work clearly and accurately presented and does it cite the current literature?
Partly

Is the study design appropriate and does the work have academic merit?
Yes

Are sufficient details of methods and analysis provided to allow replication by others?
Partly

If applicable, is the statistical analysis and its interpretation appropriate?
Partly

Are all the source data underlying the results available to ensure full reproducibility?
Yes

Are the conclusions drawn adequately supported by the results?
Partly

Competing Interests: No competing interests were disclosed.

Reviewer Expertise: Land-atmosphere interactions, micrometeorology, plant ecophysiology, carbon cycle

I confirm that I have read this submission and believe that I have an appropriate level of expertise to confirm that it is of an acceptable scientific standard, however I have significant reservations, as outlined above.

Author Response 03 Dec 2025

Ara Cho

In Eq 1 the authors do not account for the change of air flow on the outlet of the cuvette due to the extra moisture brought about by transpiration (see Appendix 2 of von Caemmerer and Farquhar 1981 - noted vCF81 from now - or the LICOR's manual). These equations also do not account for the fact that, unlike the LICOR's IRGA, the QCLS instrument measures CO2 (and COS) mixing ratios on a dry air basis. Note also that a different equation should be used to estimate transpiration (see Eq B5 in vCF81).

We thank the reviewer for pointing out this important issue regarding outlet air flow and the mixing ratio basis. We note that this effect was initially considered during model development; however, implementing a full correction would require the outflowing H_2O mole fraction—estimated by the model—to be fed back as an input variable to adjust the

outlet flow, which is beyond the current model framework. Therefore, we chose not to apply this correction explicitly but verified that its effect is minor.
In the revised manuscript, we have stated that our analysis is based on dry-air mixing ratios, consistent with the QCLS instrument, while the model internally uses wet-air mixing ratios. The conversion between these two bases is explicitly introduced in Equation 10. Regarding the outlet mass flow, we have now added an explanation and citation to von Caemmerer & Farquhar (1981, Appendix 2, Eqs.B3-B5), which describe the correction for increased outlet flow due to transpired water vapor. Under our experimental conditions ([H2O]_out = 15–30 mmol mol^{-1}), this correction leads to a change in calculated fluxes of $\leq$ 3%, which we consider negligible for the conceptual interpretation of CO_2, COS, and H_2O fluxes. Importantly, this correction was not applied to either the observed or modeled fluxes, so the model–observation comparison remains internally consistent. We have added a statement in the Methods acknowledging this assumption and its potential effect (<3%).

Here, the [gas]_in and [gas]_out represent the mole fractions of COS (pmol mol^{-1}) and CO_2 (µmol mol^{-1}) in the air entering and exiting the chamber, which are measured by the QCLS on a dry-air basis. The leaf area S (m^2) was 9 cm^2. Although transpiration slightly increases the outlet air flow due to the addition of water vapor (von Caemmerer & Farquhar, 1981, Appendix 2), the resulting increase in total molar flow (< 3% under $[H_2O]$_out = 15–30 mmol mol^{-1}) was neglected in Equation 1 for simplicity. Since this was only a small effect, it was not considered in the flux calculations and was consistently omitted throughout the model analysis. The CO_2 leaf assimilation rates obtained from the QCLS measurements closely matched those from the LI-6800 (R = 0.96, mean difference = 0.18 µmol m^{-2} s^{-1}), confirming the accuracy of the CO_2 flux measurements.

In Eqs 3-5 and 6-7, the air volume in the storage term should not be the entire chamber volume, and also because the ternary correction terms are not accounted for properly. Also, in Eq 3, the flux calculation should account for the difference in mass flow entering and exiting the leaf cuvette (see comment about Eq 1) and the "flux-gradient" calculation should include ternary corrections. Eq 6 implicitly assumes that the ternary correction is only important within the stomata, and not in the leaf boundary layer, and Eqs 6-7 are inconsistent with Eq 8 that neglects ternary correction. Fortunately, these "step-by-step" equations are not needed to interpret gas exchange data, and global equations like Eq B17 in vCF81 should be used instead (but with a clear distinction of mixing ratios on a dry or wet air basis).

We thank the reviewer for the insightful comments. We agree that the air volume in the storage term should not correspond to the entire chamber volume. In our formulation (Eqs.3-5), the first term on the left-hand side represents the rate of gas accumulation (d[gas]/dt), but under steady-state conditions, this term becomes negligible. Accordingly, we have clarified in the revised manuscript that V_CV refers to the effective air volume representing the gas-exchange region near the leaf surface, rather than the total chamber volume.
We note that the ternary corrections were already included in our Eqs. 6-7 following Jarman (1974) and von Caemmerer and Farquhar (1981) (vCF81). These equations account for the coupling between H_2O diffusion and COS & CO_2 transport at the stomatal level through the

"F_H2O([gas]_b+[gas]_i)/2" term, which is formulated on a wet-air mole fraction basis consistent with the diffusion formulation in vCF81.
By contrast, the QCLS instrument measures COS and CO_2 mole fractions on a dry-air basis. To ensure consistency, the model outputs were converted from wet-air to dry-air mole fractions using the relation described in Equation 10 before comparison with observations. We have clarified this distinction in the revised manuscript.
Equation 8, by contrast, is a simplified steady-state expression used only for diagnostic evaluation (i.e., to compute AFR in Section 3.2.3), not for model calculation. Therefore, although Equations 6–8 are not fully consistent, the ternary system at the stomatal level is appropriately represented within the model.
For the boundary layer, von Caemmerer & Farquhar (1981, Equation B10) showed that the ternary correction scales as c¯E/gbc¯E/gb, where \bar{c} is the mean gas mole fraction between ambient and boundary air. Although this term cannot be precisely quantified in our dataset (as \bar{c} was not directly measured), the ternary correction at the boundary layer is expected to be negligible under our experimental conditions because g_b (~2.44 mol m^{-2} s^{-1}) was much larger than g_s and transpiration (E) was small (0.0028–0.0081 mol m^{-2} s^{-1}).
Therefore, we applied ternary corrections only at the stomatal interface (Eqs. 6–7) and neglected them in the boundary layer for computational efficiency, where their effect is theoretically minor.

Here, V_m (m^3 mol^{-1}) is the molar volume, and V_CV (m^3) is the effective air volume representing the gas-exchange region near the leaf surface. Under steady-state conditions, the first term on the left-hand side of Equation 3, Equation 4, and Equation 5, which represents the rate of gas accumulation, becomes negligible. To account for the different properties of COS and CO_2 to H_2O, the stomatal conductances (g_s,COS and g_s,CO2) and the boundary layer conductances (g_b,COS and g_b,CO2) are scaled proportionally to the conductance of water vapor (g_{sw} and g_{bw}) ...
For the COS and CO_2 exchange at the stomatal level, a ternary system with H_2O and air should be considered, because the transpiration (F_H2O (mol m^{-2} s^{-1})) is significantly larger than COS and CO_2 assimilation (Jarman, 1974; von Caemmerer and Farquhar, 1981). Thus, we added the ternary term in Eqs. 4 and 5 for the COS and CO_2 models:

...Equation 6 7...

Although accounting for the H_2O ternary system is important, its influence on the calculated mole fractions was found to be negligible. The smaller ternary effects within the leaf boundary layer were therefore not included, as they scale with E / g_bw (von Caemmerer & Farquhar, 1981, Equation B10) and are expected to be negligible under our experimental conditions (large g_bw and small E). Note that the mole fractions calculated by the model are expressed on a wet-air basis, whereas the observed mole fractions are reported on a dry-air basis. The moisture correction applied to model outputs is described at the end of this section. To test Hypothesis 2, we analyzed how the intercellular mole fraction $[gas]_i$ influences the net flux. The flux was computed using Equation 3, Equation 6, and Equation 7 to determine $[gas]_i$, and then applied to the flux-gradient relationship:

In Eq 8, ternary corrections are missing (see above and Eq B17 in vCF81).

We thank the reviewer for pointing this out. We clarify in the text that Equation 8 is not part of the model optimization or flux calculation; rather, they are used solely to define the Apparent Flux Ratio (AFR) introduced later in Section 3.2.3. This distinction ensures conceptual consistency with the vCF81 framework while keeping the equations' role in our analysis transparent.

The term $(1-[gas]_i\,[gas]_a^{-1})$ represents the effect of changes between internal and ambient mole fractions on the gas conductance and deposition velocity, termed Ambient Fraction Remaining (AFR). This concept is utilized in Sect. 3.2.3 for interpreting Hypothesis 2. Strictly speaking, the mass flow difference between the inlet and outlet and the ternary effect should be considered in Equation 8 and Equation 9. However, these effects are expected to be minor under our experimental conditions (see above), and Equation 8 and Equation 9 were used only to examine the conceptual relationship between $[gas]_i$ and flux. Therefore, for simplicity, these correction terms were omitted. Note that this omission does not affect the interpretation of AFR in Section 3.2.3.

Eq 10 is correct but the distinction between mixing ratios on a dry and wet air should be made earlier. Also, the whole sentence leading to this Eq 10 is extremely confusing and should be rewritten and simplified. In the revised manuscript, the distinction between *dry-air* and *wet-air* mixing ratios is now introduced earlier in the Methods section, prior to Equation 10, to improve clarity. The paragraph leading to Equation 10 has also been rewritten to be more concise and straightforward, highlighting only the key point: the QCLS instrument reports CO_2 and COS as *dry-air* mixing ratios, whereas the gas exchange model operates with *wet-air* mole fractions. Accordingly, Equation 10 provides the conversion between the two definitions.

<2.2.1. General concept>
Our leaf conductance model simulates the concurrent exchange of COS, CO_2, and H_2O in a plant leaf with the conditions of the laboratory experiments. Since these gases share the same stomatal pathway, their simultaneous modeling helps us understand the mechanisms of leaf conductance. The model calculates mole fractions on a wet-air basis, while the measurements are reported on a dry-air basis. Accordingly, conversions between dry- and wet-air mole fractions were applied when comparing modeled and observed concentrations (see Section 2.1.1). Additionally, the model assumes that gas exchange reaches an equilibrium that we tried to attain in the conducted experiments. All model variables that remain constant in the model are listed in Table 2. Variables that are excluded from Table 2 are targets for optimization as explained in Section 2.3.

From experiments, we measured $[gas]_{out}$, while the leaf conductance model calculates $[gas]_a$. Because the chamber air was well mixed, the modeled $[gas]_{out,est}$ is considered equivalent to $[gas]_a$ for model-observation comparison. Thus, $[gas]_{out,est}$ is used for $[gas]_a$ to interpret experimental data. In the model, the estimated mole fractions for COS and CO_2 are based on wet air, whereas the QCLS measures dry-air mole fractions. Therefore, to

compare model results with observations, the modeled wet-air mole fractions were converted to their dry-air equivalents using the observed outgoing H_2O mole fractions ($[H_2O]_{out,obs}$ (mmol mol^{-1})):

... Equation 10...
where $[H_2O]_{out,obs}$ is the observed outgoing H_2O mole fraction (mmol mol^{-1}). For $[COS]_{in,obs}$, which was measured after moisture removal, the same correction (Equation 10) was applied using $[H_2O]_{in,obs}$ instead of $[H_2O]_{out,obs}$ to convert from the dry-air to the wet-air basis before use in the conductance model.

Eq 11 and the notion of "mesophyll conductance" for water vapour is quite debated (i.e. assuming that the air is not saturated in the leaf stomatal cavity) and unjustified here where the leaves were not exposed to very dry air or high temperature or light levels. Also the value of 10 mol/m2/s for that conductance is so high (4 times larger than the boundary-layer conductance) that its effect is probably negligible, and so introducing this new variable (and Eq 13 below) is pointless. I would recommend to neglect it, as it is normally done in the LiCOR manual.

We thank the reviewer for this comment and agree that the assumption of a non-saturated intercellular airspace (RH < 100%) is relevant only under very dry or extreme conditions, which were not studied in our experiments.
To verify that this assumption does not affect our results, we retained a mesophyll conductance for water vapor (g_{m,H_2O}) in the model as a *sanity check*. Testing a wide range of g_{m,H_2O} values (<10 mol m^{-2} s^{-1}) confirmed that its effect on the computed fluxes and internal mole fractions is indeed negligible.
We will clarify in the revised text that g_{m,H_2O} was used only to test the sensitivity to possible non-saturation in the intercellular airspace, and that it does not alter the modeled outcomes under our experimental conditions.

In our experiments, we observed water evaporation from leaves. We aimed to model this evaporation at the mesophyll level and its subsequent transport out of the leaves, governed by *g_sw*. The unit of H_2O mole fractions in all layers is mmol mol^{-1}, and the unit of the flux is mmol m^{-2} s^{-1}. To represent the internal water vapor conditions, $[H_2O]_c$ was calculated assuming that water vapor within the mesophyll intercellular airspace is saturated. However, we allowed for relative humidity within the intercellular airspace (RH_i (%)) to be less than 100 %, based on previous studies (Cernusak *et al.*, 2018; Wong *et al.*, 2022). To achieve this, we introduced a mesophyll conductance for water vapor (g_{mw}) and set it to an arbitrary value of 10 mol m^{-2} s^{-1}, approximately ten times the largest observed value of *g_sw*. This parameter was included to test the sensitivity of the model to possible non-saturation within the intercellular airspace. *The optimized g_sw also showed consistent behavior. Comparisons of the optimized mean g_sw values of 0.64 mol m^{-2} s^{-1} with the prior values of 0.62 mol m^{-2} s^{-1} reveal slight differences. Errors in g_sw were reduced from 0.09 to 0.05 mol m^{-2} s^{-1}. The optimized model yielded an average relative humidity within the leaf (RH_i) of 98.82 ± 0.04 %. These results confirm that allowing for slight non-saturation in the intercellular airspace (through g_{m,H_2O}) had a negligible impact on the modeled fluxes, validating the*

assumption that the air within the intercellular airspace was effectively saturated under our experimental conditions. Simulations further confirmed that varying g_{mw} (< 10 mol m^{-2} s^{-1}) did not alter the modeled fluxes or mole fractions, indicating that its effect was negligible under our experimental conditions.

Eqs 14-17 are not needed to interpret gas exchange data, and test the three hypotheses, because only fluxes and LRU values are shown afterwards. Also in Eq 15, it should, not be CO2_i but CO2_c (at the chloroplast level).
We respectfully disagree that Equations14–17 are unnecessary. Although the main measurement outcomes presented in the Results are fluxes and LRU values, these equations are essential to interpret the underlying internal processes that directly relate to our three hypotheses (e.g., the temperature dependence of COS compensation point and the differential stomatal impacts on COS v.s. CO_2). The layer-specific intercellular mole fractions derived from these equations provide mechanistic insight into gas diffusion and were thus retained for completeness.

Regarding Equation 15, we agree that, in principle, it should be expressed as a function of the CO_2 partial pressure at the chloroplast level ($p[CO_2]_c$), as RuBisCO carboxylation occurs within the chloroplast stroma. However, our model does not explicitly include mesophyll conductance ($g_{m,CO2}$), and thus $p[CO_2]_c$ cannot be directly resolved. In such cases, it is standard practice to approximate p*CO2c* ≈*pCO2i* $[CO_2]_c \approx p[CO_2]_i$ (Harley et al., 1992), assuming negligible mesophyll resistance.

...Equation 25... where $p[CO_2]_i$ (Pa) and $p[O_2]_i$ (Pa) are the partial pressures of CO_2 and O_2 in the inter-cellular air space. K_c (Pa) and K_o (Pa) are Michaelis-Menten constants for CO_2 and O_2, respectively. Γ^*_{CO2} (Pa) stands for the CO_2 compensation point independent of dark respiration. Strictly speaking, RuBisCO carboxylation occurs within the chloroplast stroma and should depend on the chloroplast CO_2 partial pressure ($p[CO_2]_c$), rather than $p[CO_2]_i$. However, our model does not explicitly include mesophyll conductance ($g_{m,CO2}$), and thus $p[CO_2]_c$ cannot be directly resolved. Accordingly, $p[CO_2]_i$ was used as a proxy for $p[CO_2]_c$, following the classical formulation of Farquhar et al. (1980).

In Eq 18, why assuming that mesophyll conductance to COS is only biochemical? There should be a diffusional part considered. But again, this parameterisation of mesophyll conductance for COS is not needed for testing the three hypotheses and interpret gas exchange data.

We agree that, in principle, mesophyll conductance to COS (*gm,COS* $g_{m,COS}$) includes both diffusional and biochemical components. In the original text, we referred to the "biochemical" aspect because the overall conductance is strongly modulated by carbonic anhydrase (CA) activity, which catalyzes COS hydrolysis. In the revised manuscript, we clarify that *gm,COS* $g_{m,COS}$ conceptually represents the combined effect of diffusion through

mesophyll tissues and biochemical conversion by CA. Because CA activity is very fast, the apparent temperature response of *gm,COS* $g_{m,COS}$ can be largely attributed to biochemical limitation, but we acknowledge that it may also reflect diffusional effects. We also note that the inclusion of *gm,COS* $g_{m,COS}$ was essential for evaluating the potential for COS emission (Hypothesis 1), as excluding it would prevent quantifying internal COS gradients and reversibility of net fluxes. We therefore retained Equation 18 but revised the surrounding text to clarify its conceptual basis and limited purpose.

We constructed the COS model to estimate the gross COS flux rate (F_{COS}, pmol m^{-2} s^{-1}) and mole fractions of COS in each layer (pmol mol^{-1}). Accurate modeling of COS leaf uptake requires representing mesophyll conductance, which integrates both the diffusional transport of COS and biochemical conversion by CA.

Earlier approaches treated mesophyll diffusion and CA activity as linearly proportional to Rubisco's Vmax (Berry et al., 2013). However, this simplification was shown to bias COS flux estimates, leading to the introduction of a revised CA-based temperature formulation (Cho et al., 2023). More recently, Lai et al. (2024) emphasized the importance of explicitly accounting for mesophyll diffusion in COS uptake models but also noted the lack of reliable parameterization for COS-specific mesophyll diffusion.
Building on these previous findings, we modeled biochemical conductance of COS in the mesophyll ($g_{m,COS}$ (mol m^{-2} s^{-1})) using the CA activity–based function proposed by Cho et al. (2023), which implicitly represents mesophyll diffusion while minimizing estimation bias through its revised temperature dependence. This function describes the temperature dependence of CA activity using a specified Arrhenius equation and Michaelis-Menten Kinetics (Cho et al., 2023; Daniel et al., 2010; Ogée et al., 2016; Sun et al., 2015):

From a modeling perspective, only the enzyme CA is considered in determining the mesophyll conductance of COS. However, other enzymes, such as RuBisCO and phosphoenolpyruvate carboxylase (PEP-C), are known to also catalyze COS uptake (Lorimer and Pierce, 1989; Protoschill-Krebs and Kesselmeier, 1992). The contribution of RuBisCO to COS uptake is relatively minor compared to CA (Protoschill-Krebs *et al.*, 1996), and its activity has not yet been quantified.
An additional source of uncertainty arises from the simplified representation of COS mesophyll conductance in our model. While mesophyll diffusion was not explicitly parameterized, it was implicitly represented through the temperature-dependent CA activity function (Cho et al., 2023) that integrates both diffusional and biochemical processes. Nevertheless, this implicit treatment may not fully capture variations in diffusional resistance under different environmental or structural conditions, and thus its influence on the temperature dependence of COS uptake cannot be completely excluded. Future modeling studies incorporating explicit mesophyll diffusion parameterization—beyond the current CA-based formulation—would help to disentangle the relative contributions of

diffusional and biochemical controls, as well as potential COS emissions from leaves, in regulating COS exchange.

Eqs. 19-21 present three possible temperature responses for the estimated “compensation point" for COS. It is a bit strange to show results (Figure 3 with observational data points) here. I think this section (and Eq 19-21) should be brought in the Results section directly. It is not part of the Methods.

We appreciate the reviewer’s remark. We have carefully considered this suggestion. However, Figure 3 and Equations 19–21 are retained in the Methods section because they represent the initial parameterization and uncertainty characterization used for the subsequent model fitting. The figure illustrates the prior settings and error structures applied in the optimization framework, rather than observational or derived results.

For clarity, we have slightly revised the caption and text to emphasize that these correspond to model initialization steps rather than final experimental outcomes. We believe this organization helps readers distinguish between methodological setup and empirical findings presented later in the Results section.

(Revised manuscript – the red sentences were added)
Figure 3 shows these four Γ_{COS} functions (S1–S4) representing the prior temperature-dependent parameterizations tested in the modeling framework with their imposed uncertainties. The figure also shows the experimental Γ_{COS} estimates from Experiment 1, included solely for reference to illustrate the initial parameter alignment.
Figure 3. Prior temperature functions of the COS compensation point (Γ_{COS}) (lines) with their error ranges (shaded area). Blue triangles show the regression-derived Γ_{COS} from Experiment 1, included for reference to illustrate the initial parameter setup. The S1 model assumed Γ_{COS} = 0 pmol mol^{-1}. Model S2 describes Γ_{COS} as a linear relationship with T_{leaf} (a), while models S3 and S4 use an Arrhenius equation (b).

Eqs 22 neglects changes in mass flow between the inlet and outlet (see Eq B7 in vCF81) and Eqs 23-24 are also incorrect (see comment above on Eq 6-7).

We thank the reviewer for this comment. In the revised manuscript, we have clarified the assumptions regarding outlet mass-flow and ternary corrections based on the reviewer’s earlier feedback. Specifically, we now state that although transpiration slightly increases the outlet air flow, the effect (<3%) was neglected to retain easy analytical expressions, consistent with the assumption in Equation 1. Likewise, the ternary effects at the boundary layer were considered negligible under our experimental conditions (large g_bw, small E), following Equations 6–7. These clarifications have been explicitly added after Equation 22 to ensure transparency. As these approximations were consistently applied throughout the analysis (both in observations and model calculations), they do not affect the internal consistency or interpretation of our results.

Because the temperature-dependent behavior of Γ_{COS} in Experiment 1 was derived from a limited set of measurements under only a few temperatures, additional validation was

required to test whether the modeled Γ_{COS} functions are consistent across broader environmental conditions.
To support this validation, we incorporated the indirectly derived Γ_{COS} from 48 data points in Experiments 2 and 3.
By calculating $[COS]_c$ using our optimized model parameters in Equation 3, Equation 6, and Equation 7, we were able to indirectly estimate Γ_{COS} and compare it with the modeled Γ_{COS}.

First, we calculated $[COS]_b$ from the measured COS mole fractions with the rearranged Equation 3: ...Equation 3...

where $[COS]_{in}$ and $[COS]_a$, along with AF , S, and $g_{b,COS}$, were applied from Experiments 2 and 3. Due to thorough mixing within the cuvette, we assumed $[COS]_{out}$ to be equivalent to $[COS]_a$ and used it accordingly (refer to Sect. 2.2).
Although transpiration slightly increases the outlet air flow, this effect (< 3%) was neglected to simplify the analytical expressions, consistent with the assumptions described in Equation 1. This formulation follows the same assumptions as in Equation 3 regarding ternary effects at the boundary layer, which were found to be negligible under our experimental conditions. Here, $[COS]_{in}$ and $[COS]_{out}$ were converted from a dry air basis to a wet air basis. We then used the derived $[COS]_b$ to calculate $[COS]_i$ using the rearranged Equation 6:

I don’t understand why stomatal conductance is not derived directly from the measurements (see LiCOR’s manual or Eq B14-15 in vCF81). Given the high boundary-layer conductance (about 3-4 times stomatal conductance), the sensitivity of stomatal conductance to the exact choice of “K" is very small (see LICOR manual) and it is much more reliable than an “optimized” value based on a simplified model of photosynthesis (and COS uptake), with lots of unknown parameter values.

We appreciate the reviewer’s comment and agree that the LI-6800 provides reliable estimates of stomatal conductance (g_sw) based on water vapor exchange. However, in our model, we want to test whether the g_sw values from the LI-6800 (we start our optimization from these values) are consistent with the observed exchange CO_2 and COS. When adjustments within a prescribed error range are profitable for better simulations of CO_2 and COS, we allow for such adjustments in our optimization framework. This approach allows for a physically consistent representation across species and may compensate for potential biases associated with measurement uncertainties (e.g., the K parameter and cuvette humidity corrections). To our knowledge, this novel aspect in the interpretation of multi-species chamber observations has never been tested before. We therefore are keen to keep this new modelling framework in the paper, but agree with the reviewer that the model should not introduce biases by making wrong assumptions.

A corresponding further clarification has been added in the Methods section.

The LI-6800 derives *g_sw* from water vapor exchange with its own uncertainties. Because g_{sw} similarly affects the exchange of H_2O, CO_2, and COS through the same shared stomatal pathway, we optimize g_{sw} in a coupled framework using flux information from all three

gases to ensure internal consistency across species. The novelty of this framework lies in explicitly coupling these fluxes to derive a more physically consistent constraint on g_sw, while also addressing potential uncertainties in g_sw derived from LI-6800 measurements (e.g., stomatal ratio parameter K; Sect. 2.1.1).

Initial values for *g_sw* were taken from the LI-6800 measurements during Experiments 2 and 3. We applied a random error of 0.08 mol m^{-2} s^{-1}, representing the standard deviation of *g_sw* from Experiment 3, despite efforts to maintain a constant *g_sw* (± 0.06 mol m^{-2} s^{-1}). In addition, we considered an extra measurement uncertainty of 0.02 mol m^{-2} s^{-1}, based on known sources of instrumental bias—such as the leaf temperature underestimation (Garen et al., 2022) and background total leaf conductance to water observed in empty chambers (Hussain et al., 2024). We also added individual $[H_2O]_{out,obs}$ errors by normalizing $[H_2O]_{out,obs}$. The averaged initial *g_sw* value and its standard deviation (prior error) are 0.61 mol m^{-2} s^{-1} and 0.09 mol m^{-2} s^{-1}, respectively.

Also, it seems odd to estimate a compensation point for COS using a model that requires a parameterisation of this compensation point. If the idea is to compute the COS concentration in the intercellular air space, an equation similar to Eq B18 In vCF81 could be used (see also Stimler et al 2010). But in the end, the compensation point for COS is only estimated from the intercept of the regression line of FCOS vs [COS]a (Figure 4) so only COS flux calculations are needed, and sections 2.2.3, 2.2.4 and 2.3 could be removed from the manuscript.

We respectfully disagree. While it is true that the apparent COS compensation point can be empirically derived from the intercept of the F_{COS}-$[COS]_a$ relationship (as in Fig. 4), our study aims to go beyond this empirical regression and checks whether the model-data mismatches are smaller in models that include a compensation point formulation. The main objective of this work, as clearly stated in the Introduction, is to test three mechanistic hypotheses on the controls of COS exchange within leaves regarding (i) the role of stomatal and mesophyll conductances, (ii) the biochemical conversion by carbonic anhydrase, and (iii) the temperature dependence of these processes.
To evaluate these hypotheses, the model must explicitly resolve the diffusion pathway and reaction kinetics from ambient air to the chloroplast. Therefore, estimating COS mole fractions in the chloroplast $[COS]_c$ through the full conductance chain is essential. This approach allows us to assess how internal parameters influence the observed compensation behavior and to quantify their relative sensitivities.

Section 2.4 could also be removed if the modelling part is taken out (as I suggest). There is no need of a biochemical model that needs to be “parameterised” to discuss the gas exchange results presented here. As I explained above, what needs to be done instead is to compute gas exchange parameters (fluxes, conductances, etc) following the LICOR manual (but accounting for the fact that the QCLS computes mixing ratios on this dry air basis). This would make the manuscript much shorter and easier to read and follow.

We appreciate the reviewer’s suggestion and fully agree that the observational dataset itself is of high quality and allows for a clear interpretation of COS and CO_2 exchange. Indeed, the

measurements remain the central basis of our analysis.

However, the inclusion of the modelling framework (Section 2.4) is essential for the specific objectives of this study. As stated in the Introduction, our goal is not only to describe observed fluxes but to test three mechanistic hypotheses concerning the internal regulation of COS exchange: (i) temperature-dependent Γ_{COS}, (ii) stomatal conductance-dependent to internal exchange, and (iii) enzyme-specific temperature responses of CA and RuBisCO. These internal processes cannot be inferred directly from the measured fluxes, which is why a simple empirical treatment would not allow hypothesis testing. The model is therefore not a replacement for empirical analysis, but a diagnostic complement that integrates CO_2, COS, and H_2O exchange into a consistent mechanistic framework.

Finally, we repeat that this represents the first attempt to jointly optimize gas-exchange parameters across all three gas species, allowing an independent and mechanistically consistent estimation of the COS compensation point — one of the central findings of this study.

From a modeling perspective, only the enzyme CA is considered in determining the mesophyll conductance of COS. However, other enzymes, such as RuBisCO and phosphoenolpyruvate carboxylase (PEP-C), are known to also catalyze COS uptake (Lorimer and Pierce, 1989; Protoschill-Krebs and Kesselmeier, 1992). The contribution of RuBisCO to COS uptake is relatively minor compared to CA (Protoschill-Krebs et al., 1996), and its activity has not yet been quantified.
An additional source of uncertainty arises from the simplified representation of COS mesophyll conductance in our model. While mesophyll diffusion was not explicitly parameterized, it was implicitly represented through the temperature-dependent CA activity function (Cho et al., 2023) that integrates both diffusional and biochemical processes. Nevertheless, this implicit treatment may not fully capture variations in diffusional resistance under different environmental or structural conditions, and thus its influence on the temperature dependence of COS uptake cannot be completely excluded. Future modeling studies incorporating explicit mesophyll diffusion parameterization—beyond the current CA-based formulation—would help to disentangle the relative contributions of diffusional and biochemical controls, as well as potential COS emissions from leaves, in regulating COS exchange.
Beyond these structural uncertainties in the model, it is important to note that the conductance model was designed as an exploratory diagnostic tool. Its purpose was to integrate the coupled behavior of CO_2, COS, and H_2O exchange and to mechanistically interpret the observed fluxes. Despite its simplifications in not considering minor features, such as outlet mass flow change and boundary ternary effect, this framework represents the first attempt to jointly optimize gas exchange for the three gases, thereby providing a process-based means to independently estimate the COS compensation point. Overall, this approach highlights the potential of combined gas-exchange measurement and modeling to advance our understanding of COS biogeochemistry.

The discussion about measurement errors on stomatal conductance at the end of section 2.4.1 lacks some justification (where does the extra measurement error comes from?). But

this part should be removed anyway, because this measurement error was only used for the biochemical model optimization that I propose to get rid of.
While we acknowledge that stomatal conductance (g_sw) can be derived directly following the LI-6800 manual, we retained its optimization for the reasons outlined above. The optimization ensures internal consistency across all fluxes rather than relying solely on water-vapor–based conductance values.

Regarding the additional measurement uncertainty, we have now clarified its empirical basis in the revised text. The extra error term (0.02 mol m^{-2} s^{-1}) was introduced conservatively to reflect known sources of uncertainty in LI-6800 gas-exchange measurements. Specifically, Garen et al. (2022) reported that the LI-6800 can underestimate leaf temperature, which propagates into water vapor pressure and hence g_sw estimation. In addition, Hussain et al. (2024) identified a nonzero total leaf conductance to water in empty-chamber tests, suggesting small but systematic instrument offsets. These findings justify the inclusion of a measurement uncertainty term in our optimization framework.

The text in Section 2.4.1 has been revised accordingly to include these references and to emphasize that the error term was not introduced to inflate uncertainty but rather to conservatively account for known measurement limitations while maintaining robustness in the coupled CO_2–COS–H_2O optimization.

Hussain SB, Stinziano J, Pierre MO, et al.: Accurate photosynthetic parameter estimation at low stomatal conductance: effects of cuticular conductance and instrumental noise. Photosynth. Res. 2024;160:111–124. 10.1007/s11120-024-01092-8
Garen JC, Branch HA, Borrego I, et al.: Gas exchange analysers exhibit large measurement error driven by internal thermal gradients. New Phytol. 2022;236:369-384. 10.1111/nph.18347.

<2.4. Parameter optimization> ...
The LI-6800 derives g_sw from water vapor exchange with its own uncertainties. Because g_sw similarly affects the exchange of H_2O, CO_2, and COS through the same shared stomatal pathway, we optimize g_sw in a coupled framework using flux information from all three gases to ensure internal consistency across species. The novelty of this framework lies in explicitly coupling these fluxes to derive a more physically consistent constraint on g_sw, while also addressing potential uncertainties in g_sw derived from LI-6800 measurements (e.g., stomatal ratio parameter K; Sect. 2.1.1).

Initial values for *g_sw* were taken from the LI-6800 measurements during Experiments 2 and 3. We applied a random error of 0.08 mol m^{-2} s^{-1}, representing the standard deviation of *g_sw* from Experiment 3, despite efforts to maintain a constant *g_sw* (± 0.06 mol m^{-2} s^{-1}). In addition, we considered an extra measurement uncertainty of 0.02 mol m^{-2} s^{-1}, based on known sources of instrumental bias—such as the leaf temperature underestimation (Garen et al., 2022) and background total leaf conductance to water observed in empty chambers (Hussain et al., 2024). We also added individual $[H_2O]_{out,obs}$ errors by normalizing $[H_2O]_{out,obs}$. The averaged initial *g_sw* value and its standard deviation (prior error) are 0.61 mol m^{-2} s^{-1} and 0.09 mol m^{-2} s^{-1}, respectively.

In section 2.4.2 and Eq 25, the introduction of “weights" in the cost function is difficult to understand because it seems that those weights are there to wipe out differences in observational error between CO2, COS and H2O. But the cost function is normalised by these error terms for a reason, no? And again if the biochemical model optimization is removed, section 2.4 is also removed, and this comment is not relevant anymore.

We agree that the observational errors (*σobs* σ_{obs}) already normalize each flux term in the cost function. However, in our framework, the additional weighting factors (w_{CO2}, w_{COS}, w_{H2O}) serve a different purpose. They are not intended to correct for measurement errors, but rather to balance the relative influence of each gas in the multi-objective optimization. We acknowledge that the final choices are rather subjective, but we have been very careful not to over-emphasize the conclusions based on the exploratory optimization process. Specifically, the magnitudes and temporal variabilities of CO_2, COS, and H_2O fluxes differ by more than an order of magnitude, even after normalization by their observational uncertainties. As we explain in the text, without weighting the optimization would be dominated by the CO_2 term, leading to suboptimal performance for COS and H_2O. The weights therefore ensure that all three gases contribute comparably to the minimization of the total cost function.

Section 2.4.2 has been retained and revised for clarity. The introductory text now explicitly states that (i) observational errors are used for normalization, and (ii) weights are applied to achieve balanced optimization across gases with distinct flux magnitudes. We also emphasize that this coupled optimization framework is one of the novel aspects of our study, providing a unified treatment of CO_2–COS–H_2O exchange processes.

... Equation 25...
The first term of the cost function penalizes deviations of the state *x* from the prior state vector x_a. This penalty depends on *σ*, which represents the prior error in the state vector. This background term is introduced to keep state variables within reasonable boundaries (Brasseur and Jacob, 2017). The last three terms of the cost function calculate the costs associated with deviations between modeled ($[gas]_{out,est}$) and observed mole fractions ($[gas]_{out,obs}$) for COS, CO_2, and H_2O, respectively. Each term is normalized by its observational uncertainty to ensure consistent treatment of measurement errors, and each is scaled by optimization weights (W_{bg}, W_{COS}, W_{CO2}, and W_{H2O}) to balance the relative influence of each gas. These weights do not modify the observational errors but instead prevent any single gas—particularly CO_2—from dominating the total cost. The determination of these weights is described in the following section.

In section 3.1.1, you mention a “20% increase" of what? Stomatal conductance? Also it would be good to propagate errors due to the COS emission from the chamber (the scatter on Fig 1 is rather large)
We thank the reviewer for this constructive comment. We have clarified in the revised manuscript that the reported 20 % increase refers specifically to stomatal conductance (g_sw), which increased from 0.76 to 0.90 mol m^{-2} s^{-1} during the temperature adjustment at

higher T_{leaf}. This clarification is now included in Section 3.1.1.

Regarding the uncertainty propagation, we agree that the empty-chamber correction may not completely remove background variability. To assess its influence, we incorporated the residual RMSEs from the empty-chamber correction—6.9 pmol mol^{-1} for $[COS]_a$ (x-axis) and 2.73 pmol m^{-2} s^{-1} for F_{COS} (y-axis)—into the total uncertainty of the regression-derived Γ_{COS}. Both sources of uncertainty were propagated to account for their combined impact on the regression intercept and, consequently, on the estimated compensation point.

Specifically, we calculated the total propagated uncertainty as: \sigma_{\text{total}} = \sqrt{\sigma_{\text{regression}}^{2} + \sigma_{\text{chamber}}^{2}} where $\sigma_{regression}$ is the standard error from the linear fit of F_{COS} versus $[COS]_a$, and $\sigma_{chamber}$ combines the residual uncertainties from both F_{COS} and $[COS]_a$ after the empty-chamber correction. This additional uncertainty was then included in the 95 % confidence interval of Γ_{COS}. As a result, the 95 % confidence intervals of Γ_{COS} broaden from ±53.2 to ±93.4 pmol mol^{-1} at 19.8 °C and from ±26.1 to ±48.9 pmol mol^{-1} at 25.0 °C. The estimate at 19.8 °C includes zero, indicating that it is not statistically different from zero, whereas the estimate at 25.0 °C remains significantly positive, confirming a temperature-dependent increase in Γ_{COS} and clearly states whether the retrieved composition points are all statistically different from zero.

3.1.1. COS Compensation Point (Experiment 1)
Figure 4 presents the results from Experiment 1 with Sunflower 1, aimed at determining Γ_{COS} by measuring F_{COS} while controlling $[COS]_{out}$ and maintaining constant *g_sw* and T_{leaf}. Minor fluctuations in *g_sw* occurred during temperature adjustments, increasing from 0.76 to 0.90 mol m^{-2} s^{-1} at higher temperatures. F_{COS} shows a linear increase with increasing $[COS]_{out}$, in agreement with findings from earlier studies (Gimeno *et al.*, 2017; Kesselmeier and Merk, 1993; Stimler *et al.*, 2010). We quantified the regression-based Γ_{COS} using a linear function at two temperatures: Γ_{COS} was 55.0 ± 53.2 pmol mol^{-1} at 19.8 °C and 138.7 ± 26.1 pmol mol^{-1} at 25.0 °C (error estimates denote 95 % confidence interval). These results indicate that Γ_{COS} increases with rising T_{leaf}, suggesting a potential temperature dependence.

Although the empty-chamber regression effectively removed the baseline COS emission, some residual variability likely remained (RMSE = 6.9 pmol mol^{-1} for $[COS]_a$ and 2.73 pmol m^{-2} s^{-1} for F_{COS}). To evaluate the potential influence of this unresolved background variability, we propagated these errors to the regression-derived Γ_{COS}. When the uncertainty is included, the 95% confidence interval of Γ_{COS} widened from ± 53.2 to ± 93.4 pmol mol^{-1} at 19.8 °C and from ± 26.1 to ± 48.9 pmol mol^{-1} at 25.0 °C. The large uncertainty at 19.8 °C indicates that the corresponding Γ_{COS} value is statistically indistinguishable from zero. By contrast, the Γ_{COS} measured at 25 °C remains significant even when this propagated and instrumental uncertainty is considered. Even accounting for the reported QCLS uncertainty of approximately 7.5 pmol mol^{-1} for COS (Kooijmans et al., 2016), the Γ_{COS} value at 25 °C remains statistically robust.

I have not finalized the review of the end of the manuscript but I see that Figs 7-9 and most Tables except Table 1 could be removed as they show results from the biochemical model

optimization that, to me, should be removed because I do not see what it brings to the study. My suggestions would make the paper much more digest and strong, and the main message should stay almost unchanged. I hope the authors will agree with this suggestion.

We appreciate the reviewer's careful reading and constructive feedback. We understand the concern that the inclusion of biochemical model optimization results may appear to complicate the manuscript. However, we respectfully maintain our vision that the modeling framework is an integral part of the study, serving as a novel diagnostic and interpretive tool rather than the primary result.

To address the reviewer's concern about readability and focus, we have taken the following steps:
1. Clarified the model's role and rationale in the Introduction — We have added a short paragraph explaining that the coupled CO_2–COS–H_2O conductance model was developed to mechanistically interpret internal COS processes that cannot be directly inferred from laboratory measurements alone. This emphasizes that the model complements, rather than replaces, the empirical analyses.

2. Strengthened the Discussion to contextualize the modeling results — At the beginning of Section 4, we have inserted a paragraph explicitly stating that the model was used to supplement limited observational constraints (e.g., COS compensation points determined at a limited number of temperature levels) and to explore the mechanistic basis of observed COS–CO_2 differences. This addition clarifies the interpretive rather than predictive role of the model. Together, we think that these revisions enhance the manuscript's coherence and digestibility while preserving its scientific depth. We believe that this integrated experimental–modeling framework is essential to address the study's main objective: to identify the internal leaf processes governing differential COS and CO_2 flux responses.

Disentangling these hypotheses using field measurements is challenging due to interrelated and simultaneous variations of environmental conditions (e.g. T_{leaf} , VPD, and g_sw). Laboratory experiments offer the advantage of observing COS and CO_2 uptake changes at a leaf level under controlled conditions while independently varying environmental factors. To complement the experimental analysis and mechanistically interpret the observed gas-exchange responses, we developed a coupled CO_2–COS–H_2O conductance model based on a leaf conductance model previously established for GPP tracers such as the $\Delta^{17}O$ and Δ_{47} isotopic composition of CO_2 (Adnew et al., 2020; Adnew et al., 2021; Adnew et al., 2023). This model serves as a diagnostic tool that enables joint optimization of gas-exchange parameters through the shared stomatal pathway for the three gases and allows inference of internal variables, such as intercellular and chloroplast COS mole fractions, that are not directly measurable.

<4. Discussion>
This study aimed to investigate how leaf COS and CO_2 fluxes respond differently to environmental changes and to identify which internal processes within leaves govern these

differences. Laboratory experiments were conducted under controlled conditions to isolate the effects of stomatal conductance and temperature. However, to provide more insights in the internal processes that control COS exchange, we developed and optimized a coupled CO_2–COS–H_2O conductance model to mechanistically interpret the measurement data. Although the model involves some simplified representations of internal processes, these simplifications are minor and do not affect the overall interpretation. In this section, we discuss the uncertainties in both observations and model representations, the physiological implications of the observed COS compensation points, and their broader significance for biochemical parameters and the global COS budget.

Competing Interests: No competing interests were disclosed.